

NAVAL POSTGRADUATE SCHOOL

Monterey, California



THESIS

TRANSPARENT GRID TERMINATION (TGT) FOR FINITE
DIFFERENCE TIME DOMAIN (FD-TD) ELECTROMAGNETIC
FIELD COMPUTATION IN ONE, TWO, AND THREE
DIMENSIONS

by

Kewjin Wang

September 1995

Thesis Advisor:

J. E. Lebaric

Approved for public release; distribution is unlimited.

DMO QUALITY INSPECTED 1

19960305 100

REPORT DOCUMENTATION PAGE

Form Approved
OMB No. 0704-0188

Public reporting burden for this collection of information is estimated to average 1 hour per response, including the time for reviewing instruction, searching existing data sources, gathering and maintaining the data needed, and completing and reviewing the collection of information. Send comments regarding this burden estimate or any other aspect of this collection of information, including suggestions for reducing this burden, to Washington headquarters Services, Directorate for Information Operations and Reports, 1215 Jefferson Davis Highway, Suite 1204, Arlington, VA 22202-4302, and to the Office of Management and Budget, Paperwork Reduction Project (0704-0188) Washington DC 20503.

AGENCY USE ONLY (Leave blank)

2. REPORT DATE
September 1995

3. REPORT TYPE AND DATES COVERED
Master's Thesis

4. TITLE AND SUBTITLE

Transparent Grid Termination (TGT) for Finite Difference Time Domain (FD-TD) Electromagnetic Field Computation In One, Two, and Three Dimensions

5. FUNDING NUMBERS

6. AUTHOR(S)

Kewjin Wang

7. PERFORMING ORGANIZATION NAME(S) AND ADDRESS(ES)

Naval Postgraduate School
Monterey CA 93943-5000

8. PERFORMING ORGANIZATION
REPORT NUMBER:

9. SPONSORING/MONITORING AGENCY NAME(S) AND ADDRESS(ES)

10. SPONSORING/MONITORING
AGENCY REPORT NUMBER:

11. SUPPLEMENTARY NOTES

The views expressed in this thesis are those of the author and do not reflect the official policy or position of the Department of Defense or the U.S. Government.

12a. DISTRIBUTION/AVAILABILITY STATEMENT

Approved for public release; distribution is unlimited.

12b. DISTRIBUTION CODE

13. ABSTRACT (maximum 200 words)

In order to solve FD-TD electromagnetic radiation and scattering problems in free space, the computational grid should be truncated at some finite distance to simulate the solution for an infinitely large grid. One way to emulate an infinite grid is to absorb outgoing waves incident onto the grid boundary such that there is no reflection back into the grid. Waves incident to the boundary must "exit" the grid boundary without affecting the solution within the grid. Based on this idea, this thesis develops Transparent Grid Termination (TGT) in 1-D, 2-D and 3-D as an absorbing boundary. TGT performance is compared with a very large grid for which reflections do not return to the computational domain within the observation time window.

14. SUBJECT TERMS

Modeling of TGT Boundary as an Absorbing Boundary in One, Two, and Three Dimensions. Quantifying TGT quality as an Absorbing Boundary.

15. NUMBER OF PAGES:

146

16. PRICE CODE

17. SECURITY CLASSIFICATION OF REPORT
Unclassified

18. SECURITY CLASSIFICATION OF THIS PAGE
Unclassified

19. SECURITY CLASSIFICATION OF ABSTRACT
Unclassified

20. LIMITATION OF ABSTRACT
UL

NSN 7540-01-280-5500

Standard Form 298 (Rev. 2-89)

Prescribed by ANSI Std. Z39-18

Approved for public release; distribution is unlimited.

**TRANSPARENT GRID TERMINATION (TGT) FOR FINITE DIFFERENCE
TIME DOMAIN (FD-TD) ELECTROMAGNETIC FIELD COMPUTATION IN
ONE, TWO, AND THREE DIMENSIONS**

Kewjin Wang

CPT, Korean Army
B.S. Korea Military Academy, 1989

Submitted in partial fulfillment
of the requirements for the degree of


MASTER OF SCIENCE IN SYSTEMS ENGINEERING

from the

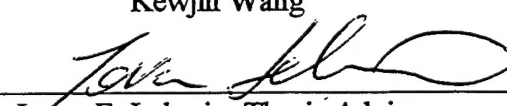
NAVAL POSTGRADUATE SCHOOL

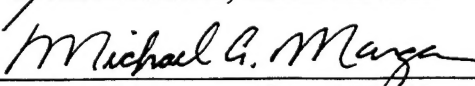
September 1995

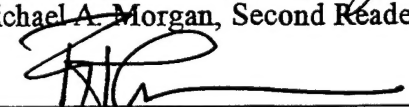
Author:


Kewjin Wang

Approved by:


Jovan E. Lebaric, Thesis Advisor


Michael A. Morgan, Second Reader


Frederic H. Levien, Chairman
Electronic Warfare Academic Group

ABSTRACT

In order to solve FD-TD electromagnetic radiation and scattering problems in free space, the computational grid should be truncated at some finite distance to simulate the solution for an infinitely large grid. One way to emulate an infinite grid is to absorb outgoing waves incident onto the grid boundary such that there is no reflection back into the grid. Waves incident to the boundary must "exit" the grid boundary without affecting the solution within the grid. Based on this idea, this thesis develops Transparent Grid Termination (TGT) in 1-D, 2-D and 3-D as an absorbing boundary. TGT performance is compared with a very large grid, for which reflections do not return to the computational domain within the observation time window.

TABLE OF CONTENTS

I. INTRODUCTION	1
A. OVERVIEW	1
B. OBJECTIVE	3
II. ANALYSIS OF TGT FOR 1-D FD-TD	7
A. FD-TD FORMULATION IN 1-D	7
1. FD-TD Equations in 1-D	7
2. Derivation of Magnetic Field Update Equation	10
3. Derivation of Electric Field Update Equation	15
B. TRANSPARENT GRID TERMINATION IN 1-D	20
1. 1-D Grid	20
2. Grid Termination	22
C. 1-D TGT RESULTS	28
III. ANALYSIS OF TGT FOR 2-D FDTD	31
A. FD-TD FORMULATION IN 2-D	31
1. FD-TD Equations in 2-D	31
2. Derivation of TE _z Magnetic Field Update Equation	35
3. Derivation of TE _z Electric Field Update Equations	40
4. Derivation of TM _z Electric Field Update Equation	47
5. Derivation of TM _z Magnetic Field Update Equations	53
B. TRANSPARENT GRID TERMINATION IN 2-D	58
1. 2-D TE _z and TM _z Grids	58
2. 2-D Grid Termination	62
C. 2-D TGT RESULTS	74
IV. ANALYSIS OF TGT FOR 3-D FD-TD	91
A. FD-TD FORMULATION IN 3-D	91
1. FD-TD Equations in 3-D	91
2. Derivation of Magnetic Field Update Equations	94
3. Derivation of Electric Field Update Equations	100

B. TRANSPARENT GRID TERMINATION IN 3-D	108
1. 3-D Grid	108
2. 3-D Grid Termination	114
C. 3-D TGT RESULTS	124
V. SUMMARY AND CONCLUSION	129
A. SUMMARY	129
B. CONCLUSIONS AND RECOMMENDATIONS	129
APPENDIX	131
A. DBIR.M	131
B. TGT_TM.M	132
LIST OF REFERENCES	135
INITIAL DISTRIBUTION LIST	137

I. INTRODUCTION

A. OVERVIEW

The analysis of electromagnetic problems in the time domain has become more common in recent decades. In this approach, the differential or integral equations for the particular problem under consideration are typically solved numerically using a short time-duration waveform as excitation. By far the most common of these techniques is the so-called finite difference time-domain (FD-TD) method.

In the FD-TD method, the problem is spatially discretized ("sampled") using a spatial step Δl , usually in a Cartesian coordinate system and temporally "sampled" using a time step Δt . The differential operators in the differential form of Maxwell's equations are approximated by finite differences or, equivalently, integrals in the integral form of Maxwell's equations are approximated by finite sums. In this research, a pulse waveform is excited at the center of the discretization grid, and the fields at the grid nodes are computed at discrete time steps. The field at a particular grid node at time t can be determined from the fields of this and adjacent nodes calculated for the previous time step $t - \Delta t$. The electric and magnetic fields obtained via the FD-TD method are the result of a "marching in time" process whose accuracy is affected by the approximations introduced at each time step. These include the grid size, time step, length of time observation, excitation waveform, and so forth.

There are several advantages to the FD-TD method. First, it is relatively simple to implement for complex objects because of spatial discretization. Inhomogeneous media is handled by assigning varying electric and magnetic properties (ϵ , μ , and σ) to individual cells. Although the FD-TD electric and magnetic field "update" equations appear complex, they contain only addition, subtraction, and multiplication. Furthermore, computer memory requirements are usually less demanding than those for the method of moments (MOM).

An important consideration in the FD-TD method is how to terminate the spatial discretization grid. The FD-TD equation derived in the following section will describe how waves propagate along an infinite grid. However, in all practical applications the grid will have to be restricted to a finite number of nodes. Therefore, a method for grid "termination" is required. The "standard" FD-TD update equations are valid for all nodes except those on the grid edges, because the grid edge nodes have fewer neighbors than the non-edge (internal) nodes. Therefore, edge nodes with a different number of neighbors have update equations different from the equations derived for the internal grid nodes. The question is how can one determine the equations for the edge nodes? One approach is to try to absorb a wave incident from inside the grid onto the boundary such that there is no reflection back into the grid. This is referred to as an absorbing boundary condition (ABC) [Ref 2]. However, the grid itself is not ideal, that is a wave does not pass through the grid without some reflection even for those nodes that are not at grid's edges (this is the consequence of spatial and temporal field sampling). Requiring that there is no

reflection off the grid edges is thus too restrictive, because there is some reflection at each and every node within the grid. We thus propose a different approach that we refer to as the Transparent Grid Termination (TGT). We start by making only one demand on the grid termination condition: that, ideally, the solution within the grid should be the same solution that one would obtain with an infinitely large grid, or in other words, that reflections off a grid edge node are the same as the reflections off any other node inside the grid. Note that if the grid were infinitely large, the grid edges would be at infinity and the equations for the grid edge nodes would be irrelevant, since the excited or scattered field would take an infinitely long time to reach the grid edges, and thus the edge equations would never really be needed. The TGT requirement is conceptually very simple and fairly straightforward to implement. We will use the multiport concept (used in analysis of linear systems) to introduce the TGT concept, and details will be shown in the following sections.

B. OBJECTIVE

The performance of the TGT in 1-D, 2-D, and 3-D can be assessed based on the residual reflection off the TGT boundary. In this thesis the total power of the electromagnetic field, excited by a unit amplitude delta pulse in the grid center, will be observed as a function of time. If the grid were ideal, the energy of the field at any node will be zero for all time after the pulse has passed that node. The total energy within an infinite ideal grid would be constant however. The total energy within a finite ideal grid

with ideal grid termination condition will be constant until the pulse has reached the grid edge and will then quickly go to zero as the pulse leaves the grid. However, because the grid is not ideal, there are some residual values at any grid node, even after the initial pulse has passed that node. Therefore, the energy within a non-ideal grid will not be constant but will fluctuate about its value for the ideal grid. These fluctuations generally decrease with time but they would exist even if the grid were infinite. If the grid is terminated, the residual energy within the grid will increase because of additional reflections off the grid edges. The global effect of the grid termination can thus be assessed by comparing the total grid powers as functions of time for the following two cases: an "infinite" grid, and a finite size grid with TGT or ABC. Note that the "infinite" grid is simulated by using a large grid and finishing the observations before the pulse that started at the grid's center has reached any of the grid edge nodes. Note that if the TGT or ABC were ideal, there would be no increase in energy within the grid after the pulse has reached the grid edges. If the TGT is not ideal, the relative change of the energy within the grid (compared to the case of an "infinite" grid) is a measure of TGT "quality": the smaller the change, the better the TGT would be. We will thus compare the total energies within the TGT boundary for a large grid with Dirichlet boundary condition (any boundary condition is appropriate for this "infinite" grid simulation because the reflections off the edges of the large grid do not reach the smaller grid boundary within the observation time-window) and the smaller grid with the TGT boundary. Once again, the large grid must provide sufficient distance between the TGT and Dirichlet boundaries such that the reflections of the Dirichlet

boundary do not reach the TGT boundary within the observation interval. The measure of residual reflection off the TGT boundary will be the difference of the energies within the TGT boundary for the "infinite" grid and the TGT. It is convenient to normalize this difference to the energy within the TGT boundary for the "infinite" grid, and express the resulting ratio in dB. The objective of this thesis is thus to determine the quality (measured in dB as described above) of the Transparent Grid Termination (TGT).

II. ANALYSIS OF TGT FOR 1-D FD-TD

A. FD-TD FORMULATION IN 1-D

1. FD-TD Equations in 1-D

The incident and the scattered electromagnetic fields and the media parameters in 1-D problems can vary with one spatial coordinate only. We will denote this coordinate as z . The fields will also be functions of time t . The media will be assumed stationary, that is, the media parameters are not functions of time t . 1-D electromagnetic fields must be Transverse Electro-Magnetic (TEM) fields, that is the field components \vec{E} and \vec{H} must be in a plane transverse to the direction of field propagation [Ref. 5]. Since we have denoted the direction of propagation as z , the fields can be denoted as transverse-to- z or TEM_z . The electric and magnetic vectors of a TEM field must be perpendicular to each other. The E and H field vectors and the direction of propagation form a triplet of orthogonal vectors, as shown below.

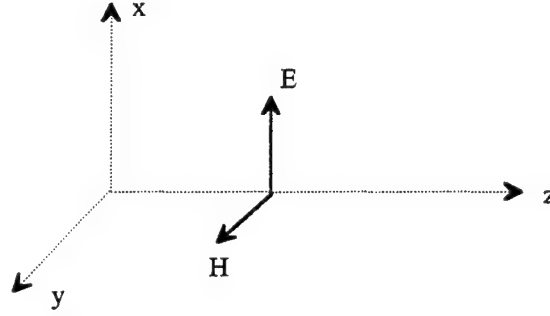


Figure 2.1. TEM Field Components.

The axes were selected such that the electric field vector is x-directed and the magnetic field vector is y-directed.

$$\vec{E}(z, t) = E_x(z, t) \vec{x} \quad (2.1)$$

$$\vec{H}(z, t) = H_y(z, t) \vec{y} \quad (2.2)$$

The electric and magnetic fields satisfy Maxwell's curl equations which express the electric and magnetic field coupling and can be written in the integral or the differential form. We will use the integral forms because they are applicable to finite (line, surface, or volume) domains whereas the differential forms are applicable to infinitesimally small domains (points). Shown below are the integral forms of Maxwell's curl equations for a TEM_z field.

$$\oint_{C_E} E_x(z, t) \vec{x} \cdot d\vec{l}_E = -\frac{\partial}{\partial t} \left\{ \iint_{S_E} \mu(z) H_y(z, t) \vec{y} \cdot d\vec{s}_E \right\} \quad (2.3)$$

$$\oint_{C_H} H_y(z, t) \vec{y} \cdot d\vec{l}_H = \frac{\partial}{\partial t} \left\{ \iint_{S_H} \varepsilon(z) E_x(z, t) \vec{x} \cdot d\vec{s}_H \right\} + \iint_{S_H} \sigma(z) E_x(z, t) \vec{x} \cdot d\vec{s}_H \quad (2.4)$$

The second equation does not have the source current term since it has been assumed that there were no source currents in the domain of interest. The contours of

integration for the electric and the magnetic field contour integrals are, in general, different and are thus labeled C_E for an electric field circulation and C_H for a magnetic field circulation. (A closed path line integral will be referred to as the circulation.) Similarly, the surfaces associated with the contours are labeled S_E for the magnetic field surface integral and S_H for the electric field surface integral. Surface integrals on the right-hand side will be referred to as fluxes. The first step in discretizing the curl equations is to select the contours for the electric and magnetic field circulation. Since the essence of Maxwell's curl equations is the coupling of the electric and magnetic fields, the contours will be selected such that this coupling is achieved in a straightforward manner, as shown below.

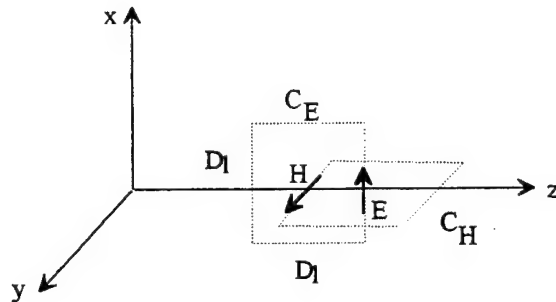


Figure 2.2. Contours for Electric and Magnetic Field Circulation and Fluxes.

The electric field contours C_E and the magnetic field contours C_H are square (Δl by Δl) contours, but in orthogonal planes. The C_E contours are in the xz-plane, while the C_H contours are in the yz-plane. The contours can be compared to links of a chain, evoking the idea of electric and magnetic field linkage. This selection of such contours leads to the so-called dual discretization grid, also referred to as the Yee lattice [Ref. 1].

2. Derivation of Magnetic Field Update Equation

The discrete equivalent of the electric field circulation will be determined next. A contour C_E is shown below.

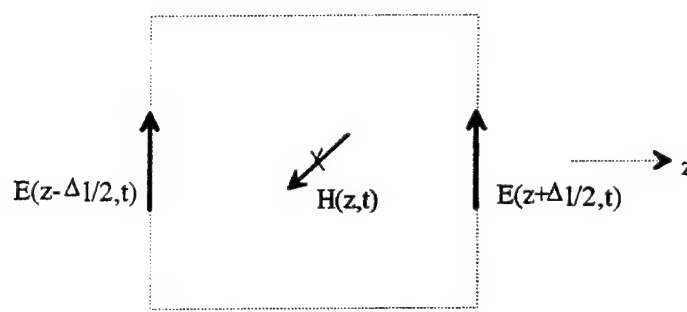


Figure 2.3. A Contour for Electric Field Circulation and Magnetic Flux Calculations.

The center of the surface S_E is assumed to have the coordinates (x, z) . A local coordinate system (ξ, ζ) can be established, with the origin at the center of the contour. Any point (x', z') within or on the contour C_E (or, equivalently, any point on the surface S_E) can be specified by its local coordinates ξ and ζ

$$x' = x + \xi \quad z' = z + \zeta \quad \text{where} \quad -\frac{\Delta l}{2} \leq \xi \leq +\frac{\Delta l}{2} \quad \text{and} \quad -\frac{\Delta l}{2} \leq \zeta \leq +\frac{\Delta l}{2}$$

The local coordinates will be used in evaluation of the line and surface integrals that constitute the integral forms of Maxwell's equations. The electric field E_x is not a function of the x -coordinate and the electric field is zero along the top and the bottom sides of the contour because there can be no z -directed field components of a TEM_z field. The circulation of the electric field around the electric field contour C_E , assuming counter-clockwise reference direction such that the normal to the surface S_E is in the direction of the magnetic field $\vec{H}(z, t)$, can be evaluated exactly

$$\oint_{C_E} E_x(z+\zeta, t) \vec{x} \cdot d\vec{l}_E = \int_{-\frac{\Delta l}{2}}^{+\frac{\Delta l}{2}} E_x(z+\frac{\Delta l}{2}, t) \vec{x} \cdot d\vec{\zeta} \vec{x} - \int_{-\frac{\Delta l}{2}}^{+\frac{\Delta l}{2}} E_x(z-\frac{\Delta l}{2}, t) \vec{x} \cdot d\vec{\zeta} \vec{x} \quad (2.5)$$

$$\oint_{C_E} E_x(z+\zeta, t) \vec{x} \cdot d\vec{l}_E = [E_x(z+\frac{\Delta l}{2}, t) - E_x(z-\frac{\Delta l}{2}, t)] \cdot \Delta l \quad (2.6)$$

The rate of change of magnetic flux through the surface S_E (within the contour C_E) can, on the other hand, be evaluated only *approximately*, since the exact way that the magnetic flux density

$$B(z, t) = \mu(z)H(z, t) \quad (2.7)$$

varies with the z -coordinate is not known a priori. Note that there is no variation of the magnetic flux density with the x -coordinate. We will next evaluate the magnetic flux approximately

$$\iint_{S_E} \mu(z+\zeta)H_y(z+\zeta, t) \vec{y} \cdot d\vec{s}_E = \int_{-\frac{\Delta l}{2}}^{+\frac{\Delta l}{2}} \int_{-\frac{\Delta l}{2}}^{+\frac{\Delta l}{2}} \mu(z+\zeta)H_y(z+\zeta, t) \vec{y} \cdot \vec{y} d\zeta d\zeta \quad (2.8)$$

The surface integral reduces to a line integral, since the integrand is not a function of the local x -coordinate ξ

$$\iint_{S_E} \mu(z+\zeta)H_y(z+\zeta, t) \vec{y} \cdot d\vec{s}_E = \Delta l \int_{-\frac{\Delta l}{2}}^{+\frac{\Delta l}{2}} \mu(z+\zeta)H_y(z+\zeta, t) d\zeta \quad (2.9)$$

There are infinitely many ways to model the variation of the magnetic flux density with the local z -coordinate ζ within the contour. Since the magnetic flux density $B(z+\zeta, t)$ is the product of the permeability $\mu(z+\zeta)$ and the magnetic field $H(z+\zeta, t)$ we first need to assume a certain variation of the magnetic field with ζ such that the integral can be evaluated over S_E . The simplest model assumes that the contour width Δl is small enough such that the magnetic field $H(z+\zeta, t)$ within the contour may be assumed constant and equal to the value at the contour's center $H(z, t)$. This is equivalent to using a piece-wise constant ("pulse" expansion) approximation of the actual magnetic field variation with the

z-coordinate. The above assumption allows that the magnetic field, although constant within a contour, can change from one contour to an other. This yields an *approximate* expression for the for the magnetic flux

$$\iint_{S_E} \mu(z+\zeta) H_y(z+\zeta, t) \vec{y} \cdot \vec{ds}_E \approx \Delta l \cdot H_y(z, t) \cdot \int_{-\frac{\Delta l}{2}}^{+\frac{\Delta l}{2}} \mu(z+\zeta) d\zeta \quad (2.10)$$

The integral of the permeability $\mu(z+\zeta)$ can be re-written in the following manner

$$\int_{-\frac{\Delta l}{2}}^{+\frac{\Delta l}{2}} \mu(z+\zeta) d\zeta = \Delta l \cdot \left[\frac{1}{\Delta l} \int_{-\frac{\Delta l}{2}}^{+\frac{\Delta l}{2}} \mu(z+\zeta) d\zeta \right] \quad (2.11)$$

The term in the brackets is recognized as the *average* permeability μ_{avg} within the contour C_E .

$$\mu_{avg}(z) = \frac{1}{\Delta l} \int_{-\frac{\Delta l}{2}}^{+\frac{\Delta l}{2}} \mu(z+\zeta) d\zeta \quad (2.12)$$

The approximate expression for the magnetic flux through S_E can now be written using the average permeability as

$$\iint_{S_E} \mu(z+\zeta) H_y(z+\zeta, t) \vec{y} \cdot \vec{ds}_E \approx (\Delta l)^2 \mu_{avg}(z) H_y(z, t) \quad (2.13)$$

Again, this approximate expression resulted from the piece-wise constant approximation of the magnetic field with respect to the z-coordinate. The main advantage of the piece-wise constant expansion employed above is its simplicity. Better accuracy can be achieved by using more involved models for the field variation with z, but at the expense of increasing the complexity and computational time. The first curl equation of Maxwell can now be replaced by an approximate equation

$$\left[E_x(z + \frac{\Delta l}{2}, t) - E_x(z - \frac{\Delta l}{2}, t) \right] \cdot \Delta l \approx -\frac{\partial}{\partial t} \{ [\mu_{avg}(z) H_y(z, t)] (\Delta l)^2 \} \quad (2.14)$$

which can be simplified (because of media stationarity) to

$$E_x(z + \frac{\Delta l}{2}, t) - E_x(z - \frac{\Delta l}{2}, t) \approx -\frac{\partial}{\partial t} \{ H_y(z, t) \} \cdot \Delta l \cdot \mu_{avg}(z) \quad (2.15)$$

This equation can also be re-written as

$$\frac{\partial}{\partial t}\{H_y(z, t)\} \approx \frac{-1}{\Delta l \cdot \mu_{avg}(z)} \left[E_x(z + \frac{\Delta l}{2}, t) - E_x(z - \frac{\Delta l}{2}, t) \right] \quad (2.16)$$

The time derivative operator in the above equation is typically replaced by the finite difference approximation [Ref 1]. However, an alternate approach is presented here, such that the approximation of the field temporal variation is shown to be analogous to the approximations already introduced for the field spatial variation. The above equation is integrated with respect to time to get an approximate equation for the magnetic field at the present time t

$$H_y(z, t) \approx \frac{-1}{\Delta l \cdot \mu_{avg}(z)} \left[\int_0^t E_x(z + \frac{\Delta l}{2}, \tau) d\tau - \int_0^t E_x(z - \frac{\Delta l}{2}, \tau) d\tau \right] \quad (2.17)$$

A similar integral equation can be written for the magnetic field at the same spatial location but at an earlier time $t - \Delta t$

$$H_y(z, t - \Delta t) \approx \frac{-1}{\Delta l \cdot \mu_{avg}(z)} \left[\int_0^{t-\Delta t} E_x(z + \frac{\Delta l}{2}, \tau) d\tau - \int_0^{t-\Delta t} E_x(z - \frac{\Delta l}{2}, \tau) d\tau \right] \quad (2.18)$$

Subtracting the two equations we get

$$H_y(z, t) - H_y(z, t - \Delta t) \approx \frac{-1}{\Delta l \cdot \mu_{avg}(z)} \left[\int_{t-\Delta t}^t E_x(z + \frac{\Delta l}{2}, \tau) d\tau - \int_{t-\Delta t}^t E_x(z - \frac{\Delta l}{2}, \tau) d\tau \right] \quad (2.19)$$

which can be also written as an "**update**" equation (assuming that the previous field value at the same location is known)

$$H_y(z, t) \approx H_y(z, t - \Delta t) - \frac{1}{\Delta l \cdot \mu_{avg}(z)} \left[\int_{t-\Delta t}^t E_x(z + \frac{\Delta l}{2}, \tau) d\tau - \int_{t-\Delta t}^t E_x(z - \frac{\Delta l}{2}, \tau) d\tau \right] \quad (2.20)$$

The integrals on the right-hand side can not be evaluated exactly, because the exact temporal variation of the electric fields within the Δt interval prior to t is generally not known, just like the spatial integral for the magnetic flux could not have been evaluated exactly because the exact variation of the magnetic field within the contour was not known. However, the integrals can be evaluated approximately by assuming a certain

variation of the electric field with the temporal variable τ . The simplest approach, consistent with the assumptions made for the field spatial variation, would be to assume that the interval Δt is small enough such that the electric field can be assumed approximately constant within Δt and equal to the value at the center of the time interval $(t-\Delta t, t)$

$$E(z + \frac{\Delta l}{2}, \tau) \approx E(z + \frac{\Delta l}{2}, t - \frac{\Delta t}{2}) \quad \text{for } t - \Delta t \leq \tau \leq t \quad (2.21)$$

$$E(z - \frac{\Delta l}{2}, \tau) \approx E(z - \frac{\Delta l}{2}, t - \frac{\Delta t}{2}) \quad \text{for } t - \Delta t \leq \tau \leq t \quad (2.22)$$

The above represents a piece-wise constant approximation of the electric field variation with respect to the temporal variable t . The approximate expression for the magnetic field at location z and the time t now becomes

$$H_y(z, t) \approx H_y(z, t - \Delta t) - \frac{\Delta t}{\Delta l \cdot \mu_{avg}(z)} \left[E_x(z + \frac{\Delta l}{2}, t - \frac{\Delta t}{2}) - E_x(z - \frac{\Delta l}{2}, t - \frac{\Delta t}{2}) \right] \quad (2.23)$$

The above equation can be written in a somewhat different form, using the identity

$$\frac{1}{\mu} = \frac{1}{\mu_0} \frac{1}{\mu_r} = \frac{\sqrt{\epsilon_0}}{\sqrt{\epsilon_0}} \frac{1}{\sqrt{\mu_0}} \frac{1}{\sqrt{\mu_0} \mu_r} = \frac{1}{\sqrt{\mu_0 \epsilon_0}} \frac{1}{\sqrt{\frac{\mu_0}{\epsilon_0}}} \frac{1}{\mu_r} = v_0 \frac{1}{Z_0} \frac{1}{\mu_r} = v_0 Y_0 \frac{1}{\mu_r} \quad (2.24)$$

where the free space velocity of propagation is denoted v_0 , the intrinsic impedance of free space is denoted Z_0 ($Z_0 \approx 377\Omega$), and μ_r denotes relative permittivity. Introducing the grid "propagation" velocity

$$v_{grid} = \frac{\Delta l}{\Delta t} \quad (2.25)$$

we can write the approximate "update" equation for the magnetic field as

$$H_y(z, t) \approx H_y(z, t - \Delta t) - Y_0 \frac{v_0}{v_{grid}} \frac{1}{\mu_{r,avg}(z)} \left[E_x(z + \frac{\Delta l}{2}, t - \frac{\Delta t}{2}) - E_x(z - \frac{\Delta l}{2}, t - \frac{\Delta t}{2}) \right] \quad (2.26)$$

The equation simplifies for the case of non-magnetic media ($\mu_r=1$)

$$H_y(z, t) \approx H_y(z, t - \Delta t) - Y_0 \frac{v_0}{v_{grid}} \left[E_x(z + \frac{\Delta l}{2}, t - \frac{\Delta t}{2}) - E_x(z - \frac{\Delta l}{2}, t - \frac{\Delta t}{2}) \right] \quad (2.27)$$

The last two equations show that the magnetic field H and the electric field E are evaluated at points shifted spatially by $\Delta l/2$, and at instants separated in time by $\Delta t/2$. The relationship between spatial and temporal "samples" of the electric and the magnetic fields is thus the same the samples are shifted with respect to each other by one-half of the sampling interval. This is the essence of the Yee lattice and applies to "sampling" of 2-D and 3-D fields as well. Dual approximate equations for the electric field "updates" can now be derived using the same procedure shown for the magnetic field update equations.

3. Derivation of Electric Field Update Equation

We start with the Maxwell's curl equation for the circulation of the magnetic field

$$\oint_{C_H} H_y(z, t) \vec{x} \cdot d\vec{l}_H = \frac{\partial}{\partial t} \left\{ \iint_{S_H} \epsilon(z) E_x(z, t) \vec{x} \cdot d\vec{s}_H \right\} + \iint_{S_H} \sigma(z) E_x(z, t) \vec{x} \cdot d\vec{s}_H \quad (2.28)$$

The discrete equivalent of the magnetic field circulation will be determined first, using the contour shown below.

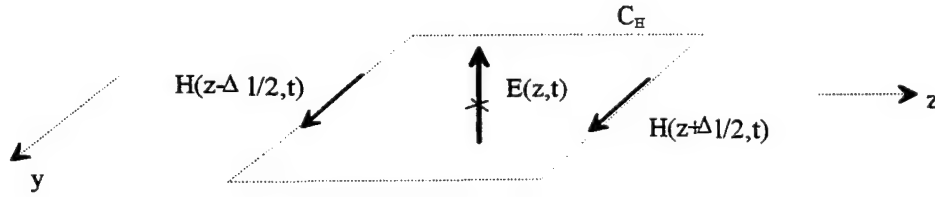


Figure 2.4. A Contour for Magnetic Field Circulation and Electric Flux Calculations.

A local coordinate system (ψ, ζ) can be established, with the origin at the center of the contour. Any point (y', z') within or on the contour C_H (or, equivalently, any point on the surface S_H) can be specified by its local coordinates

$$y' = y + \psi \quad z' = z + \zeta \quad \text{where} \quad -\frac{\Delta l}{2} \leq \psi \leq +\frac{\Delta l}{2} \quad \text{and} \quad -\frac{\Delta l}{2} \leq \zeta \leq +\frac{\Delta l}{2}$$

The circulation of the magnetic field around C_H , assuming counter-clockwise reference direction such that the normal to the surface S_H is in the direction of the electric field $\vec{E}(z, t)$, is therefore given *exactly* by the following simple expression

$$\oint_{C_H} H_y(z + \zeta, t) \vec{y} \cdot d\vec{l}_H = \int_{-\frac{\Delta l}{2}}^{+\frac{\Delta l}{2}} H_y(z - \frac{\Delta l}{2}, t) \vec{y} \cdot d\psi \vec{y} - \int_{-\frac{\Delta l}{2}}^{+\frac{\Delta l}{2}} H_y(z + \frac{\Delta l}{2}, t) \vec{y} \cdot d\psi \vec{y} \quad (2.29)$$

$$\oint_{C_H} H_y(z + \zeta, t) \vec{y} \cdot d\vec{l}_H = [H_y(z - \frac{\Delta l}{2}, t) - H_y(z + \frac{\Delta l}{2}, t)] \cdot \Delta l \quad (2.30)$$

The rate of change of the electric flux through the surface S_H can only be evaluated *approximately*, since the exact way that the electric flux density

$$D(z, t) = \varepsilon(z)H(z, t) \quad (2.31)$$

varies in the z -direction is not known a priori. First we evaluate the flux integrals

$$\iint_{S_H} \varepsilon(z + \zeta) E_x(z + \zeta, t) \vec{x} \cdot d\vec{s}_H = \int_{-\frac{\Delta l}{2}}^{+\frac{\Delta l}{2}} \int_{-\frac{\Delta l}{2}}^{+\frac{\Delta l}{2}} \varepsilon(z + \zeta) E_x(z + \zeta, t) \vec{x} \cdot \vec{x} d\psi d\zeta \quad (2.32)$$

$$\iint_{S_H} \sigma(z + \zeta) E_x(z + \zeta, t) \vec{x} \cdot d\vec{s}_H = \int_{-\frac{\Delta l}{2}}^{+\frac{\Delta l}{2}} \int_{-\frac{\Delta l}{2}}^{+\frac{\Delta l}{2}} \sigma(z + \zeta) E_x(z + \zeta, t) \vec{x} \cdot \vec{x} d\psi d\zeta \quad (2.33)$$

Since the integrands are not functions of the local y -coordinate ψ the surface integrals simplify to line integrals

$$\iint_{S_H} \varepsilon(z + \zeta) E_x(z + \zeta, t) \vec{x} \cdot d\vec{s}_H = \Delta l \int_{-\frac{\Delta l}{2}}^{+\frac{\Delta l}{2}} \varepsilon(z + \zeta) E_x(z + \zeta, t) d\zeta \quad (2.34)$$

$$\iint_{S_H} \sigma(z + \zeta) E_x(z + \zeta, t) \vec{x} \cdot d\vec{s}_H = \Delta l \int_{-\frac{\Delta l}{2}}^{+\frac{\Delta l}{2}} \sigma(z + \zeta) E_x(z + \zeta, t) d\zeta \quad (2.35)$$

Next, we assume that the contour width Δl is small enough such that the electric field $E(z + \zeta, t)$ within the contour may be assumed constant and equal to the value at the contour's center $E(z, t)$. This assumption yields *approximate* expressions for the flux integrals

$$\iint_{S_H} \varepsilon(z + \zeta) E_x(z + \zeta, t) \vec{x} \cdot d\vec{s}_H = \Delta l \cdot E_x(z, t) \cdot \int_{-\frac{\Delta l}{2}}^{+\frac{\Delta l}{2}} \varepsilon(z + \zeta) d\zeta \quad (2.36)$$

$$\iint_{S_H} \sigma(z + \zeta) E_x(z + \zeta, t) \vec{x} \cdot d\vec{s}_H = \Delta l \cdot E_x(z, t) \cdot \int_{-\frac{\Delta l}{2}}^{+\frac{\Delta l}{2}} \sigma(z + \zeta) d\zeta \quad (2.37)$$

or, using the average permittivity and conductivity

$$\iint_{S_H} \varepsilon(z + \zeta) E_x(z + \zeta, t) \vec{x} \cdot d\vec{s}_H = (\Delta l)^2 \cdot \varepsilon_{avg}(z) \cdot E_x(z, t) \quad (2.38)$$

$$\iint_{S_H} \sigma(z + \zeta) E_x(z + \zeta, t) \vec{x} \cdot d\vec{s}_H = (\Delta l)^2 \cdot \sigma_{avg}(z) \cdot E_x(z, t) \quad (2.39)$$

The second curl equation of Maxwell can now be replaced by an approximate equation

$$\left[H_y(z - \frac{\Delta l}{2}, t) - H_y(z + \frac{\Delta l}{2}, t) \right] \cdot \Delta l \approx \frac{\partial}{\partial t} \left\{ [\varepsilon_{avg}(z) E_x(z, t)] (\Delta l)^2 \right\} + (\Delta l)^2 \cdot \sigma_{avg}(z) \cdot E_x(z, t) \quad (2.40)$$

which can be simplified (because of media stationarity) to

$$H_y(z - \frac{\Delta l}{2}, t) - H_y(z + \frac{\Delta l}{2}, t) \approx \varepsilon_{avg}(z) \cdot \Delta l \cdot \frac{\partial}{\partial t} \{ E_x(z, t) \} + \Delta l \cdot \sigma_{avg}(z) \cdot E_x(z, t) \quad (2.41)$$

The approximate equation can be re-written as

$$\frac{\partial}{\partial t} \{ E_x(z, t) \} \approx \frac{1}{\Delta l \cdot \varepsilon_{avg}(z)} \left[H_y(z - \frac{\Delta l}{2}, t) - H_y(z + \frac{\Delta l}{2}, t) \right] - \frac{\sigma_{avg}(z)}{\varepsilon_{avg}(z)} \cdot E_x(z, t) \quad (2.42)$$

The above equation is integrated with respect to time to get an approximate equation for the electric field at the present time t

$$E_x(z, t) \approx \frac{1}{\Delta l \cdot \varepsilon_{avg}(z)} \left[\int_0^t H_y(z - \frac{\Delta l}{2}, \tau) d\tau - \int_0^t H_y(z + \frac{\Delta l}{2}, \tau) d\tau \right] - \frac{\sigma_{avg}(z)}{\varepsilon_{avg}(z)} \int_0^t E_x(z, \tau) d\tau \quad (2.43)$$

A similar equation can be written for the electric field at the same spatial location

but at an earlier time $t - \Delta t$

$$E_x(z, t - \Delta t) \approx \frac{1}{\Delta l \cdot \varepsilon_{avg}(z)} \left[\int_0^{t-\Delta t} H_y(z - \frac{\Delta l}{2}, \tau) d\tau - \int_0^{t-\Delta t} H_y(z + \frac{\Delta l}{2}, \tau) d\tau \right] - \frac{\sigma_{avg}(z)}{\varepsilon_{avg}(z)} \int_0^{t-\Delta t} E_x(z, \tau) d\tau \quad (2.44)$$

Subtracting the two equations we get

$$E_x(z, t) \approx E_x(z, t - \Delta t) + \frac{1}{\Delta l \cdot \varepsilon_{avg}(z)} \left[\int_{t-\Delta t}^t H_y(z - \frac{\Delta l}{2}, \tau) d\tau - \int_{t-\Delta t}^t H_y(z + \frac{\Delta l}{2}, \tau) d\tau \right] - \frac{\sigma_{avg}(z)}{\varepsilon_{avg}(z)} \int_{t-\Delta t}^t E_x(z, \tau) d\tau \quad (2.45)$$

Assuming that the interval Δt is small enough such that the magnetic fields can be assumed approximately constant within Δt and equal to the value at the center of the time interval Δt

$$H(z + \frac{\Delta l}{2}, \tau) \approx H(z + \frac{\Delta l}{2}, t - \frac{\Delta t}{2}) \quad \text{for } t - \Delta t \leq \tau \leq t \quad (2.46)$$

$$H(z - \frac{\Delta l}{2}, \tau) \approx H(z - \frac{\Delta l}{2}, t - \frac{\Delta t}{2}) \quad \text{for } t - \Delta t \leq \tau \leq t \quad (2.47)$$

we get

$$E_x(z, t) \approx E_x(z, t - \Delta t) + \quad (2.48)$$

$$\frac{\Delta t}{\Delta l \cdot \epsilon_{avg}(z)} \left[H_y(z - \frac{\Delta l}{2}, t - \frac{\Delta t}{2}) - H_y(z + \frac{\Delta l}{2}, t - \frac{\Delta t}{2}) \right] - \frac{\sigma_{avg}(z)}{\epsilon_{avg}(z)} \int_{t-\Delta t}^t E_x(z, \tau) d\tau$$

The above equation can be written in a somewhat different form

$$E_x(z, t) \approx E_x(z, t - \Delta t) + \quad (2.49)$$

$$\frac{\Delta t}{\Delta l \cdot \epsilon_{avg}(z)} \left[H_y(z - \frac{\Delta l}{2}, t - \frac{\Delta t}{2}) - H_y(z + \frac{\Delta l}{2}, t - \frac{\Delta t}{2}) \right] - \Delta t \frac{\sigma_{avg}(z)}{\epsilon_{avg}(z)} \left[\frac{1}{\Delta t} \int_{t-\Delta t}^t E_x(z, \tau) d\tau \right]$$

The term in the brackets is recognized as the average value of the electric field within the interval $(t-\Delta t, t)$. The above equation can be written in a more compact form using the identity

$$\frac{1}{\epsilon} = \frac{1}{\epsilon_0} \frac{1}{\epsilon_r} = \frac{\sqrt{\mu_0}}{\sqrt{\mu_0}} \frac{1}{\sqrt{\epsilon_0}} \frac{1}{\sqrt{\epsilon_0}} \frac{1}{\epsilon_r} = \frac{1}{\sqrt{\mu_0 \epsilon_0}} \sqrt{\frac{\mu_0}{\epsilon_0}} \frac{1}{\epsilon_r} = v_0 Z_0 \frac{1}{\epsilon_r} \quad (2.50)$$

where the free space velocity of propagation is denoted v_0 , the intrinsic impedance of free space is denoted Z_0 ($Z_0 \approx 377\Omega$) and ϵ_r denotes relative permittivity. Introducing the grid "propagation" velocity

$$v_{grid} = \frac{\Delta l}{\Delta t} \quad (2.51)$$

we can write the approximate equation for the electric field "updates" as

$$E_x(z, t) \approx E_x(z, t - \Delta t) + \quad (2.52)$$

$$Z_0 \frac{v_0}{v_{grid} \epsilon_{r,avg}(z)} \left\{ H_y(z - \frac{\Delta l}{2}, t - \frac{\Delta t}{2}) - H_y(z + \frac{\Delta l}{2}, t - \frac{\Delta t}{2}) - \Delta l \cdot \sigma_{avg}(z) \left[\frac{1}{\Delta t} \int_{t-\Delta t}^t E_x(z, \tau) d\tau \right] \right\}$$

or

$$E_x(z, t) \approx E_x(z, t - \Delta t) + \quad (2.53)$$

$$Z_0 \frac{v_0}{v_{grid} \epsilon_{r,avg}(z)} \left[H_y(z - \frac{\Delta l}{2}, t - \frac{\Delta t}{2}) - H_y(z + \frac{\Delta l}{2}, t - \frac{\Delta t}{2}) - \Delta l \cdot \sigma_{avg}(z) E_{x,avg(\Delta t)}(z, t) \right]$$

The average of the electric field between $t - \Delta t$ and t , denoted $E_{x,avg(\Delta t)}$ can not be calculated exactly because the exact temporal variation of the electric field is not known a priori. However, assuming a linear variation within Δt interval, the average field is the average of the values at $t - \Delta t$ and t

$$E_{x,avg(\Delta t)}(z, t) \approx \frac{E_x(z, t - \Delta t) + E_x(z, t)}{2} \quad (2.54)$$

Substituting the time-average $E_{x,avg(\Delta t)}(z)$ into the update equation we get

$$E_x(z, t) \approx E_x(z, t - \Delta t) + \quad (2.55)$$

$$Z_0 \frac{v_0}{v_{grid} \epsilon_{r,avg}(z)} \left[H_y(z - \frac{\Delta l}{2}, t - \frac{\Delta t}{2}) - H_y(z + \frac{\Delta l}{2}, t - \frac{\Delta t}{2}) - \Delta l \cdot \sigma_{avg}(z) \cdot \frac{E_x(z, t - \Delta t) + E_x(z, t)}{2} \right]$$

which gives the final equation for the electric field updates as

$$E_x(z, t) \approx \frac{1 - \frac{1}{2} \frac{v_0}{v_{grid}} \frac{Z_0 \cdot \Delta l \cdot \sigma_{avg}(z)}{\epsilon_{r,avg}(z)}}{1 + \frac{1}{2} \frac{v_0}{v_{grid}} \frac{Z_0 \cdot \Delta l \cdot \sigma_{avg}(z)}{\epsilon_{r,avg}(z)}} E_x(z, t - \Delta t) + \quad (2.56)$$

$$\frac{Z_0 \frac{v_0}{v_{grid} \epsilon_{r,avg}(z)}}{1 + \frac{1}{2} \frac{v_0}{v_{grid}} \frac{Z_0 \cdot \Delta l \cdot \sigma_{avg}(z)}{\epsilon_{r,avg}(z)}} \left[H_y(z - \frac{\Delta l}{2}, t - \frac{\Delta t}{2}) - H_y(z + \frac{\Delta l}{2}, t - \frac{\Delta t}{2}) \right]$$

The equation simplifies greatly for the case of non-conductive media ($\sigma=0$)

$$E_x(z, t) \approx E_x(z, t - \Delta t) + Z_0 \frac{v_0}{v_{grid} \epsilon_{r,avg}(z)} \left[H_y(z - \frac{\Delta l}{2}, t - \frac{\Delta t}{2}) - H_y(z + \frac{\Delta l}{2}, t - \frac{\Delta t}{2}) \right] \quad (2.57)$$

In the case of free-space ($\epsilon_r=1$), the equation simplifies further

$$E_x(z, t) \approx E_x(z, t - \Delta t) + Z_0 \frac{v_0}{v_{grid}} \left[H_y(z - \frac{\Delta l}{2}, t - \frac{\Delta t}{2}) - H_y(z + \frac{\Delta l}{2}, t - \frac{\Delta t}{2}) \right] \quad (2.58)$$

These electric field "update" equations also show that the electric field E and the magnetic field H should be evaluated at points shifted spatially by $\Delta l/2$, and at instants separated in time by $\Delta t/2$.

B. TRANSPARENT GRID TERMINATION IN 1-D

1. 1-D Grid

The electric and magnetic field update equations have been derived using local coordinate systems, with origins at the centers of the magnetic and electric contours, respectively. These equations now need to be "converted" to a global coordinate system, that is to the grid of equi-distant sampling points along the z -axis (for 1-D). We will assume that our domain ("grid") is a line segment of length L . The fields are sampled using a spatial step $\Delta l = L/N_z$. The electric and magnetic field sample locations are "interleaved", as shown below for $N_z = 5$. The first and the last spatial sampling points form the grid edges. The spatial edge samples can be either electric field samples or magnetic field samples. Although the selection of the field for the grid edges makes no difference in principle, we will in general use electric field samples for the grid edges.

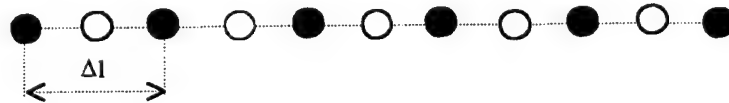


Figure 2.5. 1-D E-field (black) and H-field (white) nodes.

We would evaluate the fields within the grid first, since a known incident field propagates from the center. *Electric* field update equations can now be "converted" to electric field grid equations by replacing the variables z and t with the grid coordinates of the electric field spatial and temporal sampling points

$$z \rightarrow k\Delta l, k = 0, 1 \dots N_z \quad \text{and} \quad t \rightarrow n\Delta t, n = 0, 1 \dots N_t$$

The electric field update equation for non-conductive media is

$$E_x(k\Delta l, n\Delta t) \approx E_x(k\Delta l, n\Delta t - \Delta t) \quad (2.59)$$

$$Z_0 \frac{v_0}{v_{grid} \epsilon_{r,avg}(k\Delta l)} \left[H_y(k\Delta l - \frac{\Delta l}{2}, n\Delta t - \frac{\Delta t}{2}) - H_y(k\Delta l + \frac{\Delta l}{2}, n\Delta t - \frac{\Delta t}{2}) \right]$$

The notation can be simplified further by omitting the common Δl and Δt terms, and using a superscript for the index of the temporal sampling point

$$E_x^n(k) \approx E_x^{n-1}(k) + Z_0 \left(\frac{v_0}{v_{grid}} \right) \frac{1}{\epsilon_{r,avg}(k)} \left[H_y^{n-\frac{1}{2}}(k - \frac{1}{2}) - H_y^{n-\frac{1}{2}}(k + \frac{1}{2}) \right] \quad (2.60)$$

The electric field grid equation for conductive media, using the same notation as above, is

$$E_x^n(k) \approx \frac{1 - \frac{1}{2} \left(\frac{v_0}{v_{grid}} \right) \frac{Z_0 \cdot \Delta l \cdot \sigma_{avg}(k)}{\epsilon_{r,avg}(k)}}{1 + \frac{1}{2} \left(\frac{v_0}{v_{grid}} \right) \frac{Z_0 \cdot \Delta l \cdot \sigma_{avg}(k)}{\epsilon_{r,avg}(k)}} E_x^{n-1}(k) + \quad (2.61)$$

$$\frac{Z_0 \left(\frac{v_0}{v_{grid}} \right) \frac{1}{\epsilon_{r,avg}(k)}}{1 + \frac{1}{2} \left(\frac{v_0}{v_{grid}} \right) \frac{Z_0 \cdot \Delta l \cdot \sigma_{avg}(k)}{\epsilon_{r,avg}(k)}} \left[H_y^{n-\frac{1}{2}}(k - \frac{1}{2}) - H_y^{n-\frac{1}{2}}(k + \frac{1}{2}) \right]$$

Finally, the free-space electric field grid equation is

$$E_x^n(k) \approx E_x^{n-1}(k) + Z_0 \left(\frac{v_0}{v_{grid}} \right) \left[H_y^{n-\frac{1}{2}}(k - \frac{1}{2}) - H_y^{n-\frac{1}{2}}(k + \frac{1}{2}) \right] \quad (2.62)$$

Similarly, *magnetic* field update equations can be converted to magnetic field grid equations by replacing the variables z and t with the grid coordinates of the magnetic field spatial and temporal sampling points

$$z \rightarrow (k + \frac{1}{2})\Delta l, k = 0, 1 \dots N_z - 1 \quad \text{and} \quad t \rightarrow (n + \frac{1}{2})\Delta t, n = 0, 1 \dots N_t - 1$$

The magnetic field grid equation, using the same notation as for the electric field grid equation, is

$$H_y^{n+\frac{1}{2}}(k + \frac{1}{2}) \approx H_y^{n-\frac{1}{2}}(k + \frac{1}{2}) - Y_0 \left(\frac{v_0}{v_{grid}} \right) \frac{1}{\mu_{r,avg}(k + \frac{1}{2})} [E_x^n(k+1) - E_x^n(k)] \quad (2.63)$$

or, for non-magnetic media

$$H_y^{n+\frac{1}{2}}(k + \frac{1}{2}) \approx H_y^{n-\frac{1}{2}}(k + \frac{1}{2}) - Y_0 \left(\frac{v_0}{v_{grid}} \right) [E_x^n(k+1) - E_x^n(k)] \quad (2.64)$$

The electric and magnetic field grid equations have the following general form

$$E_x^{new} = C_{E1} E_x^{old} + C_{E2} \nabla H_y^{old} \quad (2.65)$$

$$H_y^{new} = C_{H1} H_y^{old} + C_{H2} \nabla E_x^{old} \quad (2.66)$$

where C's are constants (real numbers) that depend on the media properties and the velocity ratio v_0/v_{grid} , and "del" operator represents the spatial derivative (gradient). This general form of the grid equations can be interpreted as follows: *"the new value of E/H field at a grid node is equal to the weighted sum of the old value of the E/H field at the same node and the spatial variation of the old H/E field between the two nearest-neighbor nodes."*

2. Grid Termination

The grid equations derived above are valid for all the nodes *except* for the nodes on the grid edges. The reason is that the grid edge nodes have only one neighbor node instead of two like any node that is not on the grid edge. The edge nodes with a single "neighbor" thus need to have equations different than the equations we have derived for the "non-edge" grid nodes with two "neighbors". TGT requirement is conceptually very simple and straightforward to implement in 1-D. To that effect we will use the concept of

a multiport (a two-port in 1-D). It does not matter, in principle, whether the edge node is an E field or an H field node. We will assume that the edge node for the two-port model is an E field node. The input port of the two-port will be the nearest node "of the same kind". Since we have assumed an E field node for the output port, the input port will be the nearest E field node inside the grid. We could have also selected an E field node as the output port and the nearest H-field node as the input port. However, the selection of the same kind of node for both input and output ports has the advantage that the TGT results obtained in this manner can be also used to solve the wave equation (a second order partial differential equation) that has only one field as the variable and the grid with only one kind of nodes. The figure below shows the two ports for the two (1-D) grid edge nodes.

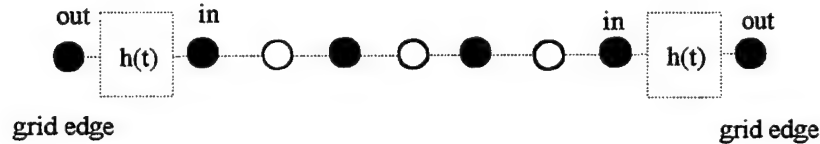


Figure 2.6. Modeling 1-D Grid Terminations as Two-ports.

The fields at the output ports $E(0,t)$ and $E(L,t)$ can be expressed as convolutions of the fields at the input ports $E(\Delta l,t)$ and $E(L-\Delta l,t)$ and the two port impulse response $h(t)$. (The impulse responses for the two-ports on the left and on the right edges are identical, by symmetry).

$$E_x(0,t) = E_x(\Delta l,t) * h(t) = \int_0^t E_x(\Delta l,\tau) h(t-\tau) d\tau \quad (2.67)$$

$$E_x(L,t) = E_x(L-\Delta l,t) * h(t) = \int_0^t E_x(L-\Delta l,\tau) h(t-\tau) d\tau \quad (2.68)$$

The discretized forms of these equations, involving samples of the fields at $t=n\Delta t$, are the discretized convolutions

$$E_x^n(0) = \sum_{p=0}^{p=n} E_x^p(1) \cdot h^{n-p} \quad (2.69)$$

$$E_x^n(N_z) = \sum_{p=0}^{p=n} E_x^p(N_z - 1) \cdot h^{n-p} \quad (2.70)$$

The convolution equations express the fields at the edges as weighted sums of the time histories of the fields "just inside" the grid. In that respect they are equations of the same type as the equations for the non-edge grid nodes, except that they involve, in general, summations with more terms. However, the impulse response $h(t)$, as will be shown, is a rapidly converging (to zero) function which reduces the number of relevant terms in the convolution sum. The impulse response $h(t)$ (actually its "sampled" form h^n) needs to be determined only once, for a selected grid velocity $v_{\text{grid}} = \Delta l / \Delta t$. The issue remains how to determine the impulse response? The discretized impulse response h^n will be determined using the discrete equivalent of the Dirac delta function which we will denote as δ^n . Since there are two grid edges and two input ports (Fig. 2.6) one input port will be set to zero and δ^n will be applied to the other input port. Since, in 1-D, there is only one h^n to determine we will set $E_x(\Delta l, t)$ to zero and apply the Dirac delta function as $E_x(L - \Delta l, t)$

$$E_x^n(N_z - 1) = \delta^n \quad (2.71)$$

$$E_x^n(1) = 0 \quad (2.72)$$

This is depicted in Figure 2.7. Note that the impulse response h^n is observed at $z = L$ and that the grid extends, theoretically, to infinity *past* the observation point $z = L$. Since $\delta^n = 0$ for $n > 0$, the grid to the left of the $(L - \Delta l)$ node is effectively isolated from

the observation point at L . This means that, to find h ", we may just consider the grid to the right of the $L-\Delta l$ node, as shown below.

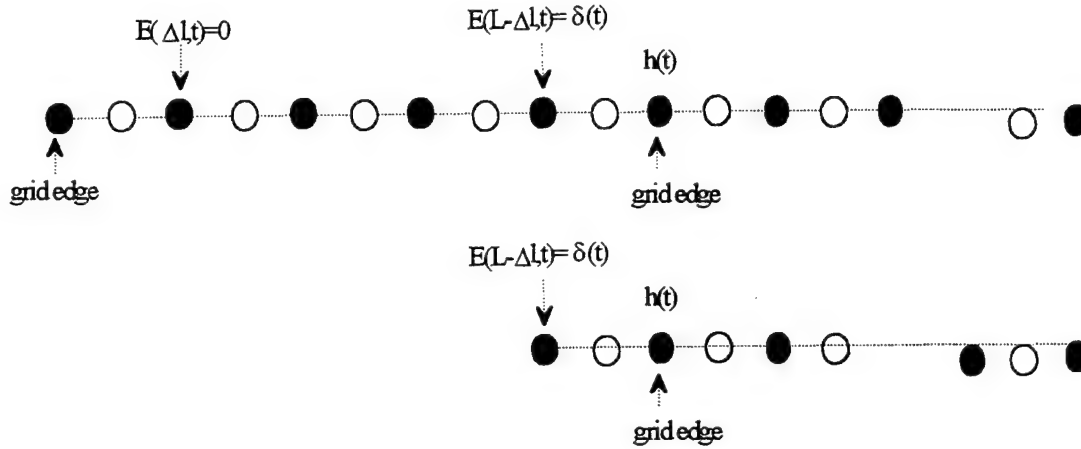


Figure 2.7. Determining the Impulse Response.

The impulse response needs to be obtained as if the grid were not terminated at all to the right of the observation point at $z = L$. If the grid were terminated, the "reflectionless" termination condition would be needed and this is exactly what we do not have and are trying to find. A grid extending to infinity does not require a termination and thus "avoids" the termination problem. Although it is not possible, in practice, to extend the grid to infinity, the grid can be made large enough such that any "reflections" off the new grid edge would have arrived *after* the impulse response has "converged" to a small selected value that we consider as "zero". The time it takes the impulse to "propagate" to this new grid edge and back to the observation point is

$$T_d = \frac{2D}{v_{grid}} = \frac{2N_D \Delta l}{\frac{\Delta l}{\Delta t}} = 2N_D \Delta t \quad (2.73)$$

where D is the distance between the observation point and the new grid's edge and N_D is the number of nodes between the observation point and the new grid's edge. The duration of the impulse response h^n that will not be "corrupted" by the reflections will be $2N_D$. Finally, it is assumed that the space outside the grid is free-space, and the grid equations for the electric and magnetic fields will thus be the free-space equations

$$E_x^n(k) = E_x^{n-1}(k) + Z_0 \left(\frac{v_0}{v_{grid}} \right) \left[H_y^{n-\frac{1}{2}}(k - \frac{1}{2}) - H_y^{n-\frac{1}{2}}(k + \frac{1}{2}) \right] \quad (2.74)$$

$$H_y^{n+\frac{1}{2}}(k + \frac{1}{2}) = H_y^{n-\frac{1}{2}}(k + \frac{1}{2}) + Y_0 \left(\frac{v_0}{v_{grid}} \right) [E_x^n(k) - E_x^n(k+1)] \quad (2.75)$$

The order of the terms in the brackets for the magnetic field equation has been reversed, such that the electric and magnetic field grid equations will have the same sign (+) in front of the brackets. The above equations can be also written in a different form, to reduce the number of multiplication's that would need to be done at each time step.

Multiplying the magnetic field equation by Z_0 we get

$$Z_0 H_y^{n+\frac{1}{2}}(k + \frac{1}{2}) = Z_0 H_y^{n-\frac{1}{2}}(k + \frac{1}{2}) + \left(\frac{v_0}{v_{grid}} \right) [E_x^n(k) - E_x^n(k+1)] \quad (2.76)$$

An auxiliary variable h_y may be introduced

$$h_y = Z_0 H_y \quad (2.77)$$

and the electric and magnetic field grid equations can be written using h_y instead of H_y

$$E_x^n(k) = E_x^{n-1}(k) + \left(\frac{v_0}{v_{grid}} \right) \left[h_y^{n-\frac{1}{2}}(k - \frac{1}{2}) - h_y^{n-\frac{1}{2}}(k + \frac{1}{2}) \right] \quad (2.78)$$

$$h_y^{n+\frac{1}{2}}(k + \frac{1}{2}) = h_y^{n-\frac{1}{2}}(k + \frac{1}{2}) + \left(\frac{v_0}{v_{grid}} \right) [E_x^n(k) - E_x^n(k+1)] \quad (2.79)$$

The equations for the electric field (E_x) and for the magnetic field multiplied by Z_0 ($Z_0 H_y$) have identical forms, involving only one parameter, the velocity ratio v_0/v_{grid} . The boundary impulse response h^n , to be obtained using these equations, will thus be valid only

for a selected velocity ratio or, equivalently for the selected grid velocity $v_{\text{grid}} = \Delta l / \Delta t$. The boundary impulse response h^n , obtained using the equations for $v_0/v_{\text{grid}} = 1$, is shown below. Note that the plotting program interpolates linearly the values between the sampling points $n\Delta t$.

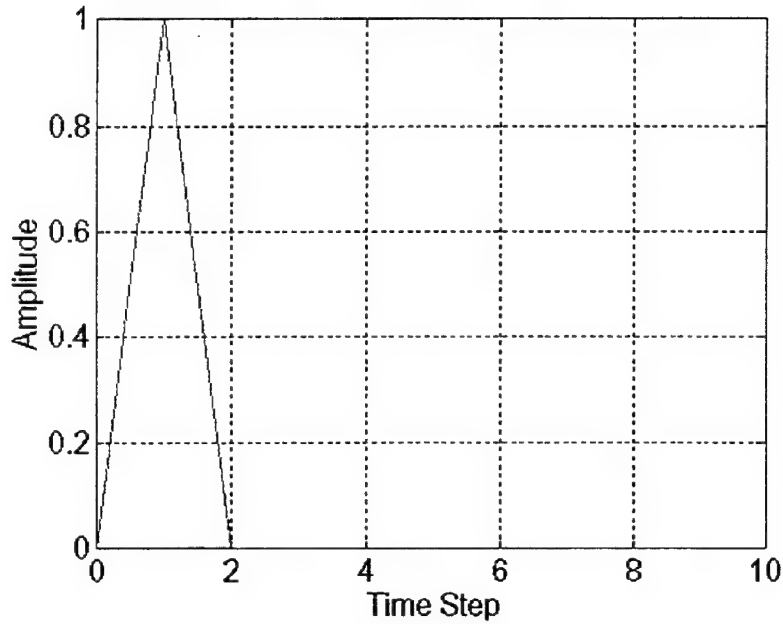


Figure 2.8. Boundary Impulse Response.

The boundary impulse response for 1-D is very simple

$$h^n = \delta^1 \quad (2.80)$$

The impulse response is non-zero only for $n = 1$ where it has the value of 1, which is a delta impulse delayed by Δt and may also be written as

$$h(t) = \delta(t - \Delta t) \quad (2.81)$$

We can now write the grid equations for 1-D grid edges as follows

$$E_x^n(0) = \sum_{p=0}^{p=n} E_x^p(1) \cdot h^{n-p} = E_x^{n-1}(1) \cdot h^1 = E_x^{n-1}(1) \quad (2.82)$$

$$E_x^n(N_z) = \sum_{p=0}^{p=n} E_x^p(N_z - 1) \cdot h^{n-p} = E_x^{n-1}(N_z - 1) \cdot h^1 = E_x^{n-1}(N_z - 1) \quad (2.83)$$

The above equations state that the fields at the grid edges are updated by simply taking the previous values of their nearest neighbors inside the grid. Although the boundary impulse responses are not so simple for 2-D and 3-D, they can be determined using essentially the same procedure as shown for 1-D.

C. 1-D TGT RESULTS

We apply the geometrical model shown in Figure 2.6. The nodes on the edges are E field nodes. The source is the electric field at the center node and the source waveform is a unit amplitude delta pulse. This represents, in 1-D, a uniform plane wave propagating from the center into +z and -z directions. By applying the "standard" FD-TD equation for the nodes inside the grid and the TGT equations for the grid edges we obtain the power within the grid as a function of time as shown below. It is clear that the power within the grid is constant until the wave has "left" the grid when it falls to zero abruptly. The 1-D grid with TGT termination thus behaves like an "ideal" grid.

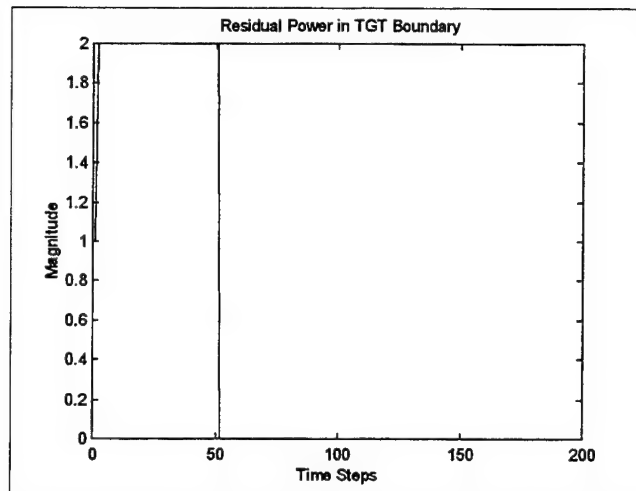


Figure 2.9. Residual Power for TGT.

We will next compare this result with that for an "infinite" grid. Note that the power is calculated within the same grid region as in the previous figure.

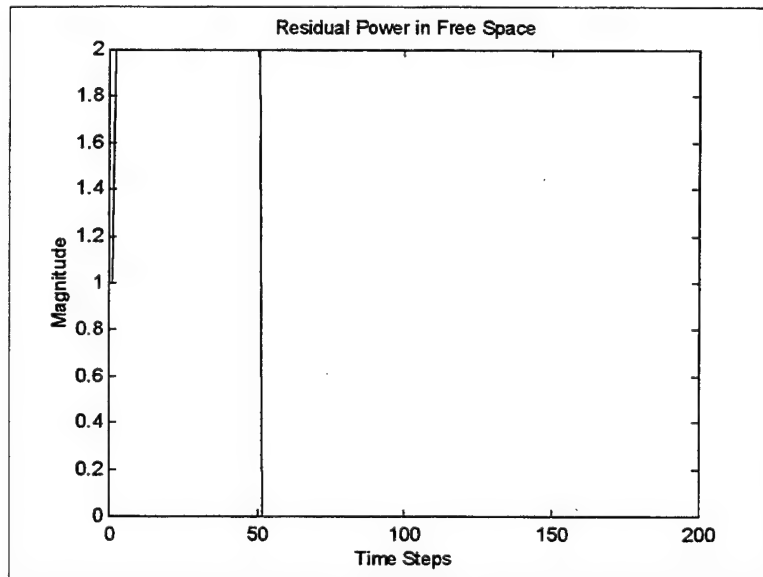


Figure 2.10. Residual Power for an "Infinite" Grid.

Subtracting the residual powers for the TGT and the "infinite" boundary we get the result shown below. Note that the TGT boundary for 1-D gives the same result as an infinite grid would.

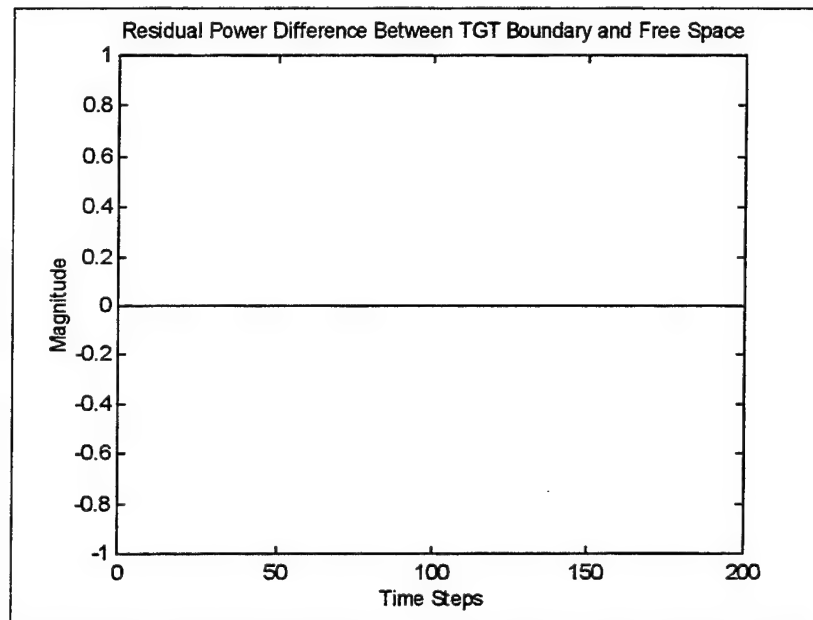


Figure 2.11. Residual Power Difference for TGT and an Infinite Grid.

III. ANALYSIS OF TGT FOR 2-D FDTD

A. FD-TD FORMULATION IN 2-D

1. FD-TD Equations in 2-D

The electromagnetic fields and the media parameters in 2-D problems do not vary with one spatial coordinate. We will denote this coordinate as z . The field invariance with the z -coordinate can be mathematically expressed as

$$\frac{\partial \vec{E}}{\partial z} = 0 \quad \text{and} \quad \frac{\partial \vec{H}}{\partial z} = 0 \quad (3.1)$$

The electric and magnetic fields will thus be functions of the spatial coordinates x and y , and time t . The media will be assumed stationary. An arbitrary 2-D electromagnetic field can be expressed as a linear combination (superposition) of Transverse Electric (TE) and Transverse Magnetic fields [Ref 5]. The TE_z field components are E_x , E_y , and H_z

$$\vec{E}_{TE}(x, y, t) = E_x(x, y, t) \vec{x} + E_y(x, y, t) \vec{y} \quad (3.2)$$

$$\vec{H}_{TE}(x, y, t) = H_z(x, y, t) \vec{z} \quad (3.3)$$

and a TE_z field can be represented as shown below (the z -axis direction is out of the plane of the paper).

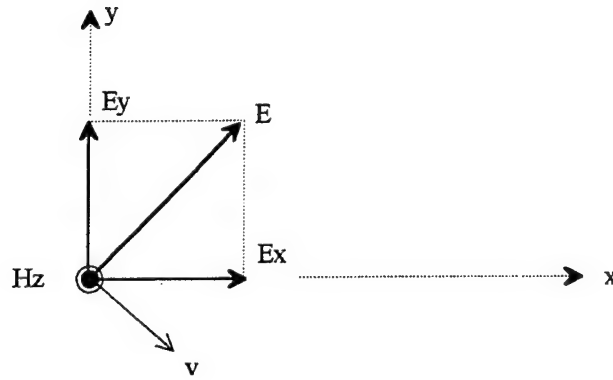


Figure 3.1. TE_z Field.

The direction of propagation is indicated by the propagation velocity vector \vec{v} . The unit vector in the direction of propagation and the electric and magnetic field vectors form a triplet of mutually orthogonal vectors. The "dual" TM_z field has the components H_x , H_y , and E_z

$$\vec{H}_{TM}(x, y, t) = H_x(x, y, t) \vec{x} + H_y(x, y, t) \vec{y} \quad (3.4)$$

$$\vec{E}_{TM}(x, y, t) = E_z(x, y, t) \vec{z} \quad (3.5)$$

as shown below.

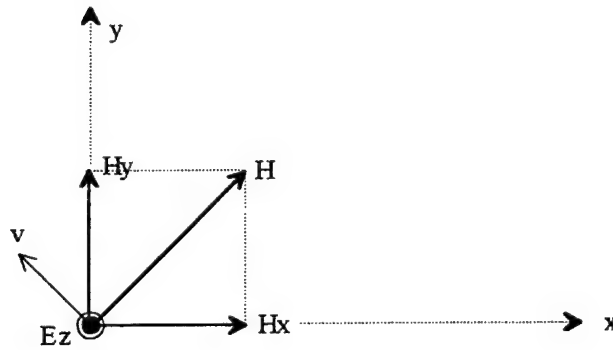


Figure 3.2. TM_z Field.

Our objective is to determine the discretized forms of Maxwell's curl equations in the integral form for TE_z fields

$$\oint_{C_E} \left[E_x(x, y, t) \vec{x} + E_y(x, y, t) \vec{y} \right] \cdot d\vec{l}_E = -\frac{\partial}{\partial t} \left\{ \iint_{S_E} \mu(x, y) H_z(x, y, t) \vec{z} \cdot d\vec{s}_E \right\} \quad (3.6)$$

$$\oint_{C_H} \left[H_z(x, y, t) \vec{z} \right] \cdot d\vec{l}_H = \frac{\partial}{\partial t} \left\{ \iint_{S_H} \varepsilon(x, y) \left[E_x(x, y, t) \vec{x} + E_y(x, y, t) \vec{y} \right] \cdot d\vec{s}_H \right\} + \quad (3.7)$$

$$+ \iint_{S_H} \sigma(x, y) \left[E_x(x, y, t) \vec{x} + E_y(x, y, t) \vec{y} \right] \cdot d\vec{s}_H$$

and for TM_z fields

$$\oint_{C_E} \left[E_z(x, y, t) \vec{z} \right] \cdot d\vec{l}_E = -\frac{\partial}{\partial t} \left\{ \iint_{S_E} \mu(x, y) \left[H_x(x, y, t) \vec{x} + H_y(x, y, t) \vec{y} \right] \cdot d\vec{s}_E \right\} \quad (3.8)$$

$$\oint_{C_H} \left[H_x(x, y, t) \vec{x} + H_y(x, y, t) \vec{y} \right] \cdot d\vec{l}_H = \quad (3.9)$$

$$\frac{\partial}{\partial t} \left\{ \iint_{S_H} \varepsilon(x, y) \left[E_z(x, y, t) \vec{z} \right] \cdot d\vec{s}_H \right\} + \iint_{S_H} \sigma(x, y) \left[E_z(x, y, t) \vec{z} \right] \cdot d\vec{s}_H$$

Note that the the second curl equations do not have the source current terms, since it has been assumed that there were no source currents in the domain of interest. The contours of integration for the electric and the magnetic field circulations are, in general, different and are thus labeled C_E for an electric field contour and C_H for a magnetic field contour. Similarly, the surfaces associated with the contours are labeled S_E for the magnetic flux and S_H for the electric flux. The electric and magnetic field contours for a TE_z field are shown below.

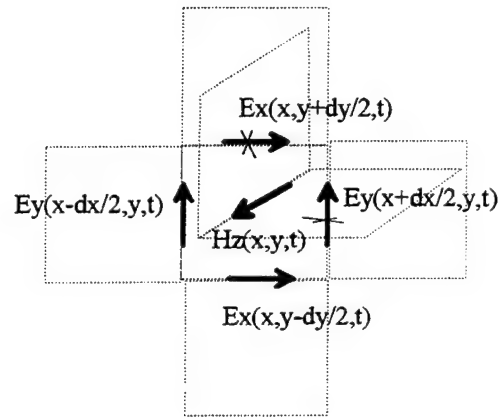


Figure 3.3. Contours for TE_z Electric and Magnetic Field Circulations and Fluxes.

The electric field contours C_E and the magnetic field contours C_H are square (Δl by Δl) contours, but in orthogonal planes. The C_E contours are in the xy -plane, while the C_H contours are in the yz -plane. The contours can be compared to links of a (2-D) chain fence, evoking the idea of electric and magnetic field linkage in two orthogonal directions. The "dual" C_E and C_H contours for a TM_z field are shown below

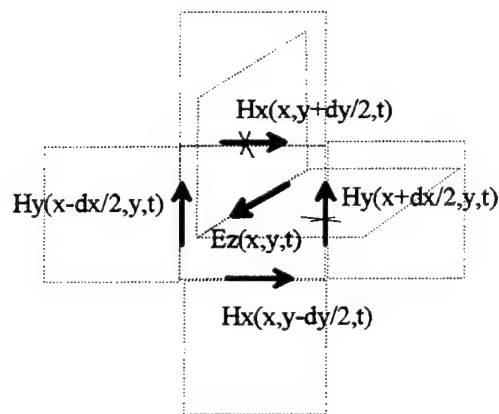


Figure 3.4. Contours for TM_z Electric and Magnetic Field Circulations and Fluxes.

The electric and magnetic contours and their associated surfaces will be used to discretize Maxwell's curl equations.

2. Derivation of TE_z Magnetic Field Update Equation

The discrete equivalent of the TE_z electric field circulation will be determined next.

A contour C_E is shown below

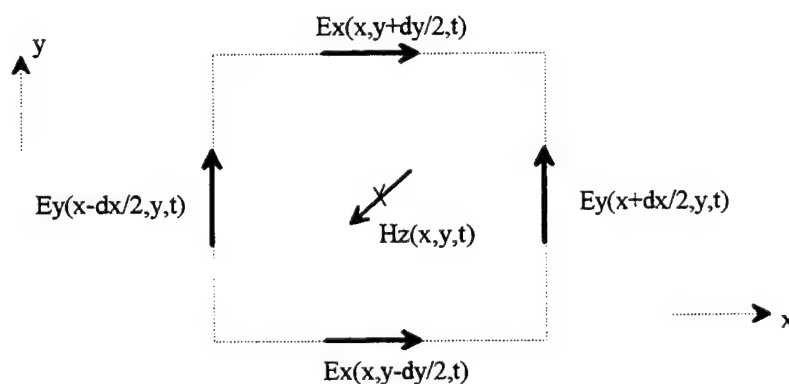


Figure 3.5. A Contour for TE_z Electric Field Circulation and Magnetic Flux Calculations.

The center of the surface S_E is assumed to have the coordinates (x, y) . We will assume a uniform grid with $\Delta x = \Delta y = \Delta l$. A local coordinate system (ξ, ψ) will be established, with the origin at the center of the contour such that any point (x', y') within or on the contour C_E can be specified by its local coordinates ξ and ψ

$$x' = x + \xi \quad y' = y + \psi \quad \text{where} \quad -\frac{\Delta l}{2} \leq \xi \leq +\frac{\Delta l}{2} \quad \text{and} \quad -\frac{\Delta l}{2} \leq \psi \leq +\frac{\Delta l}{2}$$

The local coordinates will be used in evaluation of the line and surface integrals that constitute the integral forms of Maxwell's equations. The circulation of the electric field around the electric field contour C_E , assuming counter-clockwise reference direction such that the normal to the surface S_E is in the direction of the magnetic field $\vec{H}(x, y, t)$,

can be evaluated *approximately*, assuming that the electric fields are constant over the length Δl , along the edges of the $(\Delta l \text{ by } \Delta l)$ square contour

$$\oint_{C_E} \left[E_x(x', y', t) \vec{x} + E_y(x', y', t) \vec{y} \right] \cdot d\vec{l}_E \approx \left[E_x(x, y - \frac{\Delta l}{2}, t) + E_y(x + \frac{\Delta l}{2}, y, t) - E_x(x, y + \frac{\Delta l}{2}, t) - E_y(x - \frac{\Delta l}{2}, y, t) \right] \Delta l \quad (3.10)$$

The magnetic flux through the surface S_E can be calculated using the local coordinates

$$\iint_{S_E} \mu(x', y') H_z(x', y', t) \vec{z} \cdot d\vec{s}_E = \int_{-\frac{\Delta l}{2}}^{+\frac{\Delta l}{2}} \int_{-\frac{\Delta l}{2}}^{+\frac{\Delta l}{2}} \mu(x + \xi, y + \psi) H_z(x + \xi, y + \psi, t) \vec{z} \cdot \vec{z} d\xi d\psi \quad (3.11)$$

There are infinitely many ways to model the variation of the magnetic flux density with the local coordinates ξ and ψ within the contour. We first need to postulate a certain variation of the magnetic field with ξ and ψ such that the integral can be evaluated over S_E . The simplest model assumes that the contour width Δl is small enough such that the magnetic field $H(x + \xi, y + \psi, t)$ within the contour may be assumed constant and equal to the value at the contour's center $H(x, y, t)$.

$$H_z(x + \xi, y + \psi, t) \approx H_z(x, y, t) \quad (3.12)$$

This is equivalent to using a piece-wise constant or 2-D "pulse" expansion approximation of the actual magnetic field variation with the z-coordinate. The above assumption allows that magnetic field, although constant within a contour, can change from one contour to an other. This yields an *approximate* expression for the magnetic flux

$$\iint_{S_E} \mu(x', y') H_z(x', y', t) \vec{z} \cdot d\vec{s}_E \approx H_z(x, y, t) \cdot \int_{-\frac{\Delta l}{2}}^{+\frac{\Delta l}{2}} \int_{-\frac{\Delta l}{2}}^{+\frac{\Delta l}{2}} \mu(x + \xi, y + \psi) d\xi d\psi \quad (3.13)$$

The integral of the permeability $\mu(x + \xi, y + \psi)$ can be re-written in the following manner

$$\int_{-\frac{\Delta l}{2}}^{+\frac{\Delta l}{2}} \int_{-\frac{\Delta l}{2}}^{+\frac{\Delta l}{2}} \mu(x+\xi, y+\psi) d\xi d\psi = (\Delta l)^2 \cdot \left[\frac{1}{(\Delta l)^2} \int_{-\frac{\Delta l}{2}}^{+\frac{\Delta l}{2}} \int_{-\frac{\Delta l}{2}}^{+\frac{\Delta l}{2}} \mu(x+\xi, y+\psi) d\xi d\psi \right] \quad (3.14)$$

The term in the brackets is recognized as the *average* permeability μ_{avg} within the contour C_E

$$\mu_{avg}(x, y) = \frac{1}{(\Delta l)^2} \int_{-\frac{\Delta l}{2}}^{+\frac{\Delta l}{2}} \int_{-\frac{\Delta l}{2}}^{+\frac{\Delta l}{2}} \mu(x+\xi, y+\psi) d\xi d\psi \quad (3.15)$$

The approximate expression for the magnetic flux through S_E can now be written using the average permeability as

$$\iint_{S_E} \mu(x', y') H_z(x', y', t) \vec{z} \cdot d\vec{s}_E \approx (\Delta l)^2 \mu_{avg}(x, y) H_z(x, y, t) \quad (3.16)$$

Again, this approximate expression resulted from the piece-wise constant approximation of the magnetic field with respect to x and y-coordinates. The main advantage of the piece-wise constant expansion employed above is its simplicity. Better accuracy can be achieved by using more involved models for the field variation with x and y, but at the expense of increasing the computational time. The first curl equation of Maxwell can now be replaced by an approximate equation

$$\left[E_x(x, y - \frac{\Delta l}{2}, t) + E_y(x + \frac{\Delta l}{2}, y, t) - E_x(x, y + \frac{\Delta l}{2}, t) - E_y(x - \frac{\Delta l}{2}, y, t) \right] \cdot \Delta l \approx \quad (3.17)$$

$$-\frac{\partial}{\partial t} \{ [\mu_{avg}(x, y) H_z(x, y, t)] (\Delta l)^2 \}$$

which can be simplified as below because of media stationarity

$$E_x(x, y - \frac{\Delta l}{2}, t) + E_y(x + \frac{\Delta l}{2}, y, t) - E_x(x, y + \frac{\Delta l}{2}, t) - E_y(x - \frac{\Delta l}{2}, y, t) \approx \quad (3.18)$$

$$-\frac{\partial}{\partial t} \{ H_z(x, y, t) \} \cdot \Delta l \cdot \mu_{avg}(x, y)$$

This equation can also be re-written as

$$\frac{\partial}{\partial t} \{ H_z(x, y, t) \} \quad (3.19)$$

$$\frac{-1}{\Delta l \cdot \mu_{avg}(x, y)} \left[E_x(x, y - \frac{\Delta l}{2}, t) + E_y(x + \frac{\Delta l}{2}, y, t) - E_x(x, y + \frac{\Delta l}{2}, t) - E_y(x - \frac{\Delta l}{2}, y, t) \right]$$

The time derivative operator in the above equation is typically "replaced" by the finite difference approximation. However, just like in 1-D, we present an alternate approach, such that the approximation of the field time variation is shown to be analogous to the approximations already introduced for the field spatial variation. The above equation is integrated with respect to time to get an approximate equation for the magnetic field at the present time t

$$H_z(x, y, t) \approx \frac{-1}{\Delta l \cdot \mu_{avg}(x, y)} \times \quad (3.20)$$

$$\left[\int_0^t E_x(x, y - \frac{\Delta l}{2}, \tau) d\tau - \int_0^t E_x(x, y + \frac{\Delta l}{2}, \tau) d\tau + \int_0^t E_y(x + \frac{\Delta l}{2}, y, \tau) d\tau - \int_0^t E_y(x - \frac{\Delta l}{2}, y, \tau) d\tau \right]$$

A similar integral equation can be written for the magnetic field at the same spatial location but at an earlier time $t - \Delta t$

$$H_z(x, y, t - \Delta t) \approx \frac{-1}{\Delta l \cdot \mu_{avg}(x, y)} \times \quad (3.21)$$

$$\left[\int_0^{t-\Delta t} E_x(x, y - \frac{\Delta l}{2}, \tau) d\tau - \int_0^{t-\Delta t} E_x(x, y + \frac{\Delta l}{2}, \tau) d\tau + \int_0^{t-\Delta t} E_y(x + \frac{\Delta l}{2}, y, \tau) d\tau - \int_0^{t-\Delta t} E_y(x - \frac{\Delta l}{2}, y, \tau) d\tau \right]$$

Subtracting the two equations we get

$$H_z(x, y, t) \approx H_z(x, y, t - \Delta t) - \frac{1}{\Delta l \cdot \mu_{avg}(x, y)} \times \quad (3.22)$$

$$\left[\int_{t-\Delta t}^t E_x(x, y - \frac{\Delta l}{2}, \tau) d\tau - \int_{t-\Delta t}^t E_x(x, y + \frac{\Delta l}{2}, \tau) d\tau + \int_{t-\Delta t}^t E_y(x + \frac{\Delta l}{2}, y, \tau) d\tau - \int_{t-\Delta t}^t E_y(x - \frac{\Delta l}{2}, y, \tau) d\tau \right]$$

The integrals on the right-hand side can not be evaluated exactly, because the exact temporal variation of the electric fields within the Δt interval prior to t is generally not known. However, the integrals can be evaluated approximately by assuming a certain variation of the electric field with the temporal variable τ . The simplest approach, consistent with the assumptions made for the field spatial variation, would be to assume that the interval Δt is small enough such that the electric field can be assumed

approximately constant within Δt and equal to the value at the center of the time interval

$(t-\Delta t, t)$

$$E_x(x, y - \frac{\Delta l}{2}, \tau) \approx E_x(x, y - \frac{\Delta l}{2}, t - \frac{\Delta t}{2}) \quad \text{for } t - \Delta t \leq \tau \leq t \quad (3.23)$$

$$E_x(x, y + \frac{\Delta l}{2}, \tau) \approx E_x(x, y + \frac{\Delta l}{2}, t - \frac{\Delta t}{2}) \quad \text{for } t - \Delta t \leq \tau \leq t \quad (3.24)$$

$$E_y(x - \frac{\Delta l}{2}, y, \tau) \approx E_y(x - \frac{\Delta l}{2}, y, t - \frac{\Delta t}{2}) \quad \text{for } t - \Delta t \leq \tau \leq t \quad (3.25)$$

$$E_y(x + \frac{\Delta l}{2}, y, \tau) \approx E_y(x + \frac{\Delta l}{2}, y, t - \frac{\Delta t}{2}) \quad \text{for } t - \Delta t \leq \tau \leq t \quad (3.26)$$

The above represents a piece-wise constant approximation of the electric field variation with respect to the temporal variable t . The approximate expression for the magnetic field at location (x, y) and at the time t now becomes

$$H_z(x, y, t) \approx H_z(x, y, t - \Delta t) - \frac{\Delta t}{\Delta l \cdot \mu_{avg}(x, y)} \times \quad (3.27)$$

$$\left[E_x(x, y - \frac{\Delta l}{2}, t - \frac{\Delta t}{2}) - E_x(x, y + \frac{\Delta l}{2}, t - \frac{\Delta t}{2}) + E_y(x + \frac{\Delta l}{2}, y, t - \frac{\Delta t}{2}) - E_y(x - \frac{\Delta l}{2}, y, t - \frac{\Delta t}{2}) \right]$$

The above equation can be written in a somewhat different form, using the identity

$$\frac{1}{\mu} = \frac{1}{\mu_0 \mu_r} = \frac{\sqrt{\epsilon_0}}{\sqrt{\epsilon_0}} \frac{1}{\sqrt{\mu_0} \sqrt{\mu_0}} \frac{1}{\mu_r} = \frac{1}{\sqrt{\mu_0 \epsilon_0}} \frac{1}{\sqrt{\frac{\mu_0}{\epsilon_0}}} \frac{1}{\mu_r} = v_0 \frac{1}{Z_0} \frac{1}{\mu_r} = v_0 Y_0 \frac{1}{\mu_r} \quad (3.28)$$

where the free space velocity of propagation is denoted v_0 , the intrinsic impedance of free space is denoted Z_0 ($Z_0 \approx 377\Omega$), and μ_r denotes relative permittivity. Introducing the grid "propagation" velocity

$$v_{grid} = \frac{\Delta l}{\Delta t} \quad (3.29)$$

we can write the approximate "update" equation for the magnetic field as

$$H_z(x, y, t) \approx H_z(x, y, t - \Delta t) - Y_0 \frac{v_0}{v_{grid} \mu_{r,avg}(x, y)} \times \quad (3.30)$$

$$\left[E_x(x, y - \frac{\Delta l}{2}, t - \frac{\Delta t}{2}) - E_x(x, y + \frac{\Delta l}{2}, t - \frac{\Delta t}{2}) + E_y(x + \frac{\Delta l}{2}, y, t - \frac{\Delta t}{2}) - E_y(x - \frac{\Delta l}{2}, y, t - \frac{\Delta t}{2}) \right]$$

The equation simplifies for the case of non-magnetic media ($\mu_r=1$)

$$H_z(x, y, t) \approx H_z(x, y, t - \Delta t) - Y_0 \frac{v_0}{v_{grid}} \times \quad (3.31)$$

$$\left[E_x(x, y - \frac{\Delta l}{2}, t - \frac{\Delta t}{2}) - E_x(x, y + \frac{\Delta l}{2}, t - \frac{\Delta t}{2}) + E_y(x + \frac{\Delta l}{2}, y, t - \frac{\Delta t}{2}) - E_y(x - \frac{\Delta l}{2}, y, t - \frac{\Delta t}{2}) \right]$$

The last two equations show that the magnetic field H and the electric field E are evaluated at points shifted spatially by $\Delta l/2$, and at instants separated in time by $\Delta t/2$, just like in 1-D. The relationship between spatial and temporal "samples" of the electric and the magnetic fields is thus the same and the samples are shifted with respect to each other by one-half of the sampling interval. The approximate equations for the electric field "updates" can be derived using the same procedure shown for the magnetic field update equations.

3. Derivation of TE_z Electric Field Update Equations

We will start with the Maxwell's curl equation for the circulation of the magnetic field

$$\oint_{C_H} H_z(x, y, t) \vec{z} \cdot d\vec{l}_H = \frac{\partial}{\partial t} \left\{ \iint_{S_H} \varepsilon(x, y) [E_x(x, y, t) \vec{x} + E_y(x, y, t) \vec{y}] \cdot d\vec{s}_H \right\} + \iint_{S_H} \sigma(x, y) [E_x(x, y, t) \vec{x} + E_y(x, y, t) \vec{y}] \cdot d\vec{s}_H \quad (3.32)$$

The discrete equivalent of the magnetic field circulation needs to be determined for two sample contours a contour in a plane parallel to the yz -coordinate plane, and a contour in a plane parallel to xz -coordinate plane.

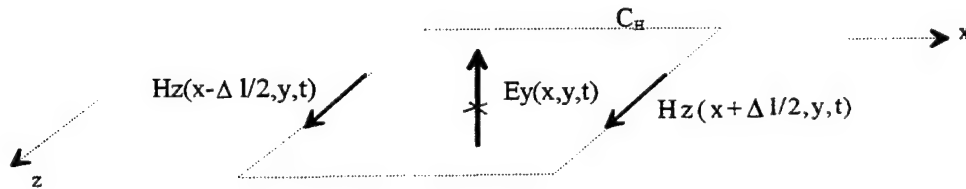


Figure 3.6. A Contour for Updating E_y .

A local coordinate system (ξ, ζ) will be used, with the origin at the center of the contour. Any point (x', z') within or on the contour C_H can be specified by its local coordinates

$$x' = x + \xi \quad z' = z + \zeta \quad \text{where} \quad -\frac{\Delta l}{2} \leq \xi \leq +\frac{\Delta l}{2} \quad \text{and} \quad -\frac{\Delta l}{2} \leq \zeta \leq +\frac{\Delta l}{2}$$

The circulation of the magnetic field around C_H , assuming counter-clockwise reference direction such that the normal to the surface S_H is in the direction of the electric field $E_y(x, y, t)$, is therefore given *exactly* by the following simple expression (because there is no magnetic field variation with the z -coordinate)

$$\oint_{C_H} H_z(x', y', t) \vec{z} \cdot d\vec{l}_H = \int_{-\frac{\Delta l}{2}}^{+\frac{\Delta l}{2}} H_z(x - \frac{\Delta l}{2}, y, t) \vec{z} \cdot d\vec{\zeta} - \int_{-\frac{\Delta l}{2}}^{+\frac{\Delta l}{2}} H_z(x + \frac{\Delta l}{2}, y, t) \vec{z} \cdot d\vec{\zeta} \quad (3.33)$$

$$\oint_{C_H} H_z(x', y', t) \vec{z} \cdot d\vec{l}_H = [H_z(x - \frac{\Delta l}{2}, y, t) - H_z(x + \frac{\Delta l}{2}, y, t)] \cdot \Delta l \quad (3.34)$$

The electric flux through the surface S_H can only be evaluated *approximately*, since the exact way that the electric flux density $D_y(x, y, t) = \epsilon(x, y)E_y(x, y, t)$ varies with x and y is not known a priori. First we need to evaluate the flux integrals

$$\iint_{S_H} \epsilon(x', y', t) E_y(x', y', t) \vec{y} \cdot d\vec{s}_H = \int_{-\frac{\Delta l}{2}}^{+\frac{\Delta l}{2}} \int_{-\frac{\Delta l}{2}}^{+\frac{\Delta l}{2}} \epsilon(x + \xi, y + \psi) E_y(x + \xi, y + \psi, t) \vec{y} \cdot \vec{y} d\xi d\zeta \quad (3.35)$$

$$\iint_{S_H} \sigma(x', y') E_y(x', y', t) \vec{y} \cdot d\vec{s}_H = \int_{-\frac{\Delta l}{2}}^{+\frac{\Delta l}{2}} \int_{-\frac{\Delta l}{2}}^{+\frac{\Delta l}{2}} \sigma(x + \xi, y + \psi) E_y(x + \xi, y + \psi, t) \vec{y} \cdot \vec{y} d\xi d\zeta \quad (3.36)$$

Since the integrands are not functions of the local z -coordinate ζ and the local coordinate $\psi=0$, the surface integrals are simplified to line integrals

$$\iint_{S_H} \epsilon(x + \xi, y) E_y(x + \xi, y, t) \vec{y} \cdot d\vec{s}_H = \Delta l \int_{-\frac{\Delta l}{2}}^{+\frac{\Delta l}{2}} \epsilon(x + \xi, y) E_y(x + \xi, y, t) d\xi \quad (3.37)$$

$$\iint_{S_H} \sigma(x + \xi, y) E_y(x + \xi, y, t) \vec{y} \cdot d\vec{s}_H = \Delta l \int_{-\frac{\Delta l}{2}}^{+\frac{\Delta l}{2}} \sigma(x + \xi, y) E_y(x + \xi, y, t) d\xi \quad (3.38)$$

Next, we assume that the contour side Δl is small enough such that the electric field $E(x+\xi, y, t)$ within the contour may be assumed constant and equal to the value at the contour's center $E(x, y, t)$. This assumption yields *approximate* expressions for the flux integrals

$$\iint_{S_H} \epsilon(x+\xi, y) E_y(x+\xi, y, t) \vec{y} \cdot \vec{ds}_H \approx \Delta l \cdot E_y(x, y, t) \cdot \int_{-\frac{\Delta l}{2}}^{+\frac{\Delta l}{2}} \epsilon(x+\xi, y) d\xi \quad (3.39)$$

$$\iint_{S_H} \sigma(x+\xi, y) E_y(x+\xi, y, t) \vec{y} \cdot \vec{ds}_H \approx \Delta l \cdot E_y(x, y, t) \cdot \int_{-\frac{\Delta l}{2}}^{+\frac{\Delta l}{2}} \sigma(x+\xi, y) d\xi \quad (3.40)$$

or, using the permittivity and conductivity averaged in the x-direction

$$\iint_{S_H} \epsilon(x+\xi, y) E_y(x+\xi, y, t) \vec{y} \cdot \vec{ds}_H \approx (\Delta l)^2 \cdot E_y(x, y, t) \cdot \epsilon_{avgx}(x, y) \quad (3.41)$$

$$\iint_{S_H} \sigma(x+\xi, y) E_y(x+\xi, y, t) \vec{y} \cdot \vec{ds}_H \approx (\Delta l)^2 \cdot E_y(x, y, t) \cdot \sigma_{avgx}(x, y) \quad (3.42)$$

The second curl equation of Maxwell can now be replaced by an approximate equation

$$\left[H_z(x - \frac{\Delta l}{2}, y, t) - H_z(x + \frac{\Delta l}{2}, y, t) \right] \cdot \Delta l \approx \quad (3.43)$$

$$\frac{\partial}{\partial t} \{ [\epsilon_{avgx}(x, y) E_y(x, y, t)] (\Delta l)^2 \} + (\Delta l)^2 \cdot \sigma_{avgx}(x, y) \cdot E_y(x, y, t)$$

which can be simplified to

$$H_z(x - \frac{\Delta l}{2}, y, t) - H_z(x + \frac{\Delta l}{2}, y, t) \approx \quad (3.44)$$

$$\epsilon_{avgx}(x, y) \cdot \Delta l \cdot \frac{\partial}{\partial t} \{ E_y(x, y, t) \} + \Delta l \cdot \sigma_{avgx}(x, y) \cdot E_y(x, y, t)$$

The approximate equation can now be re-written as

$$\begin{aligned} & \frac{\partial}{\partial t} \{ E_y(x, y, t) \} \approx \\ & \frac{1}{\Delta l \cdot \epsilon_{avgx}(x, y)} \left[H_z(x - \frac{\Delta l}{2}, y, t) - H_z(x + \frac{\Delta l}{2}, y, t) \right] - \frac{\sigma_{avgx}(x, y)}{\epsilon_{avgx}(x, y)} \cdot E_y(x, y, t) \end{aligned} \quad (3.45)$$

The above equation is integrated with respect to time to get an approximate equation for the electric field at the present time t

$$E_y(x, y, t) \approx \frac{1}{\Delta l \cdot \epsilon_{avgx}(x, y)} \left[\int_0^t H_z(x - \frac{\Delta l}{2}, y, \tau) d\tau - \int_0^t H_z(x + \frac{\Delta l}{2}, y, \tau) d\tau \right] \quad (3.46)$$

$$- \frac{\sigma_{avgx}(x, y)}{\epsilon_{avgx}(x, y)} \int_0^t E_y(x, y, \tau) d\tau$$

A similar equation can be written for the electric field at the same spatial location but at an earlier time $t - \Delta t$

$$E_y(x, y, t - \Delta t) \approx \frac{1}{\Delta l \cdot \epsilon_{avgx}(x, y)} \left[\int_0^{t-\Delta t} H_z(x - \frac{\Delta l}{2}, y, \tau) d\tau - \int_0^{t-\Delta t} H_z(x + \frac{\Delta l}{2}, y, \tau) d\tau \right] \quad (3.47)$$

$$- \frac{\sigma_{avgx}(x, y)}{\epsilon_{avgx}(x, y)} \int_0^{t-\Delta t} E_y(x, y, \tau) d\tau$$

Subtracting the two equations we get

$$E_y(x, y, t) - E_y(x, y, t - \Delta t) \approx \quad (3.48)$$

$$\frac{1}{\Delta l \cdot \epsilon_{avgx}(x, y)} \left[\int_{t-\Delta t}^t H_z(x - \frac{\Delta l}{2}, y, \tau) d\tau - \int_{t-\Delta t}^t H_z(x + \frac{\Delta l}{2}, y, \tau) d\tau \right]$$

$$- \frac{\sigma_{avgx}(x, y)}{\epsilon_{avgx}(x, y)} \int_{t-\Delta t}^t E_y(x, y, \tau) d\tau$$

which can also be written as

$$E_y(x, y, t) \approx \quad (3.49)$$

$$E_y(x, y, t - \Delta t) + \frac{1}{\Delta l \cdot \epsilon_{avgx}(x, y)} \left[\int_{t-\Delta t}^t H_z(x - \frac{\Delta l}{2}, y, \tau) d\tau - \int_{t-\Delta t}^t H_z(x + \frac{\Delta l}{2}, y, \tau) d\tau \right]$$

$$- \frac{\sigma_{avgx}(x, y)}{\epsilon_{avgx}(x, y)} \int_{t-\Delta t}^t E_y(x, y, \tau) d\tau$$

If the interval Δt is small, the magnetic fields can be assumed approximately constant within Δt and equal to the value at the center of the time interval Δt

$$H_z(x + \frac{\Delta l}{2}, y, \tau) \approx H_z(x + \frac{\Delta l}{2}, y, t - \frac{\Delta t}{2}) \quad \text{for } t - \Delta t \leq \tau \leq t \quad (3.50)$$

$$H_z(x - \frac{\Delta l}{2}, y, \tau) \approx H_z(x - \frac{\Delta l}{2}, y, t - \frac{\Delta t}{2}) \quad \text{for } t - \Delta t \leq \tau \leq t \quad (3.51)$$

Using the above approximation we get

$$E_y(x, y, t) \approx \quad (3.52)$$

$$E_y(x, y, t - \Delta t) + \frac{\Delta t}{\Delta l \cdot \epsilon_{avgx}(x, y)} \left[H_z(x - \frac{\Delta l}{2}, y, t - \frac{\Delta t}{2}) - H_z(x + \frac{\Delta l}{2}, y, t - \frac{\Delta t}{2}) \right]$$

$$- \frac{\sigma_{avgx}(x, y)}{\epsilon_{avgx}(x, y)} \int_{t-\Delta t}^t E_y(x, y, \tau) d\tau$$

The above equation can be written in a somewhat different form

$$E_y(x, y, t) \approx \quad (3.53)$$

$$E_y(x, y, t - \Delta t) + \frac{\Delta t}{\Delta l \cdot \epsilon_{avgx}(x, y)} \left[H_z(x - \frac{\Delta l}{2}, y, t - \frac{\Delta t}{2}) - H_z(x + \frac{\Delta l}{2}, y, t - \frac{\Delta t}{2}) \right]$$

$$- \Delta t \frac{\sigma_{avgx}(x, y)}{\epsilon_{avgx}(x, y)} \left[\frac{1}{\Delta t} \int_{t-\Delta t}^t E_y(x, y, \tau) d\tau \right]$$

The term in the brackets is recognized as the average value of the electric field component E_y at (x, y) within the interval $(t - \Delta t, t)$. The above equation can be written in a more compact form using the identity

$$\frac{1}{\epsilon} = \frac{1}{\epsilon_0} \frac{1}{\epsilon_r} = \frac{\sqrt{\mu_0}}{\sqrt{\mu_0}} \frac{1}{\sqrt{\epsilon_0}} \frac{1}{\sqrt{\epsilon_0}} \frac{1}{\epsilon_r} = \frac{1}{\sqrt{\mu_0 \epsilon_0}} \sqrt{\frac{\mu_0}{\epsilon_0}} \frac{1}{\epsilon_r} = v_0 Z_0 \frac{1}{\epsilon_r} \quad (3.54)$$

where the free space velocity of propagation is denoted v_0 , the intrinsic impedance of free space is denoted Z_0 ($Z_0 \approx 377\Omega$) and ϵ_r denotes relative permittivity. Introducing the grid "propagation" velocity

$$v_{grid} = \frac{\Delta l}{\Delta t} \quad (3.55)$$

we can write the approximate electric field "update" equation as

$$E_y(x, y, t) \approx \quad (3.56)$$

$$E_y(x, y, t - \Delta t) + Z_0 \frac{v_0}{v_{grid} \epsilon_{r,avgx}(x, y)} \left[H_z(x - \frac{\Delta l}{2}, y, t - \frac{\Delta t}{2}) - H_z(x + \frac{\Delta l}{2}, y, t - \frac{\Delta t}{2}) \right]$$

$$- Z_0 \frac{v_0}{v_{grid} \epsilon_{r,avgx}(x, y)} \cdot \Delta l \cdot \sigma_{avgx}(x, y) E_{y,avg(\Delta t)}(x, y, t)$$

The average of the electric field between $t - \Delta t$ and t , denoted $E_{x,avg(\Delta t)}$ can not be calculated exactly because the exact temporal variation of the electric field within the Δt

interval is not known a priori. However, assuming a linear variation within Δt interval, the average field is the average of the values at $t-\Delta t$ and t

$$E_{y,avg(\Delta t)}(x, y, t) \approx \frac{E_y(x, y, t - \Delta t) + E_y(x, y, t)}{2} \quad (3.57)$$

Substituting the time-average $E_{y,avg(\Delta t)}(x, y, t)$ into the update equation we get

$$\begin{aligned} E_y(x, y, t) \approx & \quad (3.58) \\ E_y(x, y, t - \Delta t) + Z_0 \frac{v_0}{v_{grid}} \frac{1}{\epsilon_{r,avgx}(x, y)} & \left[H_z(x - \frac{\Delta l}{2}, y, t - \frac{\Delta t}{2}) - H_z(x + \frac{\Delta l}{2}, y, t - \frac{\Delta t}{2}) \right] - \\ Z_0 \frac{v_0}{v_{grid}} \frac{1}{\epsilon_{r,avgx}(x, y)} \cdot \Delta l \cdot \sigma_{avgx}(x, y) \cdot & \frac{E_y(x, y, t - \Delta t) + E_y(x, y, t)}{2} \end{aligned}$$

which gives the final equation for the electric field updates as

$$\begin{aligned} E_y(x, y, t) \approx & \quad (3.59) \\ \frac{1 - \frac{1}{2} \frac{v_0}{v_{grid}} \frac{Z_0 \cdot \Delta l \cdot \sigma_{avgx}(x, y)}{\epsilon_{r,avgx}(x, y)}}{1 + \frac{1}{2} \frac{v_0}{v_{grid}} \frac{Z_0 \cdot \Delta l \cdot \sigma_{avgx}(x, y)}{\epsilon_{r,avgx}(x, y)}} E_y(x, y, t - \Delta t) + \\ \frac{Z_0 \frac{v_0}{v_{grid}} \frac{1}{\epsilon_{r,avgx}(x, y)}}{1 + \frac{1}{2} \frac{v_0}{v_{grid}} \frac{Z_0 \cdot \Delta l \cdot \sigma_{avgx}(x, y)}{\epsilon_{r,avgx}(x, y)}} & \left[H_z(x - \frac{\Delta l}{2}, y, t - \frac{\Delta t}{2}) - H_z(x + \frac{\Delta l}{2}, y, t - \frac{\Delta t}{2}) \right] \end{aligned}$$

The equation simplifies greatly for the case of non-conductive media ($\sigma=0$)

$$\begin{aligned} E_y(x, y, t) \approx & \quad (3.60) \\ E_y(x, y, t - \Delta t) + Z_0 \frac{v_0}{v_{grid}} \frac{1}{\epsilon_{r,avgx}(x, y)} & \left[H_z(x - \frac{\Delta l}{2}, y, t - \frac{\Delta t}{2}) - H_z(x + \frac{\Delta l}{2}, y, t - \frac{\Delta t}{2}) \right] \end{aligned}$$

In the case of free-space ($\epsilon_r=1$), the equation simplifies further

$$E_y(x, y, t) \approx E_y(x, y, t - \Delta t) + Z_0 \frac{v_0}{v_{grid}} \left[H_z(x - \frac{\Delta l}{2}, y, t - \frac{\Delta t}{2}) - H_z(x + \frac{\Delta l}{2}, y, t - \frac{\Delta t}{2}) \right] \quad (3.61)$$

The above equations are the update equations for the y-directed component of a TE_z electric field. Similar equations will be formulated next for the x-directed electric field component.

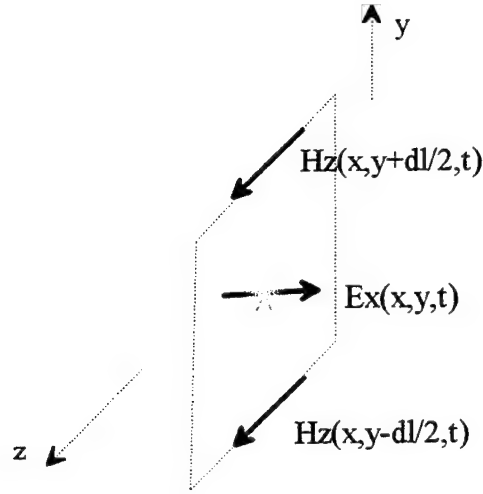


Figure 3.7. A Contour for Updating E_x .

A local coordinate system will be used, with the origin at the center of the contour. Any point (y', z') within or on the contour C_H can be specified by its local coordinates

$$y' = y + \psi \quad z' = z + \zeta \quad \text{where} \quad -\frac{\Delta l}{2} \leq \psi \leq +\frac{\Delta l}{2} \quad \text{and} \quad -\frac{\Delta l}{2} \leq \zeta \leq +\frac{\Delta l}{2}$$

Then, by applying the same procedure driven for E_y field component, we get the final equation for E_x electric field component as shown below

$$E_x(x, y, t) \approx \frac{1 - \frac{1}{2} \frac{v_0}{v_{grid}} \frac{Z_0 \cdot \Delta l \cdot \sigma_{avg}(x, y)}{\epsilon_{r, avg}(x, y)}}{1 + \frac{1}{2} \frac{v_0}{v_{grid}} \frac{Z_0 \cdot \Delta l \cdot \sigma_{avg}(x, y)}{\epsilon_{r, avg}(x, y)}} E_x(x, y, t - \Delta t) + \frac{Z_0 \frac{v_0}{v_{grid}} \frac{1}{\epsilon_{r, avg}(x, y)}}{1 + \frac{1}{2} \frac{v_0}{v_{grid}} \frac{Z_0 \cdot \Delta l \cdot \sigma_{avg}(x, y)}{\epsilon_{r, avg}(x, y)}} \left[H_z(x, y + \frac{\Delta l}{2}, t - \frac{\Delta t}{2}) - H_z(x, y - \frac{\Delta l}{2}, t - \frac{\Delta t}{2}) \right] \quad (3.62)$$

The equation simplifies greatly for the case of non-conductive media ($\sigma=0$)

$$E_x(x, y, t) \approx \quad (3.63)$$

$$E_x(x, y, t - \Delta t) + Z_0 \frac{v_0}{v_{grid} \epsilon_{r,avg}(x, y)} \left[H_z(x, y + \frac{\Delta l}{2}, t - \frac{\Delta t}{2}) - H_z(x, y - \frac{\Delta l}{2}, t - \frac{\Delta t}{2}) \right]$$

In the case of free-space ($\epsilon_r=1$), the equation simplifies further

$$E_x(x, y, t) \approx E_x(x, y, t - \Delta t) + Z_0 \frac{v_0}{v_{grid}} \left[H_z(x, y + \frac{\Delta l}{2}, t - \frac{\Delta t}{2}) - H_z(x, y - \frac{\Delta l}{2}, t - \frac{\Delta t}{2}) \right] \quad (3.64)$$

The above equations are the update equations for the x-directed component of a TE_z electric field.

4. Derivation of TM_z Electric Field Update Equation

The discrete equivalent of the TM_z magnetic field circulation will be determined next. A sample contour C_H that will be used to determine the electric field update equation is shown below

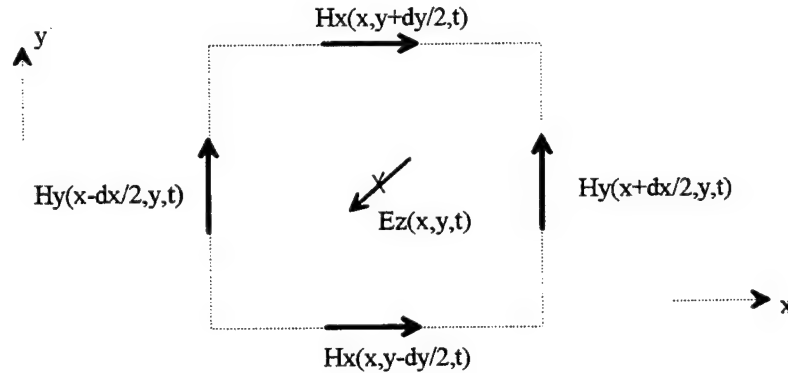


Figure 3.8. A Contour for TM_z Magnetic Field Circulation and Electric Flux Calculations.

The center of the surface S_H is assumed to have the coordinates (x, y) . We will assume a uniform grid with $\Delta x = \Delta y = \Delta l$. A local coordinate system (ξ, ψ) will be established, with the origin at the center of the contour. Any point (x', y') within or on the contour C_E can be specified by its local coordinates ξ and ψ

$$x' = x + \xi \quad y' = y + \psi \quad \text{where} \quad -\frac{\Delta l}{2} \leq \xi \leq +\frac{\Delta l}{2} \quad \text{and} \quad -\frac{\Delta l}{2} \leq \psi \leq +\frac{\Delta l}{2}$$

The local coordinates will be used in evaluation of the line and surface integrals that constitute the integral forms of Maxwell's equations. The circulation of the magnetic field around the magnetic field contour C_H , assuming counter-clockwise reference direction such that the normal to the surface S_E is in the direction of the electric field $\vec{E}(x, y, t)$, can be evaluated *approximately*, assuming that the magnetic fields are constant over the length Δl , along the edges of the $(\Delta l \text{ by } \Delta l)$ square contour

$$\oint_{C_H} \left[H_x(x', y', t) \vec{x} + H_y(x', y', t) \vec{y} \right] \bullet d\vec{l}_H \approx \left[H_x(x, y - \frac{\Delta l}{2}, t) + H_y(x + \frac{\Delta l}{2}, y, t) - H_x(x, y + \frac{\Delta l}{2}, t) - H_y(x - \frac{\Delta l}{2}, y, t) \right] \Delta l \quad (3.65)$$

The electric flux (the "displacement current") through the surface S_H and the current flux (the conduction current) can be calculated using the local coordinates

$$\iint_{S_H} \epsilon(x', y') E_z(x', y', t) \vec{z} \bullet d\vec{s}_H = \int_{-\frac{\Delta l}{2}}^{+\frac{\Delta l}{2}} \int_{-\frac{\Delta l}{2}}^{+\frac{\Delta l}{2}} \epsilon(x + \xi, y + \psi) E_z(x + \xi, y + \psi, t) \vec{z} \bullet \vec{z} d\xi d\psi \quad (3.66)$$

$$\iint_{S_H} \sigma(x', y') E_z(x', y', t) \vec{z} \bullet d\vec{s}_H = \int_{-\frac{\Delta l}{2}}^{+\frac{\Delta l}{2}} \int_{-\frac{\Delta l}{2}}^{+\frac{\Delta l}{2}} \sigma(x + \xi, y + \psi) E_z(x + \xi, y + \psi, t) \vec{z} \bullet \vec{z} d\xi d\psi \quad (3.67)$$

There are infinitely many ways to model the variation of the electric flux density with the local coordinates ξ and ψ within the contour. We first need to postulate a certain variation of the electric field with ξ and ψ such that the integral can be evaluated over S_H . The simplest model assumes that the contour width Δl is small enough such that the electric field $E(x + \xi, y + \psi, t)$ within the contour may be assumed constant and equal to the value at the contour's center $E(x, y, t)$

$$E_z(x + \xi, y + \psi, t) \approx E_z(x, y, t) \quad (3.68)$$

This is equivalent to using a piece-wise constant approximation of the actual electric field variation with the z-coordinate. The above assumption allows that, although the electric field is constant within a contour, it can change from one contour to an other. This yields *approximate* expressions for displacement and conduction currents

$$\iint_{S_H} \epsilon(x', y') E_z(x', y', t) \vec{z} \cdot \vec{ds}_E \approx E_z(x, y, t) \cdot \int_{-\frac{\Delta l}{2}}^{+\frac{\Delta l}{2}} \int_{-\frac{\Delta l}{2}}^{+\frac{\Delta l}{2}} \epsilon(x + \xi, y + \psi) d\xi d\psi \quad (3.69)$$

$$\iint_{S_H} \sigma(x', y') E_z(x', y', t) \vec{z} \cdot \vec{ds}_E \approx E_z(x, y, t) \cdot \int_{-\frac{\Delta l}{2}}^{+\frac{\Delta l}{2}} \int_{-\frac{\Delta l}{2}}^{+\frac{\Delta l}{2}} \sigma(x + \xi, y + \psi) d\xi d\psi \quad (3.70)$$

The integrals of the permittivity $\epsilon(x + \xi, y + \psi)$ and the conductivity $\sigma(x + \xi, y + \psi)$ can be re-written in the following manner

$$\int_{-\frac{\Delta l}{2}}^{+\frac{\Delta l}{2}} \int_{-\frac{\Delta l}{2}}^{+\frac{\Delta l}{2}} \epsilon(x + \xi, y + \psi) d\xi d\psi = (\Delta l)^2 \cdot \left[\frac{1}{(\Delta l)^2} \int_{-\frac{\Delta l}{2}}^{+\frac{\Delta l}{2}} \int_{-\frac{\Delta l}{2}}^{+\frac{\Delta l}{2}} \epsilon(x + \xi, y + \psi) d\xi d\psi \right] \quad (3.71)$$

$$\int_{-\frac{\Delta l}{2}}^{+\frac{\Delta l}{2}} \int_{-\frac{\Delta l}{2}}^{+\frac{\Delta l}{2}} \sigma(x + \xi, y + \psi) d\xi d\psi = (\Delta l)^2 \cdot \left[\frac{1}{(\Delta l)^2} \int_{-\frac{\Delta l}{2}}^{+\frac{\Delta l}{2}} \int_{-\frac{\Delta l}{2}}^{+\frac{\Delta l}{2}} \sigma(x + \xi, y + \psi) d\xi d\psi \right] \quad (3.72)$$

The term in the brackets is recognized as the *average* permittivity ϵ_{avg} and the *average* conductivity σ_{avg} within the contour C_H .

$$\epsilon_{avg}(x, y) = \frac{1}{(\Delta l)^2} \int_{-\frac{\Delta l}{2}}^{+\frac{\Delta l}{2}} \int_{-\frac{\Delta l}{2}}^{+\frac{\Delta l}{2}} \epsilon(x + \xi, y + \psi) d\xi d\psi \quad (3.73)$$

$$\sigma_{avg}(x, y) = \frac{1}{(\Delta l)^2} \int_{-\frac{\Delta l}{2}}^{+\frac{\Delta l}{2}} \int_{-\frac{\Delta l}{2}}^{+\frac{\Delta l}{2}} \sigma(x + \xi, y + \psi) d\xi d\psi \quad (3.74)$$

The approximate expression for the displacement and conduction currents through S_H can now be written using the average permittivity and the average conductivity as

$$\iint_{S_H} \epsilon(x', y') E_z(x', y', t) \vec{z} \cdot \vec{ds}_H \approx (\Delta l)^2 \epsilon_{avg}(x, y) E_z(x, y, t) \quad (3.75)$$

$$\iint_{S_H} \sigma(x', y') E_z(x', y', t) \vec{z} \cdot \vec{ds}_H \approx (\Delta l)^2 \sigma_{avg}(x, y) E_z(x, y, t) \quad (3.76)$$

The first curl equation of Maxwell can now be replaced by an approximate equation

$$\left[H_x(x, y - \frac{\Delta l}{2}, t) + H_y(x + \frac{\Delta l}{2}, y, t) - H_x(x, y + \frac{\Delta l}{2}, t) - H_y(x - \frac{\Delta l}{2}, y, t) \right] \cdot \Delta l \approx \quad (3.77)$$

$$\frac{\partial}{\partial t} \{ [\epsilon_{avg}(x, y) E_z(x, y, t)] (\Delta l)^2 \} + [\sigma_{avg}(x, y) E_z(x, y, t)] (\Delta l)^2$$

which can be simplified (because of media stationarity) to

$$H_x(x, y - \frac{\Delta l}{2}, t) + H_y(x + \frac{\Delta l}{2}, y, t) - H_x(x, y + \frac{\Delta l}{2}, t) - H_y(x - \frac{\Delta l}{2}, y, t) \approx \quad (3.78)$$

$$\frac{\partial}{\partial t} \{ E_z(x, y, t) \} \cdot \Delta l \cdot \epsilon_{avg}(x, y) + \sigma_{avg}(x, y) \cdot E_z(x, y, t) \cdot \Delta l$$

This equation can also be re-written as

$$\begin{aligned} & \frac{\partial}{\partial t} \{ E_z(x, y, t) \} \approx \quad (3.79) \\ & \frac{1}{\Delta l \cdot \epsilon_{avg}(x, y)} \left[H_x(x, y - \frac{\Delta l}{2}, t) + H_y(x + \frac{\Delta l}{2}, y, t) - H_x(x, y + \frac{\Delta l}{2}, t) - H_y(x - \frac{\Delta l}{2}, y, t) \right] \\ & - \frac{\sigma_{avg}(x, y)}{\epsilon_{avg}(x, y)} \cdot E_z(x, y, t) \end{aligned}$$

The above equation is integrated with respect to time to get an approximate equation for the electric field at the present time t

$$\begin{aligned} E_z(x, y, t) & \approx \frac{1}{\Delta l \cdot \epsilon_{avg}(x, y)} \times \quad (3.80) \\ & \left[\int_0^t H_x(x, y - \frac{\Delta l}{2}, \tau) d\tau - \int_0^t H_x(x, y + \frac{\Delta l}{2}, \tau) d\tau + \int_0^t H_y(x + \frac{\Delta l}{2}, y, \tau) d\tau - \int_0^t H_y(x - \frac{\Delta l}{2}, y, \tau) d\tau \right] \\ & - \frac{\sigma_{avg}(x, y)}{\epsilon_{avg}(x, y)} \cdot \int_0^t E_z(x, y, \tau) d\tau \end{aligned}$$

A similar integral equation can be written for the electric field at the same spatial location but at an earlier time t-Δt

$$\begin{aligned} E_z(x, y, t - \Delta t) & \approx \quad (3.81) \\ & \frac{1}{\Delta l \cdot \epsilon_{avg}(x, y)} \left[\int_0^{t-\Delta t} H_x(x, y - \frac{\Delta l}{2}, \tau) d\tau - \int_0^{t-\Delta t} H_x(x, y + \frac{\Delta l}{2}, \tau) d\tau + \int_0^{t-\Delta t} H_y(x + \frac{\Delta l}{2}, y, \tau) d\tau - \right. \\ & \left. \int_0^{t-\Delta t} H_y(x - \frac{\Delta l}{2}, y, \tau) d\tau \right] - \frac{\sigma_{avg}(x, y)}{\epsilon_{avg}(x, y)} \cdot \int_0^{t-\Delta t} E_z(x, y, \tau) d\tau \end{aligned}$$

Subtracting the two equations we get

$$E_z(x, y, t) \approx E_z(x, y, t - \Delta t) + \frac{1}{\Delta l \cdot \epsilon_{avg}(x, y)} \times \quad (3.82)$$

$$\left[\int_{t-\Delta t}^t H_x(x, y - \frac{\Delta l}{2}, \tau) d\tau - \int_{t-\Delta t}^t H_x(x, y + \frac{\Delta l}{2}, \tau) d\tau + \int_{t-\Delta t}^t H_y(x + \frac{\Delta l}{2}, y, \tau) d\tau - \int_{t-\Delta t}^t H_y(x - \frac{\Delta l}{2}, y, \tau) d\tau \right]$$

$$- \frac{\sigma_{avg}(x, y)}{\epsilon_{avg}(x, y)} \cdot \int_{t-\Delta t}^t E_z(x, y, \tau) d\tau$$

The integrals can be evaluated approximately by assuming a certain variation of magnetic field with the temporal variable τ . The simplest approach, consistent with the assumptions made for the field spatial variation, would be to assume that the interval Δt is small enough such that the magnetic field can be assumed approximately constant within Δt and equal to the value at the center of the time interval ($t - \Delta t, t$)

$$H_x(x, y - \frac{\Delta l}{2}, \tau) \approx H_x(x, y - \frac{\Delta l}{2}, t - \frac{\Delta t}{2}) \quad \text{for } t - \Delta t \leq \tau \leq t \quad (3.83)$$

$$H_x(x, y + \frac{\Delta l}{2}, \tau) \approx H_x(x, y + \frac{\Delta l}{2}, t - \frac{\Delta t}{2}) \quad \text{for } t - \Delta t \leq \tau \leq t \quad (3.84)$$

$$H_y(x - \frac{\Delta l}{2}, y, \tau) \approx H_y(x - \frac{\Delta l}{2}, y, t - \frac{\Delta t}{2}) \quad \text{for } t - \Delta t \leq \tau \leq t \quad (3.85)$$

$$H_y(x + \frac{\Delta l}{2}, y, \tau) \approx H_y(x + \frac{\Delta l}{2}, y, t - \frac{\Delta t}{2}) \quad \text{for } t - \Delta t \leq \tau \leq t \quad (3.86)$$

The integral of the electric field is recognized as the average value of the field within the Δt interval

$$\frac{\sigma_{avg}(x, y) \cdot \Delta t}{\epsilon_{avg}(x, y)} \cdot \left[\frac{1}{\Delta t} \int_{t-\Delta t}^t E_z(x, y, \tau) d\tau \right] = \frac{\sigma_{avg}(x, y) \cdot \Delta t}{\epsilon_{avg}(x, y)} \cdot E_{z,avg(\Delta t)}(x, y, t) \quad (3.87)$$

The average value of the electric field is approximately

$$E_{z,avg(\Delta t)}(x, y, t) \approx \frac{E_z(x, y, t) + E_z(x, y, t - \Delta t)}{2} \quad (3.88)$$

The approximate expression for the electric field at location (x, y) and at the time t now becomes

$$E_z(x, y, t) \approx E_z(x, y, t - \Delta t) + \frac{\Delta t}{\Delta l \cdot \epsilon_{avg}(x, y)} \times \quad (3.89)$$

$$\left[H_x(x, y - \frac{\Delta l}{2}, t - \frac{\Delta t}{2}) - H_x(x, y + \frac{\Delta l}{2}, t - \frac{\Delta t}{2}) + H_y(x + \frac{\Delta l}{2}, y, t - \frac{\Delta t}{2}) - H_y(x - \frac{\Delta l}{2}, y, t - \frac{\Delta t}{2}) \right]$$

$$- \frac{\sigma_{avg}(x, y) \cdot \Delta t}{\epsilon_{avg}(x, y)} \cdot \frac{E_z(x, y, t) + E_z(x, y, t - \Delta t)}{2}$$

The above equation can be written in a somewhat different form, using the identity

$$\frac{1}{\varepsilon} = \frac{1}{\varepsilon_0} \frac{1}{\varepsilon_r} = \frac{\sqrt{\mu_0}}{\sqrt{\mu_0}} \frac{1}{\sqrt{\varepsilon_0}} \frac{1}{\sqrt{\varepsilon_0}} \frac{1}{\varepsilon_r} = \frac{1}{\sqrt{\mu_0 \varepsilon_0}} \sqrt{\frac{\mu_0}{\varepsilon_0}} \frac{1}{\varepsilon_r} = v_0 Z_0 \frac{1}{\varepsilon_r} \quad (3.90)$$

where the free space velocity of propagation is denoted v_0 , the intrinsic impedance of free space is denoted Z_0 ($Z_0 \approx 377\Omega$), and ε_r denotes relative permittivity. Introducing the grid "propagation" velocity

$$v_{grid} = \frac{\Delta l}{\Delta t} \quad (3.91)$$

we can write the electric field equation more compactly

$$\begin{aligned} E_z(x, y, t) \approx & E_z(x, y, t - \Delta t) + Z_0 \frac{v_0}{v_{grid}} \frac{1}{\varepsilon_{r,avg}(x, y)} \times \\ & \left[H_x(x, y - \frac{\Delta l}{2}, t - \frac{\Delta t}{2}) - H_x(x, y + \frac{\Delta l}{2}, t - \frac{\Delta t}{2}) + H_y(x + \frac{\Delta l}{2}, y, t - \frac{\Delta t}{2}) - H_y(x - \frac{\Delta l}{2}, y, t - \frac{\Delta t}{2}) \right] \\ & - Z_0 \frac{v_0}{v_{grid}} \cdot \frac{\sigma_{avg}(x, y) \cdot \Delta l}{\varepsilon_{r,avg}(x, y)} \cdot \frac{E_z(x, y, t) + E_z(x, y, t - \Delta t)}{2} \end{aligned} \quad (3.92)$$

The electric field "update" equation is obtained by grouping the like terms in the above equation

$$\begin{aligned} E_z(x, y, t) \approx & \\ & \frac{1 - \frac{1}{2} \frac{v_0}{v_{grid}} \frac{Z_0 \cdot \sigma_{avg}(x, y) \cdot \Delta l}{\varepsilon_{r,avg}(x, y)}}{1 + \frac{1}{2} \frac{v_0}{v_{grid}} \frac{Z_0 \cdot \sigma_{avg}(x, y) \cdot \Delta l}{\varepsilon_{r,avg}(x, y)}} \cdot E_z(x, y, t - \Delta t) + \frac{Z_0 \frac{v_0}{v_{grid}} \frac{1}{\varepsilon_{r,avg}(x, y)}}{1 + \frac{1}{2} \frac{v_0}{v_{grid}} \frac{Z_0 \cdot \sigma_{avg}(x, y) \cdot \Delta l}{\varepsilon_{r,avg}(x, y)}} \times \\ & \cdot \left[H_x(x, y - \frac{\Delta l}{2}, t - \frac{\Delta t}{2}) - H_x(x, y + \frac{\Delta l}{2}, t - \frac{\Delta t}{2}) + H_y(x + \frac{\Delta l}{2}, y, t - \frac{\Delta t}{2}) - H_y(x - \frac{\Delta l}{2}, y, t - \frac{\Delta t}{2}) \right] \end{aligned} \quad (3.93)$$

The equation simplifies for the case of non-conductive media ($\sigma=0$)

$$\begin{aligned} E_z(x, y, t) \approx & E_z(x, y, t - \Delta t) + Z_0 \frac{v_0}{v_{grid}} \frac{1}{\varepsilon_{r,avg}(x, y)} \times \\ & \left[H_x(x, y - \frac{\Delta l}{2}, t - \frac{\Delta t}{2}) - H_x(x, y + \frac{\Delta l}{2}, t - \frac{\Delta t}{2}) + H_y(x + \frac{\Delta l}{2}, y, t - \frac{\Delta t}{2}) - H_y(x - \frac{\Delta l}{2}, y, t - \frac{\Delta t}{2}) \right] \end{aligned} \quad (3.94)$$

The approximate "update" equations for TMz magnetic field components will be derived next.

5. Derivation of TM_z Magnetic Field Update Equations

We will start with the Maxwell's curl equation for the circulation of the electric field

$$\oint_{C_E} E_z(x, y, t) \vec{z} \cdot d\vec{l}_E = -\frac{\partial}{\partial t} \left\{ \iint_{S_E} \epsilon(x, y) [H_x(x, y, t) \vec{x} + H_y(x, y, t) \vec{y}] \cdot d\vec{s}_E \right\} \quad (3.95)$$

The discrete equivalent of the magnetic field circulation needs to be determined for two sample contours a contour in a plane parallel to the yz-coordinate plane, and a contour in a plane parallel to xz-coordinate plane.

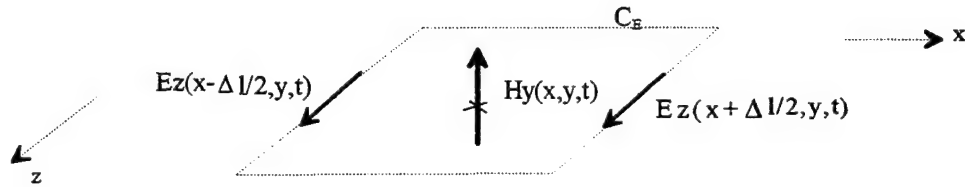


Figure 3.9. A Contour for Updating H_y .

A local coordinate system (ξ, ζ) will be used, with the origin at the center of the contour. Any point (x', z') within or on the contour C_E can be specified by its local coordinates

$$x' = x + \xi \quad z' = z + \zeta \quad \text{where} \quad -\frac{\Delta l}{2} \leq \xi \leq +\frac{\Delta l}{2} \quad \text{and} \quad -\frac{\Delta l}{2} \leq \zeta \leq +\frac{\Delta l}{2}$$

The circulation of electric field around C_E , assuming counter-clockwise reference direction such that the normal to the surface S_E is in the direction of magnetic field $H_y(x, y, t)$, is therefore given *exactly* by the following simple expression because there is no electric field variation with the z-coordinate

$$\oint_{C_E} E_z(x', y', t) \vec{z} \cdot d\vec{l}_E = \quad (3.96)$$

$$\int_{-\frac{\Delta l}{2}}^{+\frac{\Delta l}{2}} E_z(x - \frac{\Delta l}{2}, y, t) \vec{z} \cdot d\vec{\zeta} - \int_{-\frac{\Delta l}{2}}^{+\frac{\Delta l}{2}} E_z(x + \frac{\Delta l}{2}, y, t) \vec{z} \cdot d\vec{\zeta} \\ \oint_{C_E} E_z(x', y', t) \vec{z} \cdot d\vec{l}_E = [E_z(x - \frac{\Delta l}{2}, y, t) - E_z(x + \frac{\Delta l}{2}, y, t)] \cdot \Delta l \quad (3.97)$$

The magnetic flux through the surface S_E can only be evaluated *approximately*, since the exact way that the magnetic flux density

$$B_y(x, y, t) = \mu(x, y) H_y(x, y, t) \quad (3.98)$$

varies with x and y is not known a priori. First we need to evaluate the flux integral

$$\iint_{S_E} \mu(x', y', t) H_y(x', y', t) \vec{y} \cdot d\vec{s}_E = \quad (3.99) \\ \int_{-\frac{\Delta l}{2}}^{+\frac{\Delta l}{2}} \int_{-\frac{\Delta l}{2}}^{+\frac{\Delta l}{2}} \mu(x + \xi, y + \psi) H_y(x + \xi, y + \psi, t) \vec{y} \cdot \vec{y} d\xi d\psi$$

Since the integrand is not a function of the local z -coordinate ζ and the local coordinate $\psi=0$, the surface integral simplifies to a line integral

$$\iint_{S_E} \mu(x + \xi, y) H_y(x + \xi, y, t) \vec{y} \cdot d\vec{s}_E = \Delta l \int_{-\frac{\Delta l}{2}}^{+\frac{\Delta l}{2}} \mu(x + \xi, y) H_y(x + \xi, y, t) d\xi \quad (3.100)$$

Next, assume that the contour side Δl is small enough such that the magnetic field $H(x+\xi, y, t)$ within the contour may be assumed constant and equal to the value at the contour's center $H(x, y, t)$. This assumption yields an *approximate* expression for the flux integral

$$\iint_{S_E} \mu(x + \xi, y) H_y(x + \xi, y, t) \vec{y} \cdot d\vec{s}_E \approx \Delta l \cdot H_y(x, y, t) \cdot \int_{-\frac{\Delta l}{2}}^{+\frac{\Delta l}{2}} \mu(x + \xi, y) d\xi \quad (3.101)$$

or, using permeability averaged in the x -direction

$$\iint_{S_E} \mu(x + \xi, y) H_y(x + \xi, y, t) \vec{y} \cdot d\vec{s}_E \approx (\Delta l)^2 \cdot H_y(x, y, t) \cdot \mu_{avgx}(x, y) \quad (3.102)$$

The first curl equation of Maxwell can now be replaced by an approximate equation

$$[E_z(x - \frac{\Delta l}{2}, y, t) - E_z(x + \frac{\Delta l}{2}, y, t)] \cdot \Delta l \approx -\frac{\partial}{\partial t} \{ [\mu_{avgx}(x, y) H_y(x, y, t)] (\Delta l)^2 \} \quad (3.103)$$

which can be simplified to below equation, because of media stationarity

$$E_z(x - \frac{\Delta l}{2}, y, t) - E_z(x + \frac{\Delta l}{2}, y, t) \approx -\mu_{avgx}(x, y) \cdot \Delta l \cdot \frac{\partial}{\partial t} \{H_y(x, y, t)\} \quad (3.104)$$

The approximate equation can be re-written as

$$\frac{\partial}{\partial t} \{H_y(x, y, t)\} \approx \frac{-1}{\Delta l \cdot \mu_{avgx}(x, y)} \left[E_z(x - \frac{\Delta l}{2}, y, t) - E_z(x + \frac{\Delta l}{2}, y, t) \right] \quad (3.105)$$

The above equation is integrated with respect to time to get an approximate equation for the electric field at the present time t

$$H_y(x, y, t) \approx \frac{-1}{\Delta l \cdot \mu_{avgx}(x, y)} \left[\int_0^t E_z(x - \frac{\Delta l}{2}, y, \tau) d\tau - \int_0^t E_z(x + \frac{\Delta l}{2}, y, \tau) d\tau \right] \quad (3.106)$$

A similar equation can be written for the electric field at the same spatial location but at an earlier time $t - \Delta t$

$$H_y(x, y, t - \Delta t) \approx \frac{-1}{\Delta l \cdot \mu_{avgx}(x, y)} \left[\int_0^{t-\Delta t} E_z(x - \frac{\Delta l}{2}, y, \tau) d\tau - \int_0^{t-\Delta t} E_z(x + \frac{\Delta l}{2}, y, \tau) d\tau \right] \quad (3.107)$$

Subtracting the two equations we get

$$\begin{aligned} H_y(x, y, t) - H_y(x, y, t - \Delta t) &\approx \\ \frac{-1}{\Delta l \cdot \mu_{avgx}(x, y)} &\left[\int_{t-\Delta t}^t E_z(x - \frac{\Delta l}{2}, y, \tau) d\tau - \int_{t-\Delta t}^t E_z(x + \frac{\Delta l}{2}, y, \tau) d\tau \right] \end{aligned} \quad (3.108)$$

which can also be written as

$$\begin{aligned} H_y(x, y, t) &\approx \\ H_y(x, y, t - \Delta t) &+ \frac{-1}{\Delta l \cdot \mu_{avgx}(x, y)} \left[\int_{t-\Delta t}^t E_z(x - \frac{\Delta l}{2}, y, \tau) d\tau - \int_{t-\Delta t}^t E_z(x + \frac{\Delta l}{2}, y, \tau) d\tau \right] \end{aligned} \quad (3.109)$$

Assuming that the interval Δt is small enough such that the electric fields can be assumed approximately constant within Δt and equal to the value at the center of the time interval Δt

$$E_z(x + \frac{\Delta l}{2}, y, \tau) \approx E_z(x + \frac{\Delta l}{2}, y, t - \frac{\Delta t}{2}) \quad \text{for } t - \Delta t \leq \tau \leq t \quad (3.110)$$

$$E_z(x - \frac{\Delta l}{2}, y, \tau) \approx E_z(x - \frac{\Delta l}{2}, y, t - \frac{\Delta t}{2}) \quad \text{for } t - \Delta t \leq \tau \leq t \quad (3.111)$$

we get

$$\begin{aligned} H_y(x, y, t) &\approx \\ H_y(x, y, t - \Delta t) &+ \frac{\Delta t}{\Delta l \cdot \mu_{avgx}(x, y)} \left[E_z(x + \frac{\Delta l}{2}, y, t - \frac{\Delta t}{2}) - E_z(x - \frac{\Delta l}{2}, y, t - \frac{\Delta t}{2}) \right] \end{aligned} \quad (3.112)$$

The term in the brackets is recognized as the average value of the electric field component E_y at (x,y) within the interval $(t-\Delta t, t)$. The above equation can be written in a more compact form using the identity

$$\frac{1}{\mu} = \frac{1}{\mu_0 \mu_r} = \frac{\sqrt{\epsilon_0}}{\sqrt{\epsilon_0}} \frac{1}{\sqrt{\mu_0} \sqrt{\mu_0}} \frac{1}{\mu_r} = \frac{1}{\sqrt{\mu_0 \epsilon_0}} \sqrt{\frac{\epsilon_0}{\mu_0}} \frac{1}{\mu_r} = v_0 Y_0 \frac{1}{\mu_r} \quad (3.113)$$

where the free space velocity of propagation is denoted v_0 , the intrinsic admittance of free space is denoted Y_0 ($Y_0 = \frac{1}{Z_0}$, $Z_0 \approx 377\Omega$) and μ_r denotes relative permeability.

Introducing the grid "propagation" velocity

$$v_{grid} = \frac{\Delta l}{\Delta t} \quad (3.114)$$

we can write the approximate equation for the electric field "update" as

$$H_y(x, y, t) \approx H_y(x, y, t - \Delta t) + Y_0 \frac{v_0}{v_{grid} \mu_{r,avgx}(x, y)} \left\{ E_z(x + \frac{\Delta l}{2}, y, t - \frac{\Delta t}{2}) - E_z(x - \frac{\Delta l}{2}, y, t - \frac{\Delta t}{2}) \right\} \quad (3.115)$$

In the case of free-space ($\mu_r=1$), the equation simplifies to

$$H_y(x, y, t) \approx H_y(x, y, t - \Delta t) + Y_0 \frac{v_0}{v_{grid}} \left[E_z(x + \frac{\Delta l}{2}, y, t - \frac{\Delta t}{2}) - E_z(x - \frac{\Delta l}{2}, y, t - \frac{\Delta t}{2}) \right] \quad (3.116)$$

The above equations are the update equations for the y-directed component of a TM_z magnetic field. Similar equations will be formulated next for the x-directed magnetic field component.

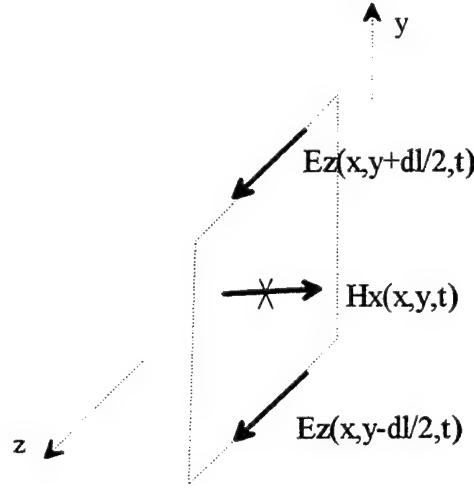


Figure 3.10. A Contour for Updating H_x .

A local coordinate system will be used, with the origin at the center of the contour. Any point (y', z') within or on the contour C_E can be specified by its local coordinates

$$y' = y + \psi \quad z' = z + \zeta \quad \text{where} \quad -\frac{\Delta l}{2} \leq \psi \leq +\frac{\Delta l}{2} \quad \text{and} \quad -\frac{\Delta l}{2} \leq \zeta \leq +\frac{\Delta l}{2}$$

By following the same procedure shown for H_y update equation, we can determine the approximate equation for the H_x magnetic field "updates" as

$$H_x(x, y, t) \approx \quad (3.117)$$

$$H_x(x, y, t - \Delta t) + Y_0 \frac{v_0}{v_{grid}} \frac{1}{\mu_{r,avg}(x, y)} \left\{ E_z(x, y - \frac{\Delta l}{2}, t - \frac{\Delta t}{2}) - E_z(x, y + \frac{\Delta l}{2}, t - \frac{\Delta t}{2}) \right\}$$

In the case of free-space ($\mu_r=1$), the equation simplifies to

$$H_x(x, y, t) \approx H_x(x, y, t - \Delta t) + Y_0 \frac{v_0}{v_{grid}} \left[E_z(x, y - \frac{\Delta l}{2}, t - \frac{\Delta t}{2}) - E_z(x, y + \frac{\Delta l}{2}, t - \frac{\Delta t}{2}) \right] \quad (3.118)$$

The above equations are the update equations for the x-directed component of a TE_z electric field.

B. TRANSPARENT GRID TERMINATION IN 2-D

1. 2-D TE_z and TM_z Grids

The electric and magnetic field update equations have been derived using local coordinate systems, with origins at the centers of the magnetic and electric contours, respectively. These equations now need to be "converted" to a global coordinate system, that is to the grid of equi-distant sampling points in the xy-plane. Since we have either TE_z or TM_z 2-D electromagnetic fields there will be TE_z and TM_z grids as well. Let us assume that our domain is an L by L square. We will assume a uniform grid, that is a discretization step Δl that is not changing with position. The fields are then "sampled" using a spatial step $\Delta l = L/(N-1)$. The electric and magnetic field sample locations are "interleaved", as shown below for $N=5$. The spatial grid edge samples can be, in principle, either electric field samples or magnetic field samples. We will select electric fields for spatial edge samples for TE_z grids and magnetic fields for TM_z grids. The "generic" 2-D grid below is thus applicable to either TE_z or TM_z fields.

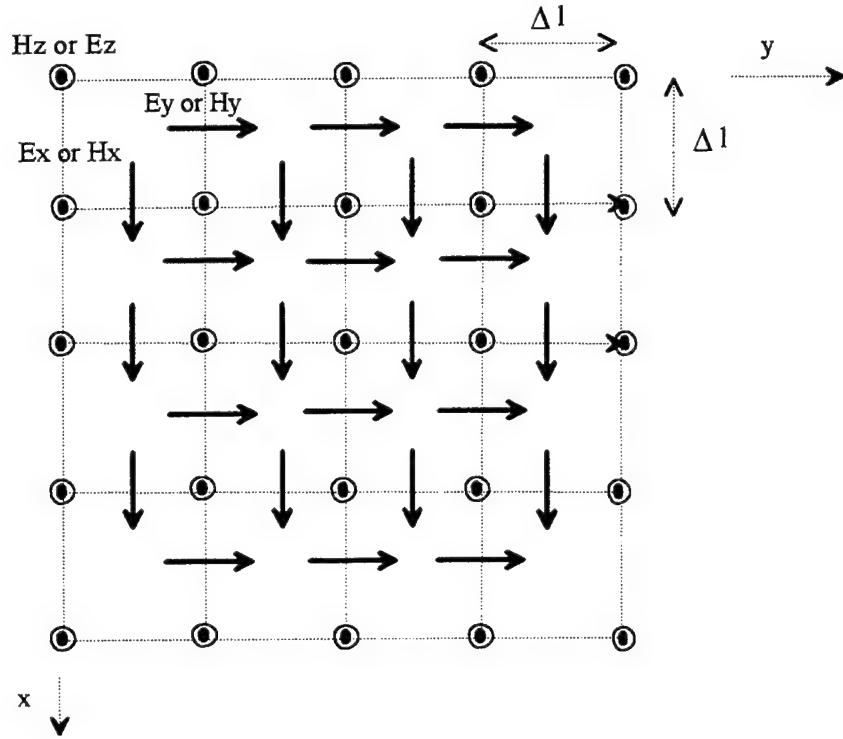


Figure 3.11. 2-D Grid

An $(N \text{ by } N)$ TE_z grid has $(N)(N)$ H_z magnetic field nodes, $(N-2)(N-1)$ E_x electric field nodes, and $(N-1)(N-2)$ E_y electric field nodes. Similarly, an $(N \text{ by } N)$ TM_z grid has $(N-2)(N-1)$ E_z electric field nodes, $(N-1)(N-2)$ H_z magnetic field nodes, and $(N+1)(N)$ H_y magnetic field nodes. TE_z electric and magnetic field "update" equations can now be "converted" to electric and magnetic field grid "update" equations by replacing the variables x , y and t with the grid coordinates of the electric field spatial and temporal sampling points

$$x \rightarrow i\Delta l, i = 0, 1 \dots N \quad y \rightarrow j\Delta l, j = 0, 1 \dots N \quad t \rightarrow n\Delta t, n = 0, 1 \dots N_t$$

The notation can be simplified by omitting the common Δl and Δt terms, and using a superscript for the index of the temporal sampling point. The grid equations for conductive media are obtained from equations (3.62 , 3.65)

$$E_x^n(i,j) \approx \frac{1 - \frac{1}{2} \frac{v_0}{v_{grid}} \frac{Z_0 \cdot \Delta l \cdot \sigma_{avg}(i,j)}{\epsilon_{r,avg}(i,j)}}{1 + \frac{1}{2} \frac{v_0}{v_{grid}} \frac{Z_0 \cdot \Delta l \cdot \sigma_{avg}(i,j)}{\epsilon_{r,avg}(i,j)}} \cdot E_x^{n-1}(x,y) \quad (3.119)$$

$$+ \frac{Z_0 \frac{v_0}{v_{grid}} \frac{1}{\epsilon_{r,avg}(i,j)}}{1 + \frac{1}{2} \frac{v_0}{v_{grid}} \frac{Z_0 \cdot \Delta l \cdot \sigma_{avg}(i,j)}{\epsilon_{r,avg}(i,j)}} \cdot \left[H_z^{n-\frac{1}{2}}(i,j+\frac{1}{2}) - H_z^{n-\frac{1}{2}}(i,j-\frac{1}{2}) \right]$$

$$E_y^n(i,j) \approx \frac{1 - \frac{1}{2} \frac{v_0}{v_{grid}} \frac{Z_0 \cdot \Delta l \cdot \sigma_{avg}(i,j)}{\epsilon_{r,avg}(i,j)}}{1 + \frac{1}{2} \frac{v_0}{v_{grid}} \frac{Z_0 \cdot \Delta l \cdot \sigma_{avg}(i,j)}{\epsilon_{r,avg}(i,j)}} \cdot E_y^{n-1}(i,j) \quad (3.120)$$

$$+ \frac{Z_0 \frac{v_0}{v_{grid}} \frac{1}{\epsilon_{r,avg}(i,j)}}{1 + \frac{1}{2} \frac{v_0}{v_{grid}} \frac{Z_0 \cdot \Delta l \cdot \sigma_{avg}(i,j)}{\epsilon_{r,avg}(i,j)}} \cdot \left[H_z^{n-\frac{1}{2}}(i-\frac{1}{2},j) - H_z^{n-\frac{1}{2}}(i+\frac{1}{2},j) \right]$$

$$H_z^n(i,j) \approx H_z^{n-1}(i,j) - Y_0 \frac{v_0}{v_{grid}} \frac{1}{\mu_{r,avg}(i,j)} \times \quad (3.121)$$

$$\left[E_x^{n-\frac{1}{2}}(i,j-\frac{1}{2}) - E_x^{n-\frac{1}{2}}(i,j+\frac{1}{2},t) + E_y^{n-\frac{1}{2}}(i+\frac{1}{2},j) - E_y^{n-\frac{1}{2}}(i-\frac{1}{2},j) \right]$$

The TE_z electric and magnetic field grid update equations for non-conductive media ($\sigma=0$) are

$$E_x^n(i,j) \approx E_x^{n-1}(i,j) + Z_0 \frac{v_0}{v_{grid}} \frac{1}{\epsilon_{r,avg}(i,j)} \cdot \left[H_z^{n-\frac{1}{2}}(i,j+\frac{1}{2}) - H_z^{n-\frac{1}{2}}(i,j-\frac{1}{2}) \right] \quad (3.122)$$

$$E_y^n(i,j) \approx E_y^{n-1}(i,j) + Z_0 \frac{v_0}{v_{grid}} \frac{1}{\epsilon_{r,avg}(i,j)} \cdot \left[H_z^{n-\frac{1}{2}}(i-\frac{1}{2},j) - H_z^{n-\frac{1}{2}}(i+\frac{1}{2},j) \right] \quad (3.123)$$

$$H_z^n(i,j) = H_z^{n-1}(i,j) + Y_0 \frac{v_0}{v_{grid} \mu_{r,avg}(i,j)} \times \quad (3.124)$$

$$\left[E_x^{n-\frac{1}{2}}(i,j+\frac{1}{2}) - E_x^{n-\frac{1}{2}}(i,j-\frac{1}{2}) + E_y^{n-\frac{1}{2}}(i-\frac{1}{2},j) - E_y^{n-\frac{1}{2}}(i+\frac{1}{2},j) \right]$$

Finally, the free-space TE_z grid equations are

$$E_x^n(i,j) \approx E_x^{n-1}(i,j) + Z_0 \frac{v_0}{v_{grid}} \cdot \left[H_z^{n-\frac{1}{2}}(i,j+\frac{1}{2}) - H_z^{n-\frac{1}{2}}(i,j-\frac{1}{2}) \right] \quad (3.125)$$

$$E_y^n(i,j) \approx E_y^{n-1}(i,j) + Z_0 \frac{v_0}{v_{grid}} \cdot \left[H_z^{n-\frac{1}{2}}(i-\frac{1}{2},j) - H_z^{n-\frac{1}{2}}(i+\frac{1}{2},j) \right] \quad (3.126)$$

$$H_z^n(i,j) = \quad (3.127)$$

$$H_z^{n-1}(i,j) + Y_0 \frac{v_0}{v_{grid}} \cdot \left[E_x^{n-\frac{1}{2}}(i,j+\frac{1}{2}) - E_x^{n-\frac{1}{2}}(i,j-\frac{1}{2}) + E_y^{n-\frac{1}{2}}(i-\frac{1}{2},j) - E_y^{n-\frac{1}{2}}(i+\frac{1}{2},j) \right]$$

Dual TM_z grid equations for conducting media are

$$H_x^n(i,j) = H_x^{n-1}(i,j) + Y_0 \frac{v_0}{v_{grid} \mu_{r,avg}(i,j)} \cdot \left[E_z^{n-\frac{1}{2}}(i,j-\frac{1}{2}) - E_z^{n-\frac{1}{2}}(i,j+\frac{1}{2}) \right] \quad (3.128)$$

$$H_y^n(i,j) = H_y^{n-1}(i,j) + Y_0 \frac{v_0}{v_{grid} \mu_{r,avg}(i,j)} \cdot \left[E_z^{n-\frac{1}{2}}(i+\frac{1}{2},j) - E_z^{n-\frac{1}{2}}(i-\frac{1}{2},j) \right] \quad (3.129)$$

$$E_z^n(i,j) \approx \frac{1 - \frac{1}{2} \frac{v_0}{v_{grid}} \frac{Z_0 \cdot \sigma_{avg}(i,j) \cdot \Delta l}{\epsilon_{r,avg}(i,j)}}{1 + \frac{1}{2} \frac{v_0}{v_{grid}} \frac{Z_0 \cdot \sigma_{avg}(i,j) \cdot \Delta l}{\epsilon_{r,avg}(i,j)}} \cdot E_z^{n-1}(i,j) + \quad (3.130)$$

$$\frac{Z_0 \frac{v_0}{v_{grid} \epsilon_{r,avg}(i,j)}}{1 + \frac{1}{2} \frac{v_0}{v_{grid}} \frac{Z_0 \cdot \sigma_{avg}(i,j) \cdot \Delta l}{\epsilon_{r,avg}(i,j)}} \cdot \left[H_x^{n-\frac{1}{2}}(i,j-\frac{1}{2}) - H_x^{n-\frac{1}{2}}(i,j+\frac{1}{2}) + H_y^{n-\frac{1}{2}}(i+\frac{1}{2},j) - H_y^{n-\frac{1}{2}}(i-\frac{1}{2},j) \right]$$

The TM_z electric field grid equation simplifies for non-conductive media

$$E_z^n(i,j) \approx E_z^{n-1}(i,j) + Z_0 \frac{v_0}{v_{grid} \epsilon_{r,avg}(i,j)} \times \quad (3.131)$$

$$\left[H_x^{n-\frac{1}{2}}(i,j-\frac{1}{2}) - H_x^{n-\frac{1}{2}}(i,j+\frac{1}{2}) + H_y^{n-\frac{1}{2}}(i+\frac{1}{2},j) - H_y^{n-\frac{1}{2}}(i-\frac{1}{2},j) \right]$$

Finally, the free-space TM_z grid equations are

$$H_x^n(i,j) = H_x^{n-1}(i,j) + Y_0 \frac{v_0}{v_{grid}} \cdot \left[E_z^{n-\frac{1}{2}}(i,j-\frac{1}{2}) - E_z^{n-\frac{1}{2}}(i,j+\frac{1}{2}) \right] \quad (3.132)$$

$$H_y^n(i,j) = H_y^{n-1}(i,j) + Y_0 \frac{v_0}{v_{grid}} \cdot \left[E_z^{n-\frac{1}{2}}(i+\frac{1}{2},j) - E_z^{n-\frac{1}{2}}(i-\frac{1}{2},j) \right] \quad (3.133)$$

$$E_z^n(i,j) \approx E_z^{n-1}(i,j) + Z_0 \frac{v_0}{v_{grid}} \cdot \left[H_x^{n-\frac{1}{2}}(i,j-\frac{1}{2}) - H_x^{n-\frac{1}{2}}(i,j+\frac{1}{2}) + H_y^{n-\frac{1}{2}}(i+\frac{1}{2},j) - H_y^{n-\frac{1}{2}}(i-\frac{1}{2},j) \right] \quad (3.134)$$

Note that TE_z electric and magnetic field grid equations in 2-D have the following general form

$$E_x^{new} = C_{Ex1} E_x^{old} + C_{Ex2} \nabla H_z^{old} \quad (3.135)$$

$$E_y^{new} = C_{Ey1} E_y^{old} + C_{Ey2} \nabla H_z^{old} \quad (3.136)$$

$$H_z^{new} = C_{H1} H_z^{old} + C_{Hx2} \nabla E_x^{old} + C_{Hy2} \nabla E_y^{old} \quad (3.137)$$

where C's are constants (real numbers) that depend on the media properties and the velocity ratio v_0/v_{grid} , and "del" operator represents the spatial derivative (gradient).

Similarly, the TM_z electric and magnetic field equations can be written as

$$H_x^{new} = C_{Hx1} H_x^{old} + C_{Hx2} \nabla E_z^{old} \quad (3.138)$$

$$H_y^{new} = C_{Hy1} H_y^{old} + C_{Hy2} \nabla E_z^{old} \quad (3.139)$$

$$E_z^{new} = C_{E1} E_z^{old} + C_{Ex2} \nabla H_x^{old} + C_{Ey2} \nabla H_y^{old} \quad (3.140)$$

2. 2-D Grid Termination

The grid equations derived previously are valid for all the nodes *except* for the nodes on the grid edges. The reason is that a grid edge node for a field component in a transverse-to-z plane has only one neighbor node instead of four like a node that is not on the grid edge, as shown below.

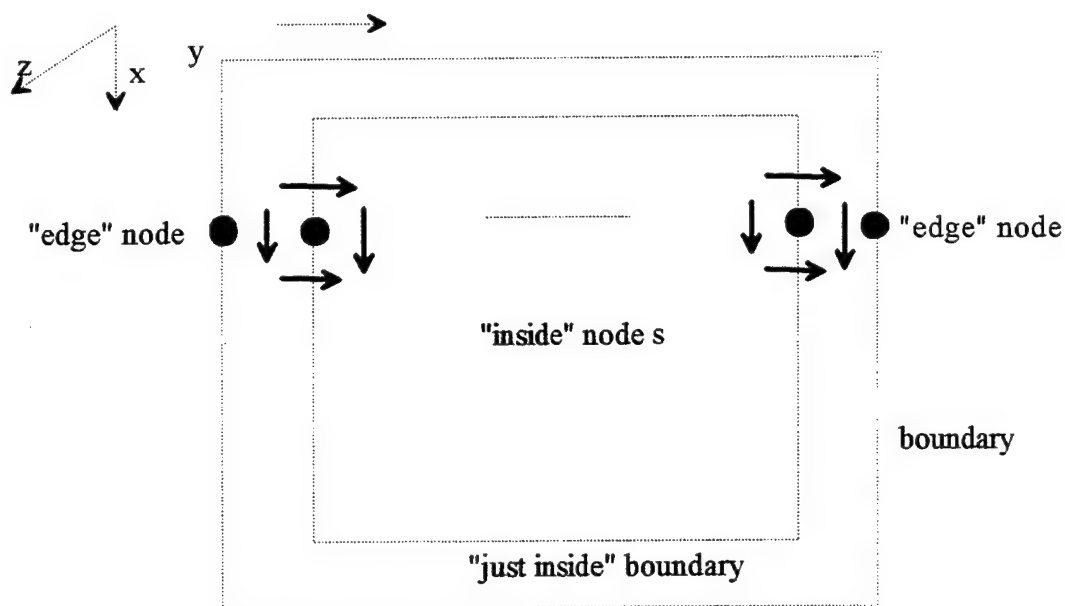


Figure 3.12. Edge Nodes of a 2-D Grid.

An equation for the circulation of the z -directed field component can not be written for an edge node because a z -directed field component on the edge shown in the figure above can not be updated using the grid equations discussed so far. Extending the ideas of transparent grid termination (TGT) and the discrete boundary impulse response (DBIR) applied for 1-D problems, the update equations for edge nodes can be devised based upon convolutions of the fields one layer inward and the pre-calculated impulse responses from the inward layer to the grid edge nodes. An edge field will be expressed as a superposition of responses, as illustrated in the figure below for a top edge grid node. (The same applies to other edge nodes as well.)

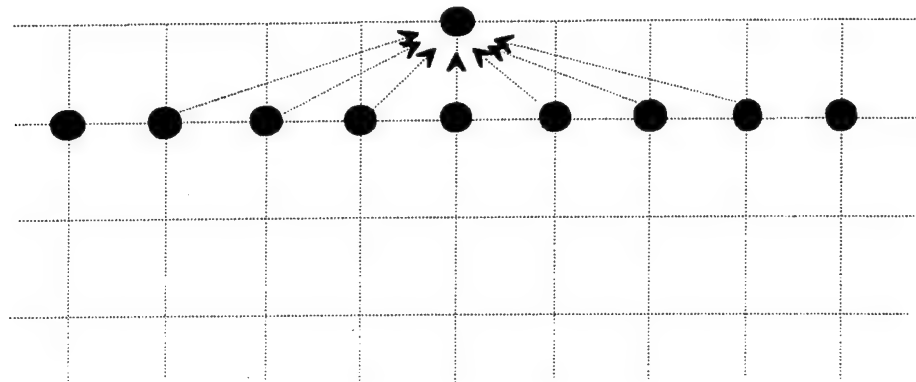


Figure 3.13. Edge Field as a Superposition of Responses.

The superposition can be also "visualized" using the concept of a multiport . The nodes on grid edges can be considered as output ports of a linear multi-port. Assuming, for simplicity, that the grid is square with N edge field nodes on each side, the total number of output ports will be $4(N-1)$. The nodes on the layer just inside the grid boundary will be considered as input ports of the linear multiport. There will be a total of $4(N-3)$ input ports. The equivalent multiport is shown below.

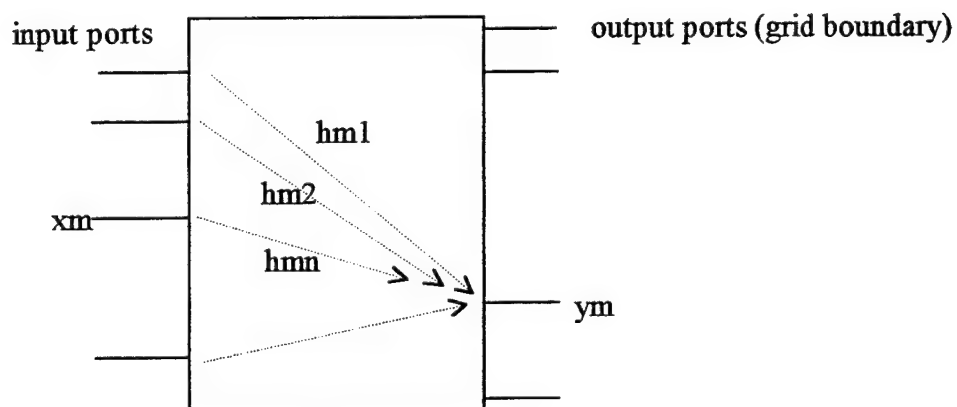


Figure 3.14. Modeling 2-D Grid Boundary as a Multiport.

The input and output fields can be either electric or magnetic fields. Furthermore, the input and output fields need not be of the same "kind", that is the input fields could be, in principle, E-fields and the output fields could be H-fields, or vice versa. However, we will select the input and output fields to be of the same "kind", that is either all E or all H fields, such that the impulse responses $h_{m,n}(t)$ will be "dimensionless". The input and output fields will be H-fields for TE_z and E-fields for TM_z fields. In this manner, the same impulse responses $h_{m,n}(t)$ can be used for both TE_z and TM_z grids. The equations will be derived for TE_z fields, that is with electric fields at the grid edges. Dual equations for the TM_z fields can be obtained simply by replacing E's with H's in the TE_z equations.

There are four sides of the square grid boundary. The top side has the electric field $E_z(0,y,t)$, the bottom side has the electric field $E_z(L,y,t)$, the left side has the electric field $E_z(x,0,t)$, and the right side has the electric field $E_z(x,L,t)$. The layer just inside will have the corresponding fields as $E_z(\Delta l,y,t)$, $E_z(L-\Delta l,y,t)$, $E_z(x,\Delta l,t)$, and $E_z(x,L-\Delta l,t)$. The limits on the values of x and y for the edges are 0 and L ($0 \leq x,y \leq L$), while the limits for the layer just inside are Δl and $L-\Delta l$ ($\Delta l \leq x,y \leq L-\Delta l$). Using the grid coordinates (i,j) the fields on the grid boundary will be, starting at the upper left corner (coordinates 0,0) and using a clockwise reference direction $E_z^n(0,j), E_z^n(i, N-1), E_z^n(N-1,j), E_z^n(i, 0)$. These can be grouped into a "vector" of electric fields on the grid boundary

$$E_{boundary}(t) = [E_z(0,j,t) \ E_z(i, N-1,t) \ E_z(N-1,j,t) \ E_z(i, 0,t)]^T \quad (3.141)$$

where T indicates transposition (the vector is a column vector, but it has been written as a transpose of a row vector to save space). In an analogous manner an electric field vector can be formed for the layer just inside the grid boundary

$$E_{just_inside}(t) = [E_z(1,j,t) \ E_z(i, N-2,t) \ E_z(N-2,j,t) \ E_z(i, 1,t)]^T \quad (3.142)$$

The advantage of the vector arrangement is that we can now use a single index (say index m) to identify a field on the grid boundary and another single index (say index n) to identify an electric field on the layer just inside the grid boundary. The use of single indices m and n allows for a direct and compact reference to the multiport representation of the grid termination problem. The electric field on the grid boundary $E_{\text{boundary}}(t)$ can be expressed as a convolution of the electric fields at the layer just inside the grid boundary $E_{\text{just_inside}}(t)$ and a *matrix* of impulse responses $H(t)$.

$$E_{\text{boundary}}(t) = H(t) * E_{\text{just_inside}}(t) \quad (3.143)$$

where the $4(N-1)$ by $4(N-3)$ matrix of impulse responses can be written as

$$H(t) = \begin{bmatrix} h_{1,1}(t) & h_{1,2}(t) & h_{1,3}(t) & . & . & . & . & h_{1,4(N-3)}(t) \\ h_{2,1}(t) & . & . & . & . & . & . & h_{2,4(N-3)}(t) \\ . & . & . & . & . & . & . & . \\ . & . & . & . & . & . & . & . \\ . & . & . & . & . & . & . & . \\ . & . & . & . & . & . & . & . \\ . & . & . & . & . & . & . & . \\ h_{4(N-1),1}(t) & h_{4(N-1),2}(t) & . & . & . & . & . & h_{4(N-1),4(N-3)}(t) \end{bmatrix} \quad (3.144)$$

The electric field at a boundary node (identified by a particular value of the index m) can be written as the product of the m -th row of the impulse response matrix $H(t)$ and the column vector of the electric fields just inside the boundary (identified by index n)

$$E_{\text{boundary}}(m, t) = \quad (3.145)$$

$$\sum_{n=1}^{n=4(N-3)} h_{m,n}(t) * E_{\text{just_inside}}(n, t) = \sum_{n=1}^{n=4(N-3)} \int_0^t E_{\text{just_inside}}(n, \tau) \cdot h_{m,n}(t - \tau) d\tau$$

where the summation is over all the nodes on the layer just inside the boundary. The discretized forms of the above equations, involving samples of electric fields at $t=k\Delta t$, are

the sums of discrete convolutions. Since a discrete convolution is itself a sum, the result for the boundary nodes will involve double summations (the expression below uses superscripts for time samples and convolution summation).

$$E_{boundary}^k(m) = \sum_{n=1}^{n=4(N-3)} \sum_{p=0}^{p=k} E_{just_inside}^p(n) \cdot h_{m,n}^{k-p} \quad (3.146)$$

The convolution equations express the fields at the edges as weighted sums (the weighting coefficients are the values of the discrete boundary impulse responses $h_{m,n}$) of the time histories of the fields "just inside" the grid. In that respect they are equations of the same type as the equations for the non-edge grid nodes (equations ?? and ??), except that they involve, in general, summations with many more terms. However, the impulse responses $h_{m,n}(t)$ converge to zero relatively fast which effectively reduces the number of significant terms in the convolution sums. The convolution sums can thus be truncated such that only a certain number of the most recent values of the electric fields just inside the boundary are needed (this reduces the number of electric fields that have to be stored and updated). The discrete boundary impulse responses $h_{m,n}(k\Delta t)$ need to be determined (and saved) only once, just like in 1-D, for a selected grid velocity $v_{grid} = \Delta l / \Delta t$. The impulse responses can be stored in a rectangular matrix form. A particularly suitable matrix form would have $4(N-1)$ rows, one row per boundary node, and $4(N-3)N_b$ columns, where N_b denotes the "truncated" length of the discrete boundary impulse responses. This form is suitable because the boundary electric fields can then be calculated as a product of such a matrix and a column vector constructed of $4(N-3)$ subvectors of length N_b . The subvectors represent the N_b most recent values of the

electric field at nodes just inside the boundary. (The choice of N_b depends on the desired amplitude "resolution", with the values over 20 giving very good results for $v_{grid}/v_0 = \sqrt{D}$, $D=2$ for two dimensional problems). These subvectors are updated at each time step by shifting all of their values down (that is "further into the past") by one, discarding the last value, and updating the first subvector element with the most recent field value calculated via standard grid update equations. The double summations are thus efficiently executed as matrix-vector multiplications.

The discretized impulse responses $h_{m,n}^k$ are determined in a manner analogous to the 1-D case, using the discrete equivalent of the delta function which we will denote as δ^k . It is convenient to use the equivalent multipoint to explain the procedure. In order to determine the discrete boundary impulse response for a particular input port n , all input ports *except* the n -th input port are set to zero and delta impulse is applied to the n -th input port. Recording all the outputs from $t=0$ to $t=N_b\Delta t$ provides us with $4N$ discrete boundary impulses of duration N_b .

$$E_{just_inside}^k(n) = \delta^k \quad (3.147)$$

$$E_{just_inside}^k(p) = 0 \quad \text{for } p = 1 \dots 4(N-3) \quad \text{and } p \neq n \quad (3.148)$$

The process is repeated $4(N-3)$ times (since there are $4(N-3)$ input ports) and the results are stored in a $4(N-1)$ by $4(N-3)N_b$ matrix. This matrix is then used to implement the transparent grid termination via the matrix multiplication by the $4(N-3)N_b$ column vector of the time-histories of the fields just inside the boundary. Depending on the values of N_b and N , there will be input nodes that are sufficiently far from an output node such that the time it takes for an input impulse to propagate to the output port exceeds N_b . In

such a case, the contribution of such an input node to the output node is known to be zero in advance. This may be used to reduce the number of operations in a TGT implementation. The process of obtaining the 2-D discrete boundary impulse responses is carried out on a "large" grid whose size should be at least $(N+N_b)$ by $(N+N_b)$, or equivalently, the distance from the TGT boundary to the boundary of the "large" grid should be at least $N_b\Delta l/2$. The termination of this "larger" grid (in typical applications $N \gg N_b$ and the "larger" grid would be only incrementally larger) is immaterial, since the reflections off its boundary do not arrive at the output nodes (where they would have corrupted the impulse responses) before the time-stepping has been terminated. When calculating the discrete boundary impulse responses (DBIR), the nodes interior to the TGT boundary need not be updated since all the nodes on the layer just inside the TGT boundary (the input ports) are zero for $t > 0$ (at $t=0$ only one node on the layer just inside the TGT boundary has the value of 1). The DBIR calculations thus require updates only for the nodes between the TGT boundary and the large grid boundary which can result in significant computational time savings if $N \gg N_b$. The update equations used for the region between the "inner" (TGT) and the outer boundaries are the free space equations, since this region is assumed to be free space. (The medium between the two boundaries can be any homogenous medium extending to infinity, but the most practical case is the free space.)

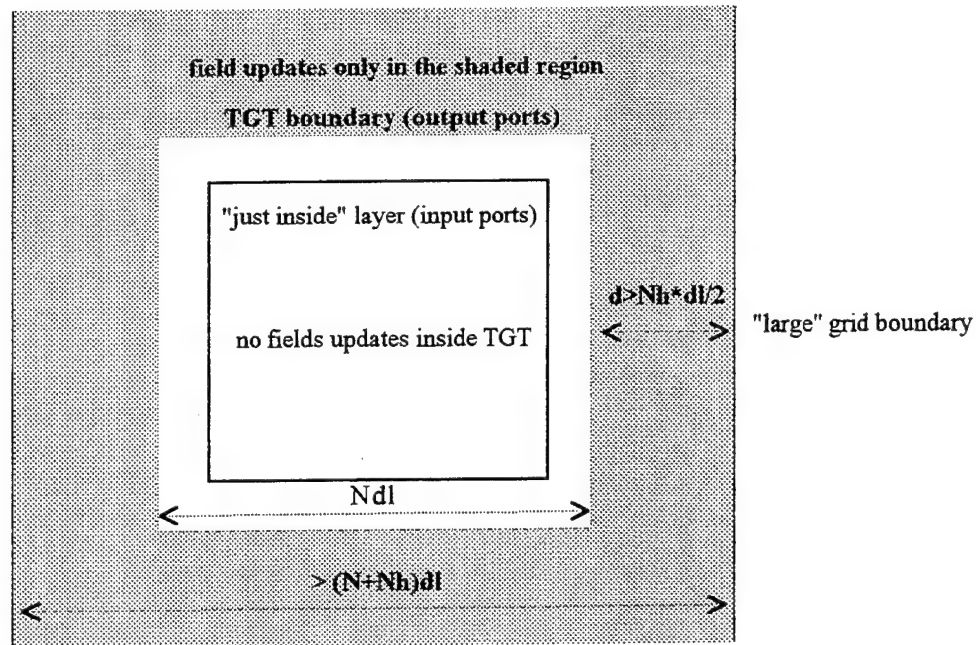


Figure 3.15. 2-D Grid for Calculation of TGT Boundary Impulse Responses.

The shape of the discrete boundary impulse response $h_{mn}(t)$ determined as described in this section will depend on the relative positions of the observation (output, index m) and the source (input, index n) nodes. In general, the more the indices differ from each other the following will be noticed

- the impulse response will start later;
- the maximum value of the impulse response will be smaller;
- the impulse response will be more "spread out" in time.

To illustrate these, three sample impulse responses are shown. The observation point (output port) is the same for all three responses, and is positioned in the center of one side of the TGT boundary. The three discrete boundary impulse responses are the responses to the delta function applied to

- a source (input node) immediately below the output node;
- an input node 5 nodes to the side of the source node immediately below the output node;
- an input node 10 nodes to the side of the source node immediately below the output node.

The velocity ratio v_0/v_{grid} for the DBIR calculations was set to $1/\sqrt{2}$. The plotting program interpolates linearly between the sampling points $k\Delta t$. The impulse response were truncated to a duration of $N_h=40$. Because of the vast change in scale (the largest value of DBIR for a source node just below is $1/2$ while the largest DBIR value for a source 5 nodes to the side is about 25 times smaller, and the largest DBIR value for a source node 10 nodes to the side is about 1,000 times smaller) the impulse responses are shown individually. The rapid decrease of the impulse response peak values with distance offers the possibility to implement TGT using "local" equations instead of using "global" convolutions. An approximate "local" TGT implementation would involve only a few input nodes nearest to an output node, while a "global" TGT implementation involves all input nodes (all the nodes on the layer just inside TGT). The loss of accuracy due to "localization" is not excessive, because of the rapid reduction of the maxima of $h_{m,n}(t)$ as the difference between m and n increases. Finally, the DBIR shown are equally applicable to TE_z and TM_z grids.

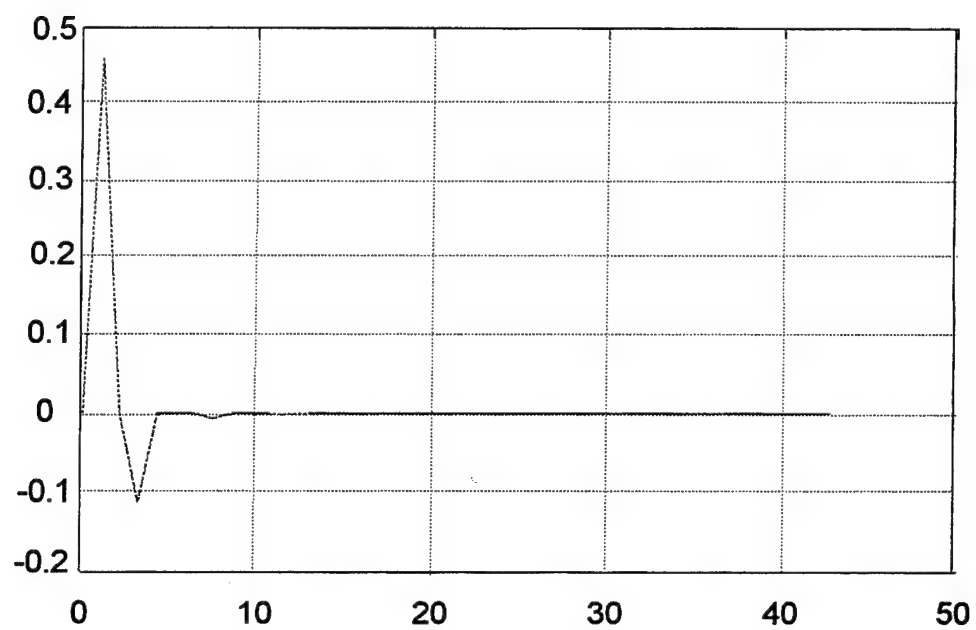


Figure 3.16. DBIR For A Source Node Directly Below An Observation Node.

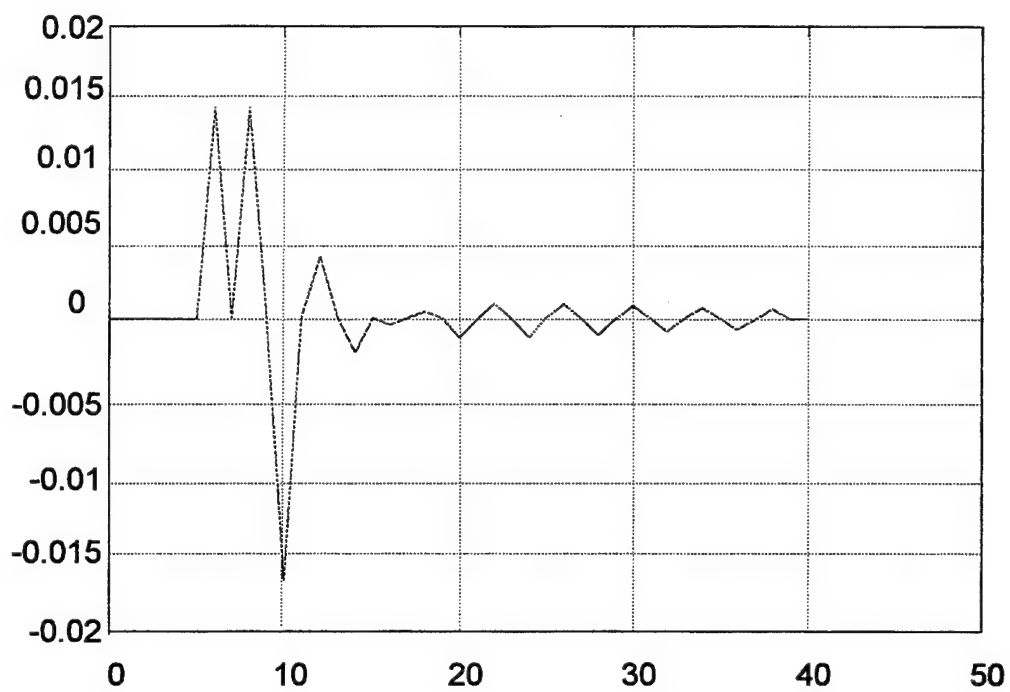


Figure 3.17a. DBIR For A Source Node 5 Nodes to the Side.

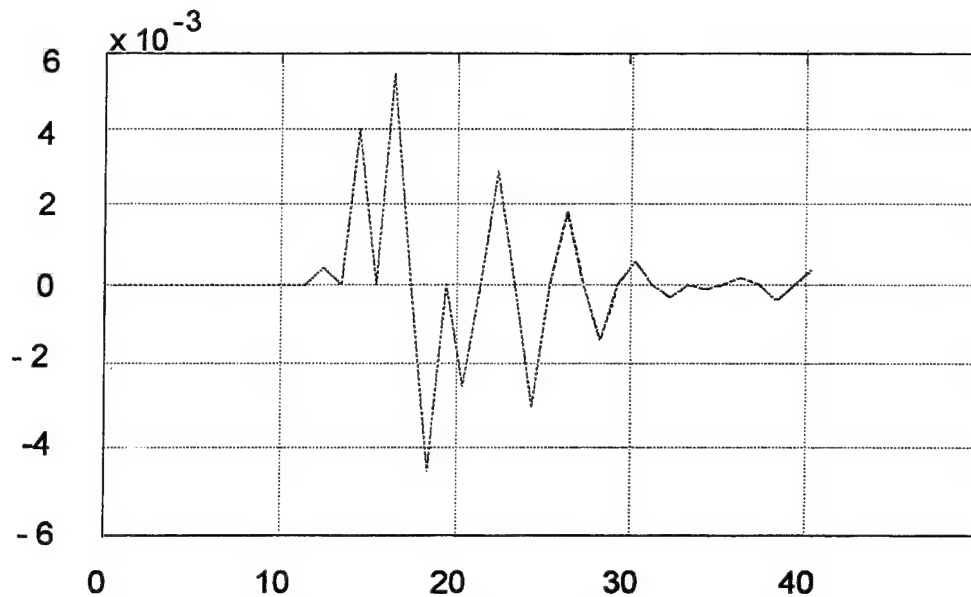


Figure 3.17b. DBIR For A Source Node 10 Nodes to the Side

C. 2-D TGT RESULTS

In order to test the TGT we will use the TM_z grid model shown in Figure 3.11. Therefore, the nodes on the grid edges are E-field nodes. Note that the results would be the same for TE_z fields, with H-fields node on the edges of the grid. The source is a unit-amplitude delta impulse of E_z electric field applied at the center node. The impulse source at the center of the grid gives rise to a cylindrical wave that propagates radially away from the grid's center. The cylindrical wave is not perfect, as its is "distorted" by the grid and develops a "wake" as it propagates through the grid. The cylindrical wave is incident to the TGT boundary. If the TGT were perfect, the total power within the grid would be the same as the total power within the same region for an infinite grid.

However, since the TGT is not perfect (because of truncation of impulse responses) there will be some increase in the total power that comes from the "reflection" off TGT. A measure of TGT performance in 2-D will be the relative increase in the total power, that is the ratio of the power increase for the TGT and the power for an infinite grid. This ratio is a function of time and, since it is normally very small it is best represented in dB

$$Q_{TGT} = 10 \cdot \log_{10} \left(\frac{P_{inf} - P_{TGT}}{P_{inf}} \right)$$

We have denoted this ratio as Q_{TGT} since it expresses the TGT "quality". We will select a square grid with 21 nodes on each side for our 2-D TGT test. The impulse responses will be truncated such that the TGT performance can be observed for various selected impulse response durations. Note that the power within the grid will be the same for the case of an infinite grid and the TGT until the outward-propagating cylindrical wave reaches the TGT. All results will be shown for the case

$$v_{grid} = \sqrt{2} \cdot v_0$$

The grid power and the TGT quality factor Q_{TGT} will be plotted as functions of time, with the coordinate origin ($t=0$) referring to the time when the outgoing cylindrical wave first reaches the TGT.

First, we truncate the impulse responses such that their duration is $t_h = 10\Delta t$. The power within the grid is plotted as well as the power difference and the relative power difference in dB (the Q_{TGT}). The plot of power vs time shows the decrease in power towards 0 as the cylindrical wave leaves the grid. If the grid and the TGT were ideal, the power will be constant until the wave reaches the grid nodes at the centers of each side

(the outgoing wave reaches these nodes first since they are closest to the grid center where the wave has originated). The power will then decrease towards zero as more and more of the wave leaves the grid. Finally, the wave would reach the four corners of the grid (these nodes are the farthest from the grid center and the wave gets to them last) and leave the grid altogether, the power within the grid being zero from then on. However, since neither the grid nor the TGT are perfect, there will be some small "residual" energy within the grid at all times, converging to zero as time progresses. The relative power difference in db (the Q_{TGT}) curve shows that, for $t < t_h$ the power "reflected" off the TGT is about 150 dB *below* the power that the same domain (within the TGT boundary) would have for an infinite grid. For $t > t_h$ the power "reflected" off the TGT is more than 20 dB *below* the power of an infinite grid. This means that the effects of the TGT are about two orders of magnitude smaller than those of the grid "imperfection" for $t > t_h$ and about 15 orders of magnitude smaller for $t < t_h$. The plots for $t_h=20$, $t_h=30$, and $t_h=40$ confirm the above as well. Note that increasing the duration of the impulse response also reduces the "reflections" off TGT for $t > t_h$. Also, note that for a grid of N nodes on the side the duration of impulse responses greater than $2N$ allows for any node on the layer just inside TGT to contribute at least one value to any of the nodes on the TGT (because there are $2N$ nodes from one corner of the TGT to the opposite corner).

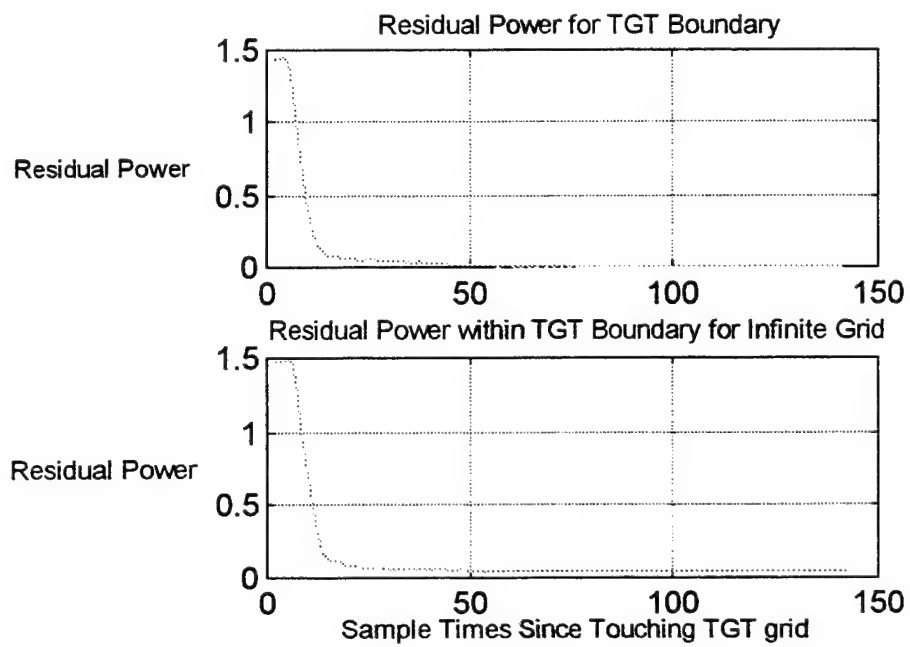


Figure 3.18. Residual Power for $t_b = 3\Delta t$.

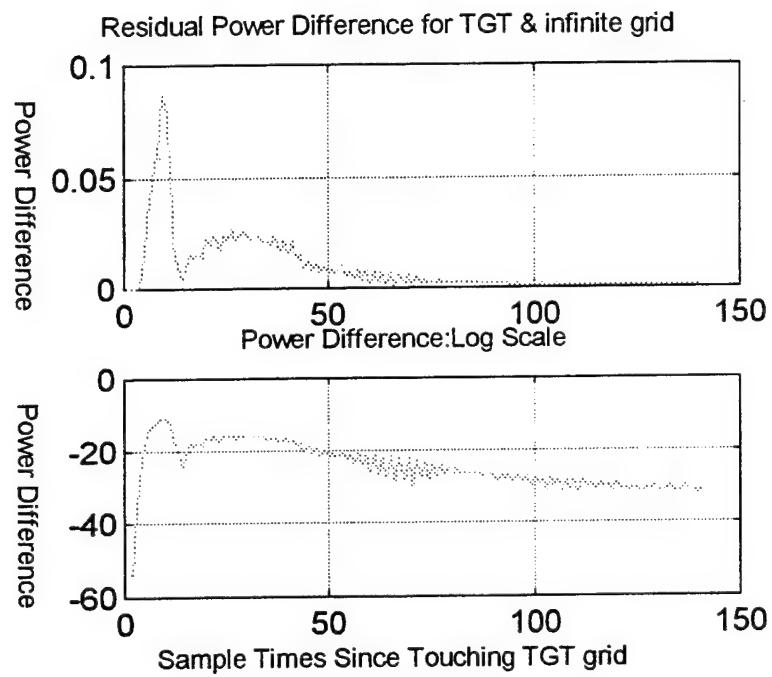


Figure 3.19. Residual Power Difference Between TGT and Infinte Boundary for $t_b=3\Delta t$.

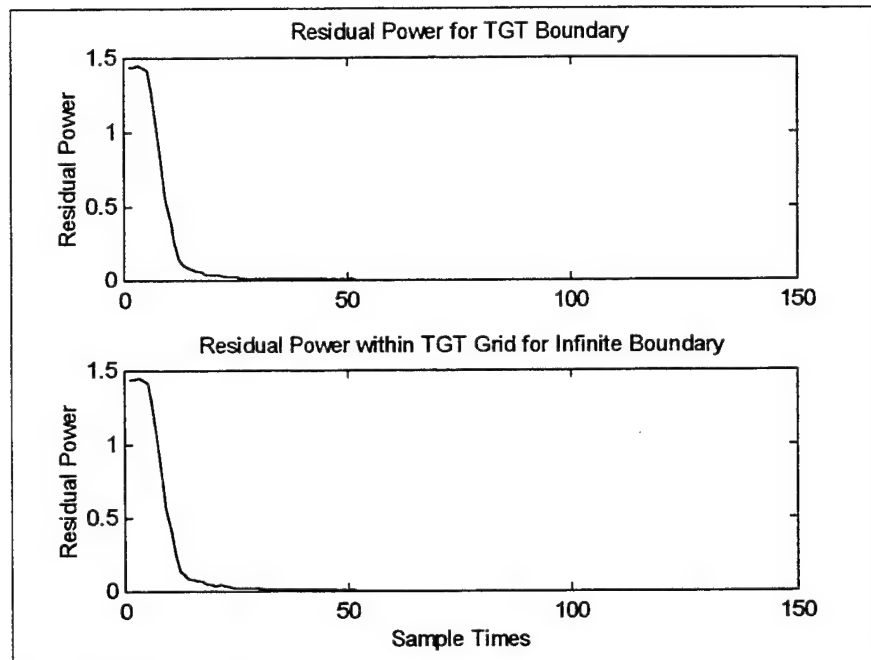


Figure 3.20. Residual Power for $t_b=10\Delta t$.

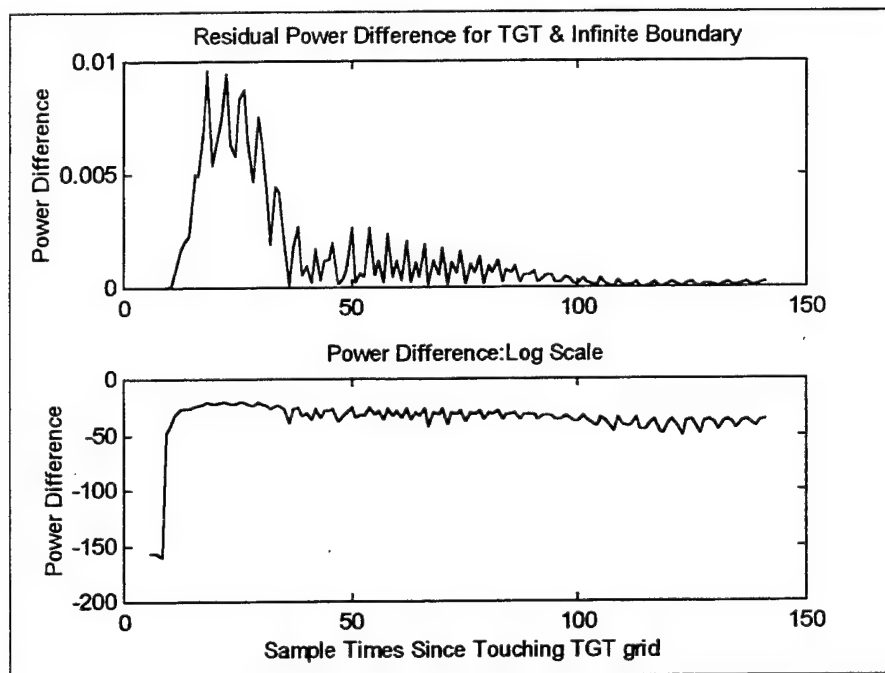


Figure 3.21. Residual Power Difference Between TGT and Infinte Boundary for $t_b=10\Delta t$.

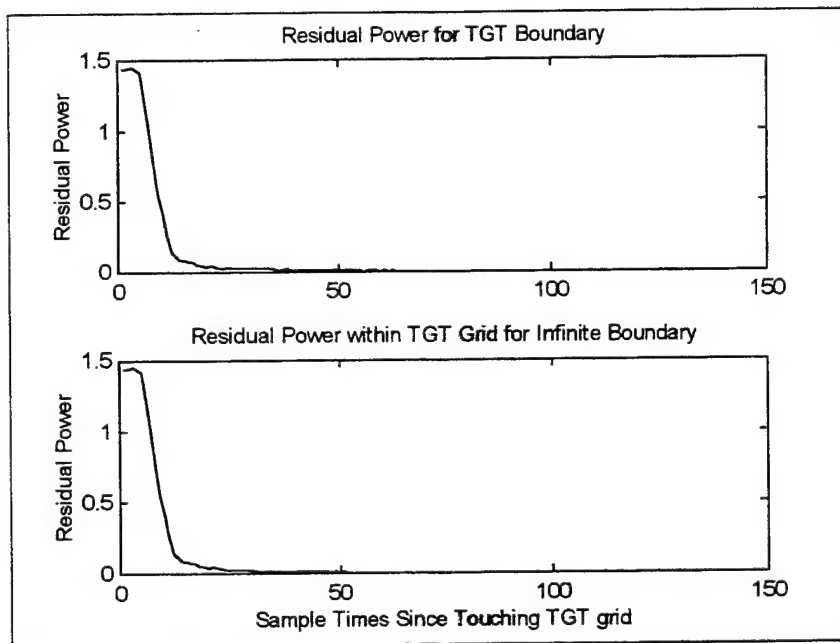


Figure 3.22. Residual Power for $t_b=20\Delta t$.

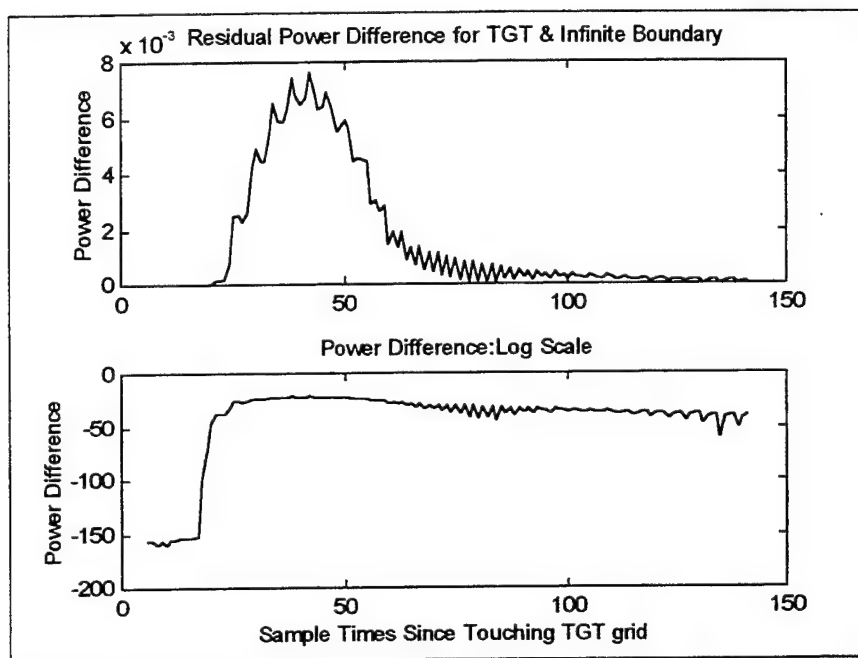


Figure 3.23. Residual Power Difference Between TGT and Infinte Boundary for $t_b=20\Delta t$.

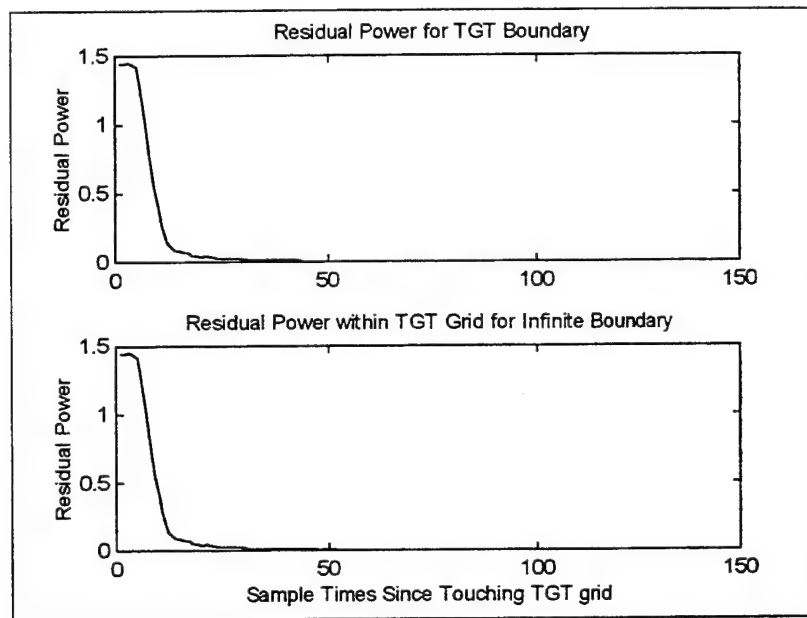


Figure 3.24. Residual Power for $t_b=30\Delta t$.

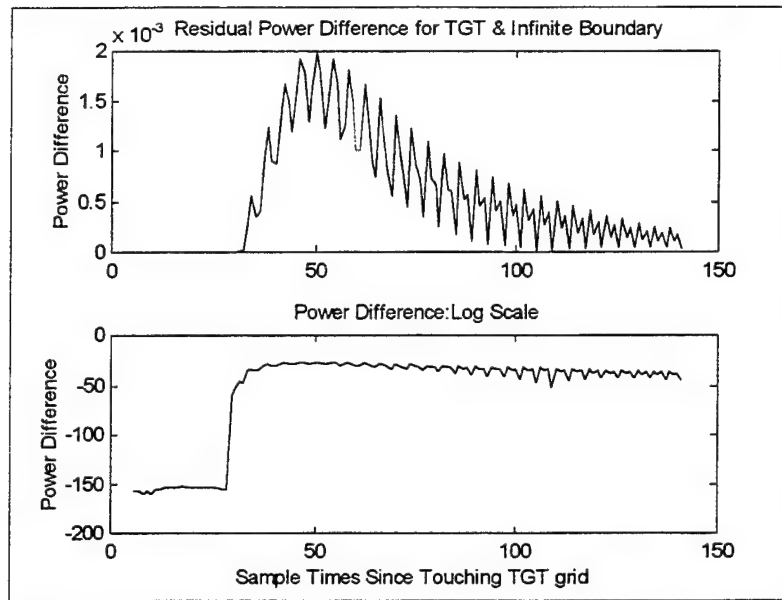


Figure 3.25. Residual Power Difference Between TGT and Infinte Boundary for $t_h=30\Delta t$.

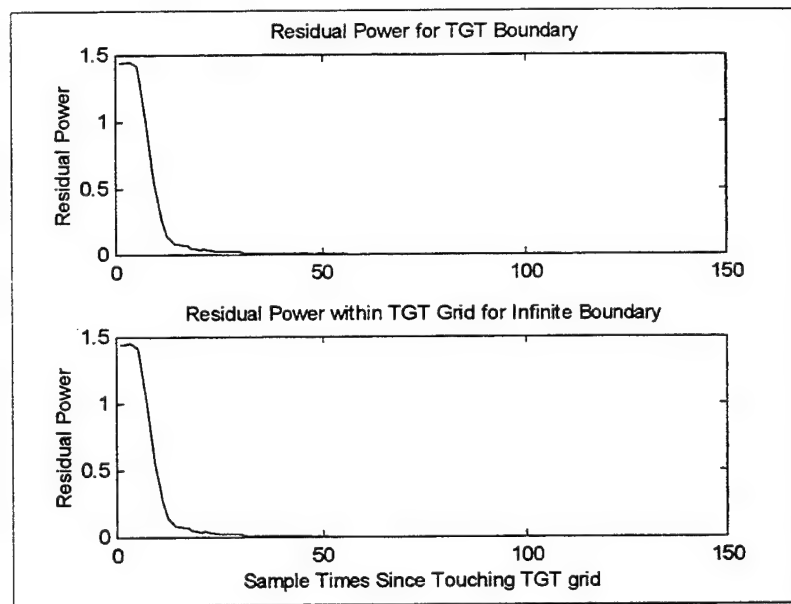


Figure 3.26. Residual Power for $t_b=40\Delta t$.

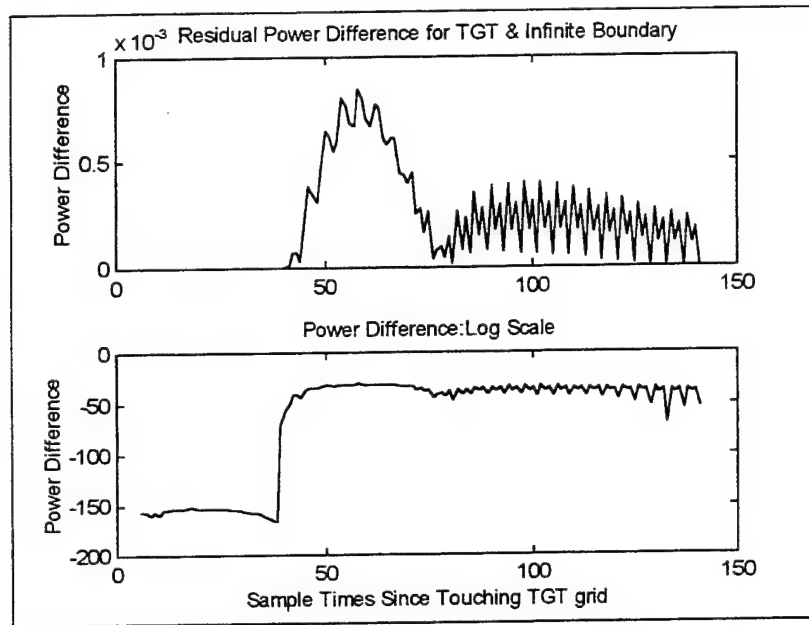


Figure 3.27. Residual Power Difference Between TGT and Infinte Boundary for $t_b = 40\Delta t$.

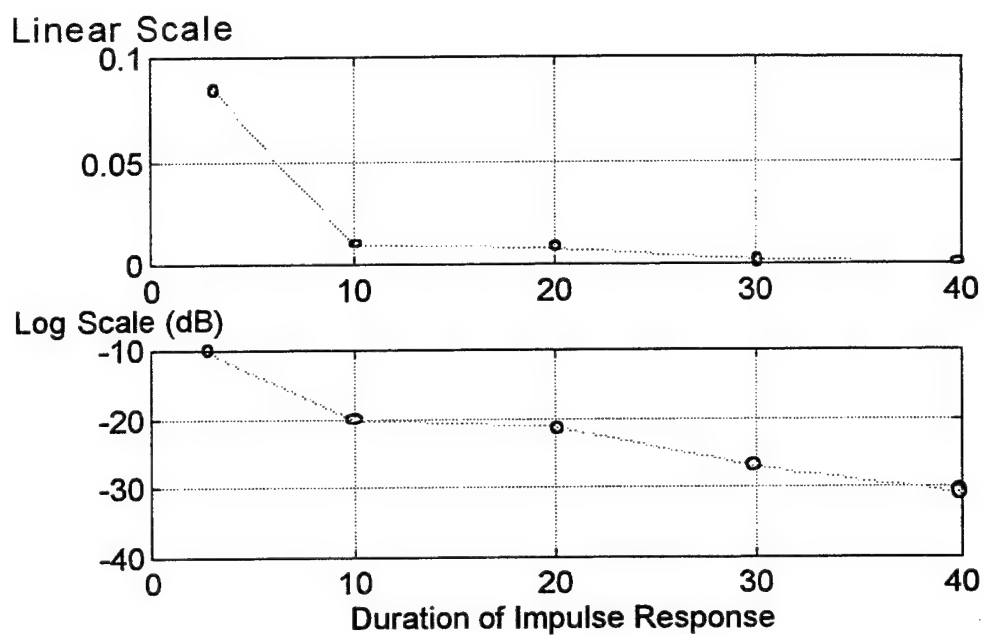


Figure 3.28. Maximum Power Difference Between TGT and Infinte Boundary as a function of Impulse Response Duration (t_b).

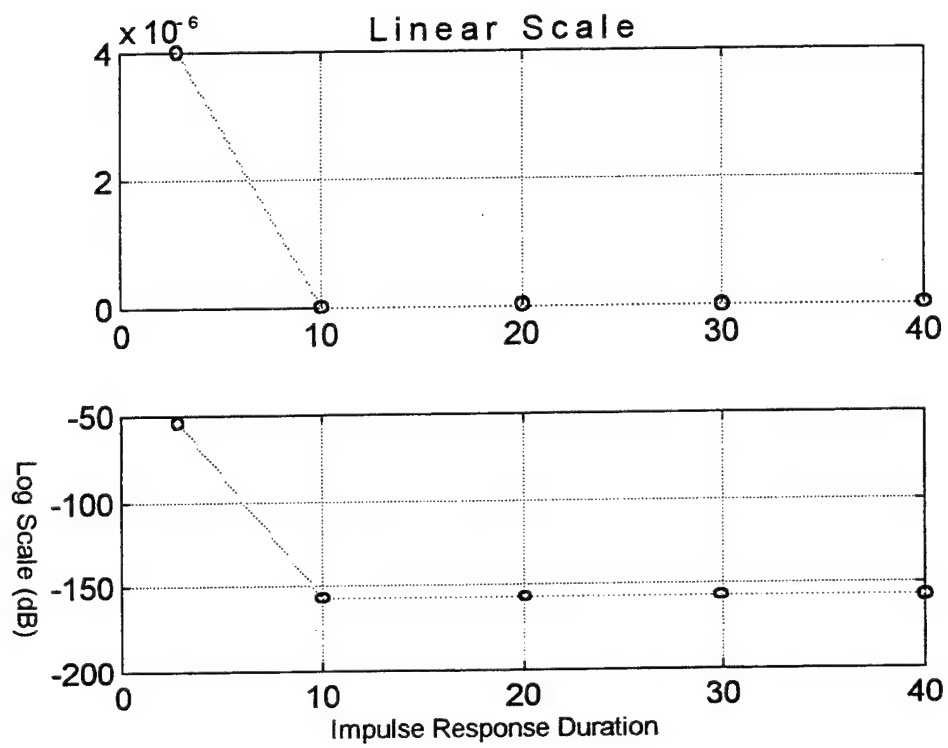


Figure 3.29. Minimum Power Difference Between TGT and Infinte Boundary as a function of Impulse Response Duration (t_b)

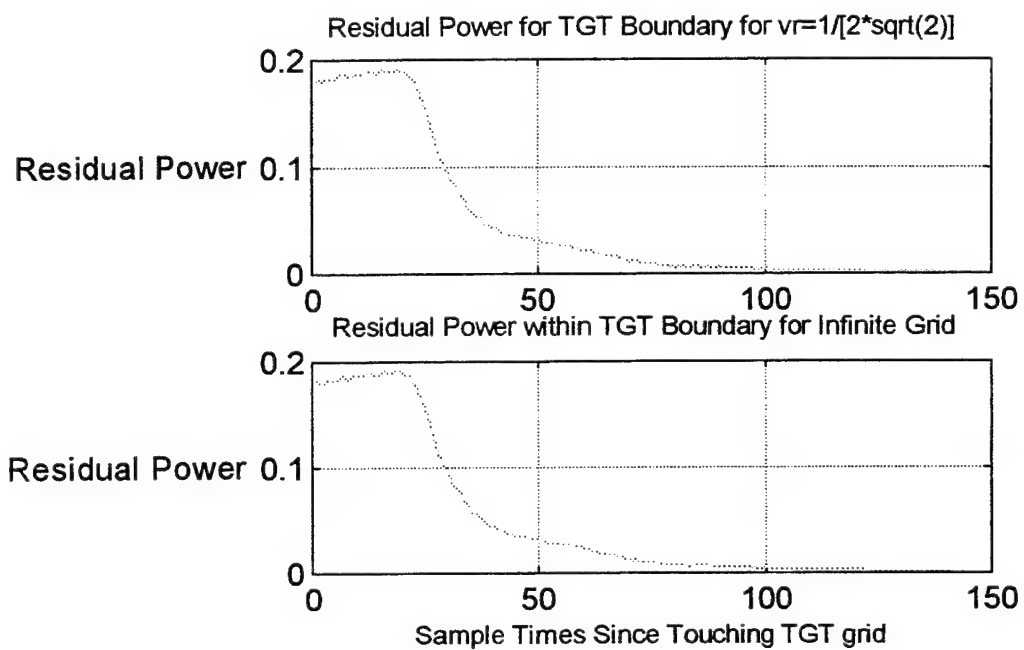


Figure 3.30. Residual Power for $t_b = 40\Delta t$, using $V_r = \frac{1}{2\sqrt{2}}$.

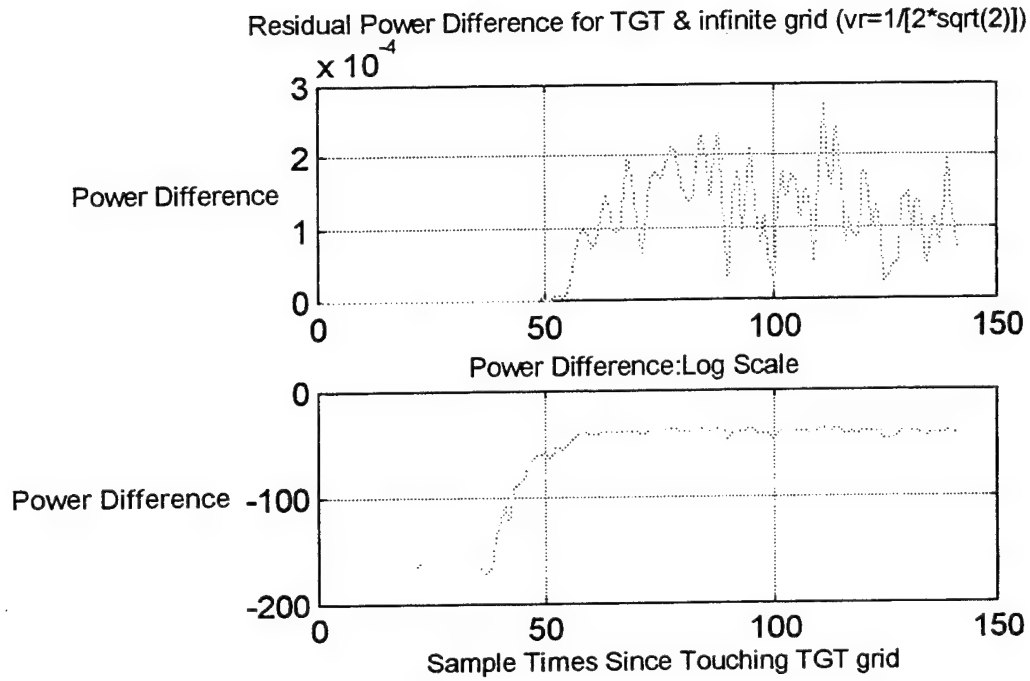


Figure 3.31. Residual Power Difference Between TGT and Infinte Boundary for $t_n = 40\Delta t$,
using $V_r = \frac{1}{2\sqrt{2}}$.

IV. ANALYSIS OF TGT FOR 3-D FD-TD

A. FD-TD FORMULATION IN 3-D

1. FD-TD Equations in 3-D

The incident and the scattered electromagnetic fields and the media parameters in 3-D problems vary with three spatial coordinates (x, y, z) , so the electric and magnetic fields will be functions of the spatial coordinates x, y, z , and time t . A 3-D electric field vector E can be represented in terms of its orthogonal components as shown below

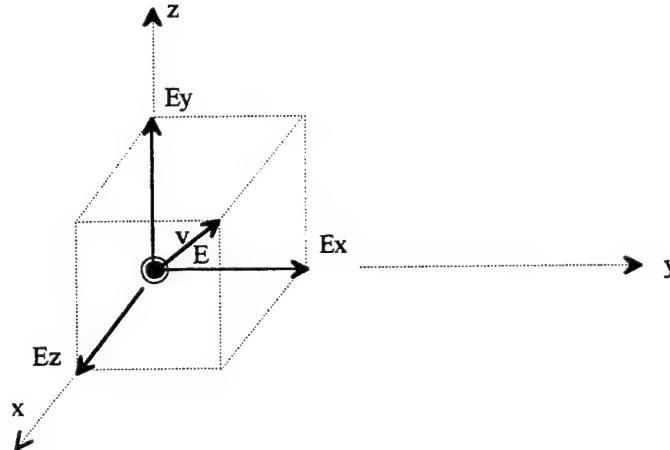


Figure 4.1. Electric Field Vector Components.

$$\vec{E}(x, y, z, t) = E_x(x, y, z, t) \vec{x} + E_y(x, y, z, t) \vec{y} + E_z(x, y, z, t) \vec{z} \quad (4.1)$$

The direction of propagation is indicated by the direction of the velocity of propagation vector \vec{v} . Similarly, for the magnetic field vector H we can write

$$\vec{H}(x, y, z, t) = H_x(x, y, z, t) \vec{x} + H_y(x, y, z, t) \vec{y} + H_z(x, y, z, t) \vec{z} \quad (4.2)$$

The electric and magnetic fields are solutions of Maxwell's equations

$$\oint_{C_E} \overrightarrow{E(x,y,z,t)} \cdot \overrightarrow{dl_E} = -\frac{\partial}{\partial t} \left\{ \iint_{S_E} \overrightarrow{B} \cdot \overrightarrow{ds_E} \right\} = -\frac{\partial}{\partial t} \left\{ \iint_{S_E} \mu(x,y,z) \overrightarrow{H(x,y,z,t)} \cdot \overrightarrow{ds_E} \right\} \quad (4.3)$$

$$\oint_{C_H} \overrightarrow{H(x,y,z,t)} \cdot \overrightarrow{dl_H} = \frac{\partial}{\partial t} \left\{ \iint_{S_H} \epsilon(x,y,z) \overrightarrow{E(x,y,z,t)} \cdot \overrightarrow{ds_H} \right\} + \iint_{S_H} \sigma(x,y,z) \overrightarrow{E(x,y,z,t)} \cdot \overrightarrow{ds_H} \quad (4.4)$$

The second curl equation does not have the source current term, since it has been assumed that there were no source currents in the domain of interest. The contours of integration for the electric and the magnetic field circulations are, in general, different and will thus be labeled C_E for an electric field contour and C_H for a magnetic field contour. Similarly, the surfaces associated with the contours will be labeled S_E for the magnetic flux and S_H for the electric flux. In order to determine the discretized forms of Maxwell's curl equations in the integral form for the 3-D, we will use 3-D Yee electric and magnetic cells [Ref 1]. One such cell is shown below.

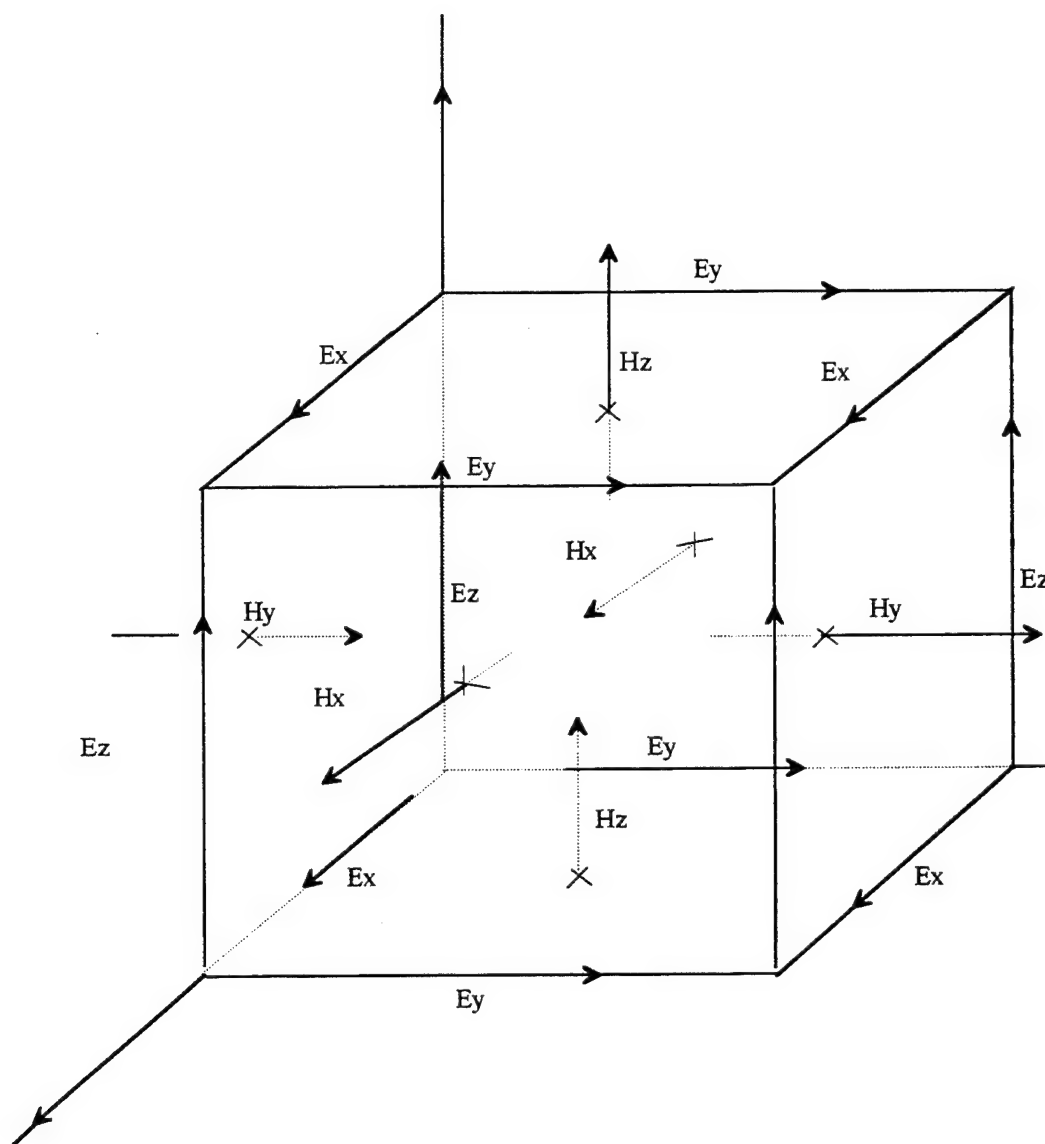


Figure 4.2. Positions of Field Components in a Yee's Electric Cell.

The electric field contours C_E and the magnetic field contours C_H are square (Δl by Δl) contours. The linked C_E and C_H contours are all orthogonal to each other, evoking the

idea of electric and magnetic field linkage in all directions. Based on Yee's cells, the electric and magnetic contours and their associated surfaces will be used to discretize Maxwell's curl equations.

2. Derivation of Magnetic Field Update Equations

We need to derive the update equations for each of the three components of magnetic field vector H . A contour C_E for deriving the update equation for $H_x(x,y,z,t)$ is shown below. This contour can be thought of as the front face of the Yee cell (cube) from the previous figure. Note that the coordinates of the four electric field components are expressed in terms of the coordinates of the contour's center.

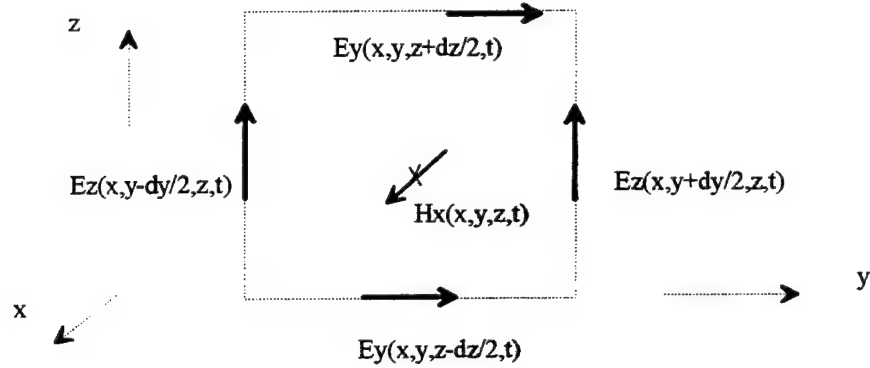


Figure 4.3. A Contour for Updating H_x .

We will assume a uniform grid with $\Delta x = \Delta y = \Delta z = \Delta l$. A local coordinate system (ξ, ψ, ς) will be established, with the origin at the center of the contour. Any point (y', z') within or on the contour C_E can be specified by its local coordinates ξ and ς

$$y' = y + \psi \quad z' = z + \varsigma \quad \text{where} \quad -\frac{\Delta l}{2} \leq \psi \leq +\frac{\Delta l}{2}, \quad -\frac{\Delta l}{2} \leq \varsigma \leq +\frac{\Delta l}{2}$$

The local coordinates will be used in the evaluation of the line and surface integrals that constitute the integral forms of Maxwell's equations. The circulation of the electric field around the electric field contour C_E , assuming counter-clockwise reference direction such that the normal to the surface S_E is in the direction of the magnetic field $\vec{H}_x(x, y, z, t)$, can be evaluated *approximately*, assuming that the electric fields are constant over their respective contour's sides of length Δl

$$\oint_{C_E} \left[E_y(x', y', z', t) \vec{x} + E_z(x', y', z', t) \vec{y} \right] \cdot d\vec{l}_E \approx \left[E_y(x, y, z - \frac{\Delta l}{2}, t) - E_y(x, y, z + \frac{\Delta l}{2}, t) + E_z(x, y + \frac{\Delta l}{2}, t) - E_z(x, y - \frac{\Delta l}{2}, t) \right] \cdot \Delta l \quad (4.5)$$

The magnetic flux through the surface S_E (the right-hand side of the first curl equation) can be calculated using the local coordinates

$$\iint_{S_E} \mu(x', y', z') H_z(x', y', z', t) \vec{z} \cdot d\vec{s}_E = \int_{-\frac{\Delta l}{2}}^{+\frac{\Delta l}{2}} \int_{-\frac{\Delta l}{2}}^{+\frac{\Delta l}{2}} \mu(x, y + \psi, z + \zeta) H_x(x, y + \psi, z + \zeta, t) \vec{x} \cdot \vec{x} d\psi d\zeta \quad (4.6)$$

There are infinitely many ways to model the variation of the magnetic flux density (with respect to local coordinates ψ and ζ) within the contour. We first need to postulate a certain variation of the magnetic field with ψ and ζ such that the integral can be evaluated over S_E . The simplest model assumes that the contour width Δl is small enough such that the magnetic field $H(x, y + \psi, z + \zeta, t)$ within the contour may be assumed constant and equal to the value at the contour's center $H(x, y, z, t)$.

$$H_x(x, y + \psi, z + \zeta, t) \approx H_x(x, y, z, t) \quad (4.7)$$

This is equivalent to using a piece-wise constant (or 2-D "pulse" expansion) approximation of the actual magnetic field variation with respect to y and z . Note that the

above assumption allows that, although the magnetic field is constant within a contour, it can change from one contour to an other. This yields an *approximate* expression for the for the magnetic flux

$$\iint_{S_E} \mu(x', y', z') H_x(x', y', z', t) \vec{z} \cdot d\vec{s}_E \approx H_x(x, y, z, t) \cdot \int_{-\frac{\Delta l}{2}}^{+\frac{\Delta l}{2}} \int_{-\frac{\Delta l}{2}}^{+\frac{\Delta l}{2}} \mu(x, y + \psi, z + \zeta) d\psi d\zeta \quad (4.8)$$

The integral of the permeability $\mu(x, y + \psi, z + \zeta)$ can be re-written in the following manner

$$\int_{-\frac{\Delta l}{2}}^{+\frac{\Delta l}{2}} \int_{-\frac{\Delta l}{2}}^{+\frac{\Delta l}{2}} \mu(x, y + \psi, z + \zeta) d\zeta d\psi = (\Delta l)^2 \cdot \left[\frac{1}{(\Delta l)^2} \int_{-\frac{\Delta l}{2}}^{+\frac{\Delta l}{2}} \int_{-\frac{\Delta l}{2}}^{+\frac{\Delta l}{2}} \mu(x, y + \psi, z + \zeta) d\psi d\zeta \right] \quad (4.9)$$

The term in the brackets is recognized as the permeability μ_{avg} averaged in the y and z-directions within the contour C_E (which is in a $x = \text{const}$ plane)

$$\mu_{avgx}(x, y, z) = \frac{1}{(\Delta l)^2} \int_{-\frac{\Delta l}{2}}^{+\frac{\Delta l}{2}} \int_{-\frac{\Delta l}{2}}^{+\frac{\Delta l}{2}} \mu(x, y + \psi, z + \zeta) d\psi d\zeta \quad (4.10)$$

The approximate expression for the magnetic flux through S_E can now be written using the average permeability as

$$\iint_{S_E} \mu(x', y', z') H_x(x', y', z', t) \vec{z} \cdot d\vec{s}_E \approx (\Delta l)^2 \mu_{avgx}(x, y, z) H_x(x, y, z, t) \quad (4.11)$$

Again, this approximate expression resulted from the piece-wise constant approximation of the magnetic field with respect to y and z-coordinates. The main advantage of the piece-wise constant expansion employed above is its simplicity. The first curl equation of Maxwell can now be replaced by an approximate equation

$$E_y(x, y, z - \frac{\Delta l}{2}, t) - E_y(x, y, z + \frac{\Delta l}{2}, t) + E_z(x, y + \frac{\Delta l}{2}, z, t) - E_z(x, y - \frac{\Delta l}{2}, z, t) \approx -\frac{\partial}{\partial t} \{ [\mu_{avgx}(x, y, z) H_x(x, y, z, t)] \Delta l \} \quad (4.12)$$

which can be simplified (because of media stationarity) to

$$E_y(x, y, z - \frac{\Delta l}{2}, t) - E_y(x, y, z + \frac{\Delta l}{2}, t) + E_z(x, y + \frac{\Delta l}{2}, z, t) - E_z(x, y - \frac{\Delta l}{2}, z, t) \approx -\frac{\partial}{\partial t} \{ H_x(x, y, z, t) \} \cdot \Delta l \cdot \mu_{avgx}(x, y, z) \quad (4.13)$$

This equation can also be re-written as

$$\frac{\partial}{\partial t} \{H_x(x, y, z, t)\} \approx \frac{-1}{\Delta l \cdot \mu_{avgx}(x, y, z)} \left[E_y(x, y, z - \frac{\Delta l}{2}, t) - E_y(x, y, z + \frac{\Delta l}{2}, t) + E_z(x, y + \frac{\Delta l}{2}, z, t) - E_z(x, y - \frac{\Delta l}{2}, z, t) \right] \quad (4.14)$$

The time derivative operator in the above equation is typically replaced by the finite difference approximation [Ref 5]. However, just like in 1-D and 2-D, we present an alternate approach, such that the approximation of the field time variation is shown to be analogous to the approximations already introduced for the field spatial variation. The above equation is integrated with respect to time to get an approximate equation for the magnetic field at the present time t

$$H_x(x, y, z, t) \approx \frac{-1}{\Delta l \cdot \mu_{avgx}(x, y, z)} \times \left[\int_0^t E_y(x, y, z - \frac{\Delta l}{2}, \tau) d\tau - \int_0^t E_y(x, y, z + \frac{\Delta l}{2}, \tau) d\tau + \int_0^t E_z(x, y + \frac{\Delta l}{2}, z, \tau) d\tau - \int_0^t E_z(x, y - \frac{\Delta l}{2}, z, \tau) d\tau \right] \quad (4.15)$$

A similar integral equation can be written for the magnetic field at the same spatial location but at an earlier time $t - \Delta t$

$$H_x(x, y, z, t - \Delta t) \approx \frac{-1}{\Delta l \cdot \mu_{avgx}(x, y, z)} \times \left[\int_0^{t-\Delta t} E_y(x, y, z - \frac{\Delta l}{2}, \tau) d\tau - \int_0^{t-\Delta t} E_y(x, y, z + \frac{\Delta l}{2}, \tau) d\tau + \int_0^{t-\Delta t} E_z(x, y + \frac{\Delta l}{2}, z, \tau) d\tau - \int_0^{t-\Delta t} E_z(x, y - \frac{\Delta l}{2}, z, \tau) d\tau \right] \quad (4.16)$$

Subtracting the two equations we get

$$H_x(x, y, z, t) \approx H_x(x, y, z, t - \Delta t) - \frac{1}{\Delta l \cdot \mu_{avgx}(x, y, z)} \times \left[\int_{t-\Delta t}^t E_y(x, y, z - \frac{\Delta l}{2}, \tau) d\tau - \int_{t-\Delta t}^t E_y(x, y, z + \frac{\Delta l}{2}, \tau) d\tau + \int_{t-\Delta t}^t E_z(x, y + \frac{\Delta l}{2}, z, \tau) d\tau - \int_{t-\Delta t}^t E_z(x, y - \frac{\Delta l}{2}, z, \tau) d\tau \right] \quad (4.17)$$

The integrals on the right-hand side can not be evaluated exactly, because the exact temporal variation of the electric fields within the Δt interval prior to t is generally not known (just like the spatial integral for the magnetic flux could not have been

evaluated exactly because the exact variation of the magnetic field within the contour was not known). However, the integrals can be evaluated approximately by assuming a certain variation of the electric field with the temporal variable τ . The simplest approach, consistent with the assumptions made for the field spatial variation, would be to assume that the interval Δt is small enough such that the electric field can be assumed approximately constant within Δt and equal to the value at the center of the time interval $(t-\Delta t, t)$

$$E_y(x, y, z - \frac{\Delta l}{2}, \tau) \approx E_y(x, y, z - \frac{\Delta l}{2}, t - \frac{\Delta t}{2}) \quad \text{for } t - \Delta t \leq \tau \leq t \quad (4.18)$$

$$E_y(x, y, z + \frac{\Delta l}{2}, \tau) \approx E_y(x, y, z + \frac{\Delta l}{2}, t - \frac{\Delta t}{2}) \quad \text{for } t - \Delta t \leq \tau \leq t \quad (4.19)$$

$$E_z(x, y + \frac{\Delta l}{2}, z, \tau) \approx E_z(x, y + \frac{\Delta l}{2}, z, t - \frac{\Delta t}{2}) \quad \text{for } t - \Delta t \leq \tau \leq t \quad (4.20)$$

$$E_z(x, y - \frac{\Delta l}{2}, z, \tau) \approx E_z(x, y - \frac{\Delta l}{2}, z, t - \frac{\Delta t}{2}) \quad \text{for } t - \Delta t \leq \tau \leq t \quad (4.21)$$

The above represents a piece-wise constant approximation of the electric field variation with respect to the temporal variable t . The approximate expression for the magnetic field at location (x, y, z) and at the time t now becomes

$$H_x(x, y, t) \approx H_x(x, y, t - \Delta t) - \frac{\Delta t}{\Delta l \cdot \mu_{avg}(x, y, z)} \times \quad (4.22)$$

$$\left[E_y(x, y, z - \frac{\Delta l}{2}, t - \frac{\Delta t}{2}) - E_y(x, y, z + \frac{\Delta l}{2}, t - \frac{\Delta t}{2}) + E_z(x, y + \frac{\Delta l}{2}, z, t - \frac{\Delta t}{2}) - E_z(x, y - \frac{\Delta l}{2}, z, t - \frac{\Delta t}{2}) \right]$$

The above equation can be written in a somewhat different form, using the identity

$$\frac{1}{\mu} = \frac{1}{\mu_0} \frac{1}{\mu_r} = \frac{\sqrt{\epsilon_0}}{\sqrt{\epsilon_0}} \frac{1}{\sqrt{\mu_0}} \frac{1}{\sqrt{\mu_0} \mu_r} = \frac{1}{\sqrt{\mu_0 \epsilon_0}} \frac{1}{\sqrt{\frac{\mu_0}{\epsilon_0}}} \frac{1}{\mu_r} = v_0 \frac{1}{Z_0} \frac{1}{\mu_r} = v_0 Y_0 \frac{1}{\mu_r} \quad (4.23)$$

where the free space velocity of propagation is denoted v_0 , the intrinsic impedance of free space is denoted Z_0 ($Z_0 \approx 377\Omega$), and μ_r denotes relative permittivity. Introducing the grid "propagation" velocity

$$v_{grid} = \frac{\Delta l}{\Delta t} \quad (4.24)$$

we can write the approximate "update" equation for the magnetic field as

$$H_x(x,y,z,t) \approx H_x(x,y,z,t-\Delta t) - Y_0 \left(\frac{v_0}{v_{grid}} \right) \frac{1}{\mu_{r,avgx}(x,y,z)} \times \quad (4.25)$$

$$\left[E_y(x,y,z-\frac{\Delta t}{2},t-\frac{\Delta t}{2}) - E_y(x,y,z+\frac{\Delta t}{2},t-\frac{\Delta t}{2}) + E_z(x,y+\frac{\Delta t}{2},z,t-\frac{\Delta t}{2}) - E_z(x,y-\frac{\Delta t}{2},z,t-\frac{\Delta t}{2}) \right]$$

The equation simplifies for the case of non-magnetic media ($\mu_r=1$)

$$H_x(x,y,z,t) \approx H_x(x,y,z,t-\Delta t) - Y_0 \left(\frac{v_0}{v_{grid}} \right) \times \quad (4.26)$$

$$\left[E_y(x,y,z-\frac{\Delta t}{2},t-\frac{\Delta t}{2}) - E_y(x,y,z+\frac{\Delta t}{2},t-\frac{\Delta t}{2}) + E_z(x,y+\frac{\Delta t}{2},z,t-\frac{\Delta t}{2}) - E_z(x,y-\frac{\Delta t}{2},z,t-\frac{\Delta t}{2}) \right]$$

The update equations for the components $H_y(x,y,z,t)$ and $H_z(x,y,z,t)$ can be derived in the same manner. Since the only differences would be due to different contour and surface orientations, the update equations for the components $H_y(x,y,z,t)$ and $H_z(x,y,z,t)$ can be obtained from the update equation for $H_x(x,y,z)$ by cyclic permutation of indices. The contour for updating $H_y(x,y,z,t)$ is shown below

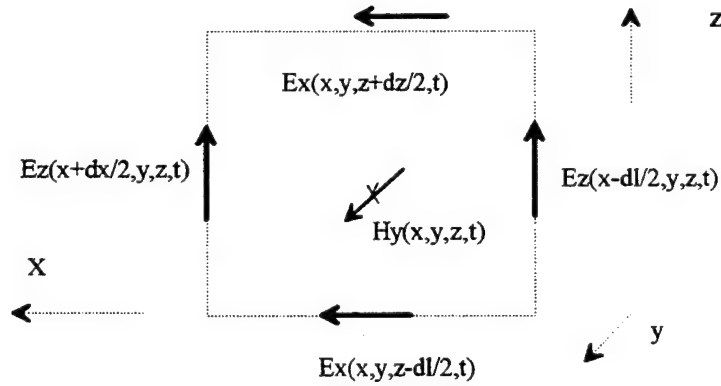


Figure 4.4. A Contour for Updating H_y .

Following the same procedure shown for updating H_x component, or simply using the cyclic permutation of indices we get the update equation for $H_y(x,y,z,t)$

$$H_y(x, y, z, t) \approx H_y(x, y, z, t - \Delta t) - Y_0 \left(\frac{v_0}{v_{grid}} \right) \frac{1}{\mu_{r,avgy}(x, y, z)} \times \quad (4.27)$$

$$\left[E_z(x - \frac{\Delta l}{2}, y, z, t - \frac{\Delta t}{2}) - E_z(x + \frac{\Delta l}{2}, y, z, t - \frac{\Delta t}{2}) + E_x(x, y, z + \frac{\Delta l}{2}, t - \frac{\Delta t}{2}) - E_x(x, y, z - \frac{\Delta l}{2}, t - \frac{\Delta t}{2}) \right]$$

Finally, the contour for updating $H_z(x, y, z, t)$ is shown below

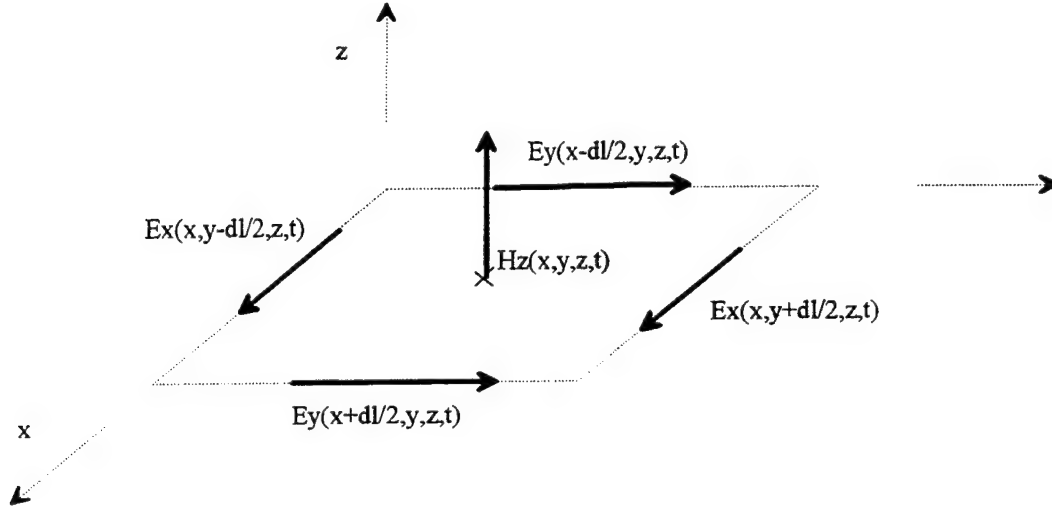


Figure 4.5. A Contour for Updating H_z .

The update equation for $H_z(x, y, z, t)$ is

$$H_z(x, y, z, t) \approx H_z(x, y, z, t - \Delta t) - Y_0 \left(\frac{v_0}{v_{grid}} \right) \frac{1}{\mu_{r,avgz}(x, y, z)} \times \quad (4.28)$$

$$\left[E_x(x, y - \frac{\Delta l}{2}, z, t - \frac{\Delta t}{2}) - E_x(x, y + \frac{\Delta l}{2}, z, t - \frac{\Delta t}{2}) + E_y(x + \frac{\Delta l}{2}, y, z, t - \frac{\Delta t}{2}) - E_y(x - \frac{\Delta l}{2}, y, z, t - \frac{\Delta t}{2}) \right]$$

In most cases the media will be non-magnetic, in which case all relative permittivity averages will be equal to 1, and the update equations will simplify accordingly.

3. Derivation of Electric Field Update Equations

We will start with the Maxwell's curl equation for the circulation of the magnetic field

$$\oint_{C_H} H_z(x,y,z,t) \vec{z} \cdot d\vec{l}_H = \frac{\partial}{\partial t} \left\{ \iint_{S_H} \varepsilon(x,y,z) [E_x(x,y,z,t) \vec{x} + E_y(x,y,z,t) \vec{y}] \cdot d\vec{s}_H \right\} + (4.29)$$

$$\iint_{S_H} \sigma(x,y,z) [E_x(x,y,t) \vec{x} + E_y(x,y,t) \vec{y}] \cdot d\vec{s}_H$$

The second term on the right-hand-side (the conduction current) is obviously going to cause the update equations for the electric field to be more complicated than the magnetic field update equations. The discrete equivalent of the magnetic field circulation needs to be determined for three sample contours: a contour in a plane parallel to the yz-coordinate plane, a contour in a plane parallel to the xz-coordinate plane, and a contour in a plane parallel to the xy-plane. The first contour provides an update equation for the x-directed component of the electric field, the second contour provides an update equation for the y-directed component of the electric field, and the third contour provides an update equation for the z-directed component of the electric field. Again, it is sufficient to derive the update equation for one electric field component only (say the x-component) since the other equations can be obtained by a simple cyclic permutation of indices.

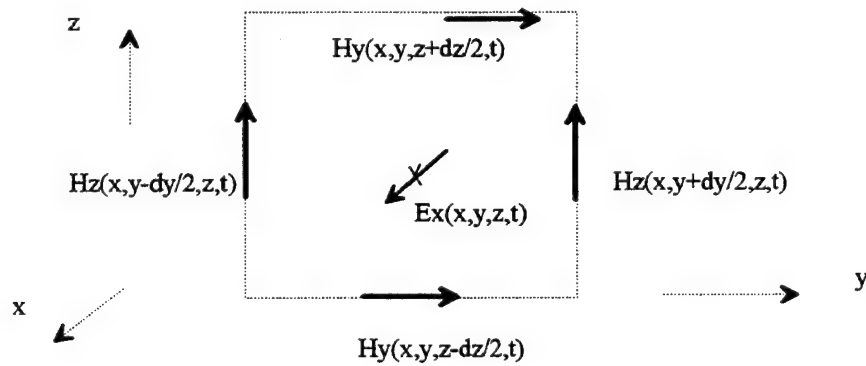


Figure 4.6. A Contour for Updating E_x .

A local coordinate system (ψ, ς) will be used, with the origin at the center of the contour. Any point (y', z') within or on the contour C_H (or, equivalently, any point on the surface S_H) can be specified by its local coordinates

$$y' = y + \psi \quad z' = z + \varsigma \quad \text{where} \quad -\frac{\Delta l}{2} \leq \varsigma \leq +\frac{\Delta l}{2}, \text{ and } -\frac{\Delta l}{2} \leq \psi \leq +\frac{\Delta l}{2}$$

The circulation of the magnetic field around C_H , assuming counter-clockwise reference direction such that the normal to the surface S_H is in the direction of the electric field $E_x(x, y, z, t)$, is *approximately*

$$\oint_{C_H} \left[H_y(x', y', z', t) \vec{y} + H_z(x', y', z', t) \vec{z} \right] \cdot d\vec{l}_H \approx \left[H_y(x, y, z - \frac{\Delta l}{2}, t) - H_y(x, y, z + \frac{\Delta l}{2}, t) + H_z(x, y + \frac{\Delta l}{2}, z, t) - H_z(x, y - \frac{\Delta l}{2}, z, t) \right] \cdot \Delta l \quad (4.30)$$

The electric flux through the surface S_H can only be evaluated *approximately*, since the exact way that the electric flux density

$$D_x(x, y, z, t) = \epsilon(x, y, z) E_x(x, y, z, t) \quad (4.31)$$

varies with y and z is not known a priori. First we re-write the flux integrals

$$\iint_{S_H} \epsilon(x', y', z', t) E_x(x', y', z', t) \vec{x} \cdot d\vec{s}_H = \int_{-\frac{\Delta l}{2}}^{+\frac{\Delta l}{2}} \int_{-\frac{\Delta l}{2}}^{+\frac{\Delta l}{2}} \epsilon(x, y + \psi, z + \varsigma) E_x(x, y + \psi, z + \varsigma, t) \vec{x} \cdot \vec{x} d\psi d\varsigma \quad (4.32)$$

$$\iint_{S_H} \sigma(x', y', z') E_x(x', y', z', t) \vec{x} \cdot d\vec{s}_H = \int_{-\frac{\Delta l}{2}}^{+\frac{\Delta l}{2}} \int_{-\frac{\Delta l}{2}}^{+\frac{\Delta l}{2}} \sigma(x, y + \psi, z + \varsigma) E_x(x, y + \psi, z + \varsigma, t) \vec{x} \cdot \vec{x} d\psi d\varsigma \quad (4.33)$$

Next, we assume that the contour side Δl is small enough such that the electric field $E(x, y + \psi, z + \varsigma, t)$ within the contour may be assumed constant and equal to the value at the contour's center $E(x, y, z, t)$. This assumption yields *approximate* expressions for the flux integrals

$$\iint_{S_H} \epsilon(x, y + \psi, z + \varsigma) E_x(x, y + \psi, z + \varsigma, t) \vec{x} \cdot d\vec{s}_H \approx E_x(x, y, z, t) \cdot \int_{-\frac{\Delta l}{2}}^{+\frac{\Delta l}{2}} \int_{-\frac{\Delta l}{2}}^{+\frac{\Delta l}{2}} \epsilon(x, y + \psi, z + \varsigma) d\psi d\varsigma \quad (4.34)$$

$$\iint_{S_H} \sigma(x, y + \psi, z + \varsigma) E_x(x, y + \psi, z + \varsigma, t) \vec{x} \cdot \vec{ds}_H \approx E_y(x, y, z, t) \cdot \int_{-\frac{\Delta l}{2}}^{+\frac{\Delta l}{2}} \int_{-\frac{\Delta l}{2}}^{+\frac{\Delta l}{2}} \sigma(x, y + \psi, z + \varsigma) d\psi d\varsigma \quad (4.35)$$

or, using the permittivity and the conductivity averaged in the y and z-directions

$$\iint_{S_H} \epsilon(x, y + \psi, z + \varsigma) E_x(x, y + \psi, z + \varsigma, t) \vec{x} \cdot \vec{ds}_H \approx (\Delta l)^2 \cdot E_x(x, y, z, t) \cdot \epsilon_{avgx}(x, y, z) \quad (4.36)$$

$$\iint_{S_H} \sigma(x, y + \psi, z + \varsigma) E_x(x, y + \psi, z + \varsigma, t) \vec{x} \cdot \vec{ds}_H \approx (\Delta l)^2 \cdot E_x(x, y, z, t) \cdot \sigma_{avgx}(x, y, z) \quad (4.37)$$

The second curl equation of Maxwell can now be replaced by an approximate equation

$$\left[H_y(x, y, z - \frac{\Delta l}{2}, t) - H_y(x, y, z + \frac{\Delta l}{2}, t) + H_z(x, y + \frac{\Delta l}{2}, z, t) - H_z(x, y - \frac{\Delta l}{2}, z, t) \right] \cdot \Delta l \approx (4.38)$$

$$\frac{\partial}{\partial t} \left\{ [\epsilon_{avgx}(x, y, z) E_y(x, y, z, t)] (\Delta l)^2 \right\} + (\Delta l)^2 \cdot \sigma_{avgx}(x, y, z) \cdot E_x(x, y, z, t)$$

The approximate curl equation can be re-written as

$$\frac{\partial}{\partial t} \{ E_x(x, y, z, t) \} \quad (4.39)$$

$$\frac{1}{\Delta l \cdot \epsilon_{avgx}(x, y, z)} \left[H_y(x, y, z - \frac{\Delta l}{2}, t) - H_y(x, y, z + \frac{\Delta l}{2}, t) + H_z(x, y + \frac{\Delta l}{2}, z, t) - H_z(x, y - \frac{\Delta l}{2}, z, t) \right]$$

$$- \frac{\sigma_{avgx}(x, y, z)}{\epsilon_{avgx}(x, y, z)} \cdot E_x(x, y, z, t)$$

The above equation is integrated with respect to time to get an approximate equation for the electric field at the present time t

$$E_x(x, y, z, t) \approx \frac{1}{\Delta l \cdot \epsilon_{avgx}(x, y, z)} \times \quad (4.40)$$

$$\left[\int_0^t H_y(x, y, z - \frac{\Delta l}{2}, \tau) d\tau - \int_0^t H_y(x, y, z + \frac{\Delta l}{2}, \tau) d\tau + \int_0^t H_z(x, y + \frac{\Delta l}{2}, z, \tau) d\tau - \int_0^t H_z(x, y - \frac{\Delta l}{2}, z, \tau) d\tau \right]$$

$$- \frac{\sigma_{avgx}(x, y, z)}{\epsilon_{avgx}(x, y, z)} \cdot \int_0^t E_x(x, y, z, \tau) d\tau$$

Similar equation can be written for the electric field at the same spatial location but

at an earlier time t-Δt

$$E_x(x, y, z, t - \Delta t) \approx \frac{1}{\Delta l \cdot \epsilon_{avgx}(x, y, z)} \times \quad (4.41)$$

$$\left[\int_0^{t-\Delta t} H_y(x, y, z - \frac{\Delta l}{2}, \tau) d\tau - \int_0^{t-\Delta t} H_y(x, y, z + \frac{\Delta l}{2}, \tau) d\tau + \int_0^{t-\Delta t} H_z(x, y + \frac{\Delta l}{2}, z, \tau) d\tau - \int_0^{t-\Delta t} H_z(x, y - \frac{\Delta l}{2}, z, \tau) d\tau \right]$$

$$- \frac{\sigma_{avgx}(x, y, z)}{\epsilon_{avgx}(x, y, z)} \int_0^{t-\Delta t} E_x(x, y, z, \tau) d\tau$$

Subtracting the two equations we get

$$E_x(x, y, z, t) \approx E_x(x, y, z, t - \Delta t) - \frac{1}{\Delta l \cdot \epsilon_{avgx}(x, y, z)} \times \quad (4.42)$$

$$\left[\int_{t-\Delta t}^t H_y(x, y, z - \frac{\Delta l}{2}, \tau) d\tau - \int_{t-\Delta t}^t H_y(x, y, z + \frac{\Delta l}{2}, \tau) d\tau + \int_{t-\Delta t}^t H_z(x, y + \frac{\Delta l}{2}, z, \tau) d\tau - \int_{t-\Delta t}^t H_z(x, y - \frac{\Delta l}{2}, z, \tau) d\tau \right]$$

$$- \frac{\sigma_{avgx}(x, y, z)}{\epsilon_{avgx}(x, y, z)} \int_{t-\Delta t}^t E_x(x, y, z, \tau) d\tau$$

Assuming that the interval Δt is small enough such that the magnetic fields can be assumed approximately constant within Δt and equal to the value at the center of the time interval Δt

$$H_y(x, y, z + \frac{\Delta l}{2}, \tau) \approx H_y(x, y, z + \frac{\Delta l}{2}, t - \frac{\Delta t}{2}) \quad \text{for } t - \Delta t \leq \tau \leq t \quad (4.43)$$

$$H_y(x, y, z - \frac{\Delta l}{2}, \tau) \approx H_y(x, y, z - \frac{\Delta l}{2}, t - \frac{\Delta t}{2}) \quad \text{for } t - \Delta t \leq \tau \leq t \quad (4.44)$$

$$H_z(x, y + \frac{\Delta l}{2}, z, \tau) \approx H_z(x, y + \frac{\Delta l}{2}, z, t - \frac{\Delta t}{2}) \quad \text{for } t - \Delta t \leq \tau \leq t \quad (4.45)$$

$$H_z(x, y - \frac{\Delta l}{2}, z, \tau) \approx H_z(x, y - \frac{\Delta l}{2}, z, t - \frac{\Delta t}{2}) \quad \text{for } t - \Delta t \leq \tau \leq t \quad (4.46)$$

we get

$$E_x(x, y, z, t) \approx E_x(x, y, z, t - \Delta t) + \frac{\Delta t}{\Delta l \cdot \epsilon_{avgx}(x, y, z)} \times \quad (4.47)$$

$$\left[H_y(x, y, z - \frac{\Delta l}{2}, t - \frac{\Delta t}{2}) - H_y(x, y, z + \frac{\Delta l}{2}, t - \frac{\Delta t}{2}) + H_z(x, y + \frac{\Delta l}{2}, z, t - \frac{\Delta t}{2}) - H_z(x, y - \frac{\Delta l}{2}, z, t - \frac{\Delta t}{2}) \right]$$

$$- \frac{\sigma_{avgx}(x, y, z)}{\epsilon_{avgx}(x, y, z)} \cdot \int_{t-\Delta t}^t E_x(x, y, z, \tau) d\tau$$

The last integral term can be expressed in different form as shown below

$$\Delta t \cdot \frac{\sigma_{avgx}(x, y, z)}{\epsilon_{avgx}(x, y, z)} \cdot \frac{1}{\Delta t} \cdot \int_{t-\Delta t}^t E_x(x, y, z, \tau) d\tau = \Delta t \cdot \frac{\sigma_{avgx}(x, y, z)}{\epsilon_{avgx}(x, y, z)} \cdot E_{x,avg(\Delta t)}(x, y, z, t) \quad (4.48)$$

The above equation can be written in more compact manner by using the identity

$$\frac{1}{\epsilon} = \frac{1}{\epsilon_0} \frac{1}{\epsilon_r} = \frac{\sqrt{\mu_0}}{\sqrt{\mu_0}} \frac{1}{\sqrt{\epsilon_0}} \frac{1}{\sqrt{\epsilon_0} \epsilon_r} = \frac{1}{\sqrt{\mu_0 \epsilon_0}} \sqrt{\frac{\mu_0}{\epsilon_0}} \frac{1}{\epsilon_r} = v_0 Z_0 \frac{1}{\epsilon_r} \quad (4.49)$$

where the free space velocity of propagation is denoted v_0 , the intrinsic impedance of free space is denoted Z_0 ($Z_0 \approx 377\Omega$) and ϵ_r denotes relative permittivity. Introducing the grid "propagation" velocity

$$v_{grid} = \frac{\Delta l}{\Delta t} \quad (4.50)$$

we can write the approximate equation for the electric field "updates" as

$$E_x(x, y, z, t) \approx E_x(x, y, z, t) + Z_0 \frac{v_0}{v_{grid} \epsilon_{r,avgx}(x, y, z)} \times \quad (4.51)$$

$$\left[H_y(x, y, z - \frac{\Delta l}{2}, t - \frac{\Delta t}{2}) - H_y(x, y, z + \frac{\Delta l}{2}, t - \frac{\Delta t}{2}) + H_z(x, y + \frac{\Delta l}{2}, z, t - \Delta t) - H_z(x, y - \frac{\Delta l}{2}, z, t - \frac{\Delta t}{2}) \right]$$

$$Z_0 \frac{v_0}{v_{grid} \epsilon_{r,avgx}(x, y, z)} \cdot \Delta l \cdot \sigma_{avgx}(x, y, z) E_{x,avg(\Delta t)}(x, y, z, t)$$

The average of the electric field between $t - \Delta t$ and t , denoted $E_{x,avg(\Delta t)}$ can not be calculated exactly because the exact temporal variation of the electric field within the Δt interval is not known a priori. However, assuming a linear variation within Δt interval, the temporal average of the field is the average of the field values at $t - \Delta t$ and t

$$E_{x,avg(\Delta t)}(x, y, z, t) \approx \frac{E_x(x, y, z, t - \Delta t) + E_x(x, y, z, t)}{2} \quad (4.52)$$

Substituting the time-average $E_{x,avg(\Delta t)}(x, y, t)$ into the update equation we get

$$E_x(x, y, z, t) \approx E_x(x, y, z, t - \Delta t) + Z_0 \frac{v_0}{v_{grid} \epsilon_{r,avgx}(x, y, z)} \times \quad (4.53)$$

$$\left[H_y(x, y, z - \frac{\Delta l}{2}, t - \frac{\Delta t}{2}) - H_y(x, y, z + \frac{\Delta l}{2}, t - \frac{\Delta t}{2}) + H_z(x, y + \frac{\Delta l}{2}, z, t - \Delta t) - H_z(x, y - \frac{\Delta l}{2}, z, t - \frac{\Delta t}{2}) \right]$$

$$- Z_0 \frac{v_0}{v_{grid} \epsilon_{r,avgx}(x, y, z)} \cdot \Delta l \cdot \sigma_{avgx}(x, y, z) \cdot \frac{E_x(x, y, z, t - \Delta t) + E_x(x, y, z, t)}{2}$$

which give the update equation for the x-component of the electric field as

$$E_x(x, y, z, t) \approx \frac{1 - \frac{1}{2} \frac{v_0}{v_{grid}} \frac{Z_0 \cdot \Delta l \cdot \sigma_{avgx}(x, y, z)}{\epsilon_{r,avgx}(x, y, z)}}{1 + \frac{1}{2} \frac{v_0}{v_{grid}} \frac{Z_0 \cdot \Delta l \cdot \sigma_{avgx}(x, y, z)}{\epsilon_{r,avgx}(x, y, z)}} E_x(x, y, z, t - \Delta t) + \quad (4.54)$$

$$\frac{Z_0 \frac{v_0}{v_{grid} \epsilon_{r,avgx}(x, y, z)}}{1 + \frac{1}{2} \frac{v_0}{v_{grid}} \frac{Z_0 \cdot \Delta l \cdot \sigma_{avgx}(x, y, z)}{\epsilon_{r,avgx}(x, y, z)}} \times$$

$$\left[H_y(x, y, z - \frac{\Delta l}{2}, t - \frac{\Delta t}{2}) - H_y(x, y, z + \frac{\Delta l}{2}, t - \frac{\Delta t}{2}) + H_z(x, y + \frac{\Delta l}{2}, z, t - \Delta t) - H_z(x, y - \frac{\Delta l}{2}, z, t - \frac{\Delta t}{2}) \right]$$

The equation simplifies greatly for the case of non-conductive media ($\sigma=0$)

$$E_x(x,y,z,t) \approx E_x(x,y,z,t-\Delta t) + Z_0 \frac{v_0}{v_{grid}} \frac{1}{\epsilon_{r,avgx}(x,y,z)} \times \quad (4.55)$$

$$\left[H_y(x,y,z-\frac{\Delta l}{2},t-\frac{\Delta t}{2}) - H_y(x,y,z+\frac{\Delta l}{2},t-\frac{\Delta t}{2}) + H_z(x,y+\frac{\Delta l}{2},z,t-\Delta t) - H_z(x,y-\frac{\Delta l}{2},z,t-\frac{\Delta t}{2}) \right]$$

In the case of free-space ($\epsilon_r=1$), the equation simplifies further

$$E_x(x,y,z,t) \approx E_x(x,y,z,t-\Delta t) + Z_0 \frac{v_0}{v_{grid}} \times \quad (4.56)$$

$$\left[H_y(x,y,z-\frac{\Delta l}{2},t-\frac{\Delta t}{2}) - H_y(x,y,z+\frac{\Delta l}{2},t-\frac{\Delta t}{2}) + H_z(x,y+\frac{\Delta l}{2},z,t-\Delta t) - H_z(x,y-\frac{\Delta l}{2},z,t-\frac{\Delta t}{2}) \right]$$

The update equations for the other two electric field components $E_y(x,y,z,t)$ and $E_z(x,y,z,t)$ can be derived in the same manner. Since the only differences are in the contour and surface orientation, the update equations for $E_y(x,y,z,t)$ and $E_z(x,y,z,t)$ can be determined by a simple cyclic permutation of indices, as shown on the next page. The contour for updating $E_y(x,y,z,t)$ is shown below.

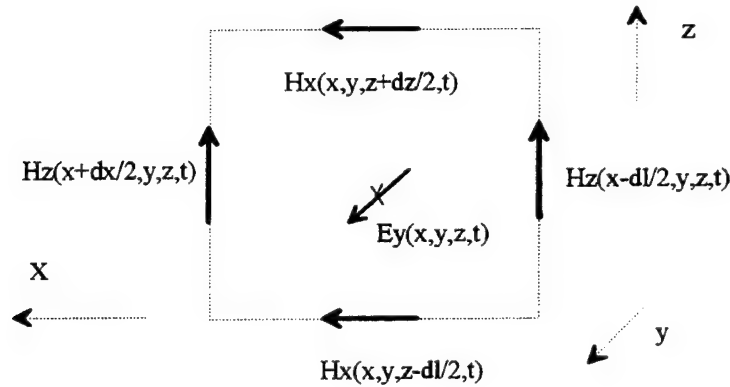


Figure 4.7. A Contour for Updating E_y

Following the same procedure as shown for the $E_x(x,y,z,t)$ update equation, or by a simple cyclic permutation of indices we obtain

$$E_y(x,y,z,t) \approx \frac{1 - \frac{1}{2} \frac{v_0}{v_{grid}} \frac{Z_0 \cdot \Delta l \cdot \sigma_{avg}(x,y,z)}{\epsilon_{r,avg}(x,y,z)}}{1 + \frac{1}{2} \frac{v_0}{v_{grid}} \frac{Z_0 \cdot \Delta l \cdot \sigma_{avg}(x,y,z)}{\epsilon_{r,avg}(x,y,z)}} E_y(x,y,z,t - \Delta t) + \quad (4.57)$$

$$\frac{Z_0 \frac{v_0}{v_{grid}} \frac{1}{\epsilon_{r,avg}(x,y,z)}}{1 + \frac{1}{2} \frac{v_0}{v_{grid}} \frac{Z_0 \cdot \Delta l \cdot \sigma_{avg}(x,y,z)}{\epsilon_{r,avg}(x,y,z)}} \times$$

$$\left[H_z(x - \frac{\Delta l}{2}, y, z, t - \Delta t) - H_z(x + \frac{\Delta l}{2}, y, z, t - \frac{\Delta t}{2}) + H_x(x, y, z + \frac{\Delta l}{2}, t - \frac{\Delta t}{2}) - H_x(x, y, z - \frac{\Delta l}{2}, t - \frac{\Delta t}{2}) \right]$$

The equation simplifies greatly for the case of non-conductive media ($\sigma=0$)

$$E_y(x,y,z,t) \approx E_y(x,y,z,t - \Delta t) + Z_0 \frac{v_0}{v_{grid}} \frac{1}{\epsilon_{r,avg}(x,y,z)} \times \quad (4.58)$$

$$\left[H_z(x - \frac{\Delta l}{2}, y, z, t - \Delta t) - H_z(x + \frac{\Delta l}{2}, y, z, t - \frac{\Delta t}{2}) + H_x(x, y, z + \frac{\Delta l}{2}, t - \frac{\Delta t}{2}) - H_x(x, y, z - \frac{\Delta l}{2}, t - \frac{\Delta t}{2}) \right]$$

In the case of free-space ($\epsilon_r=1$), the equation simplifies further

$$E_y(x,y,z,t) \approx E_y(x,y,z,t - \Delta t) + Z_0 \frac{v_0}{v_{grid}} \times \quad (4.59)$$

$$\left[H_z(x - \frac{\Delta l}{2}, y, z, t - \Delta t) - H_z(x + \frac{\Delta l}{2}, y, z, t - \frac{\Delta t}{2}) + H_x(x, y, z + \frac{\Delta l}{2}, t - \frac{\Delta t}{2}) - H_x(x, y, z - \frac{\Delta l}{2}, t - \frac{\Delta t}{2}) \right]$$

The contour for updating $E_z(x,y,z,t)$ is shown below.

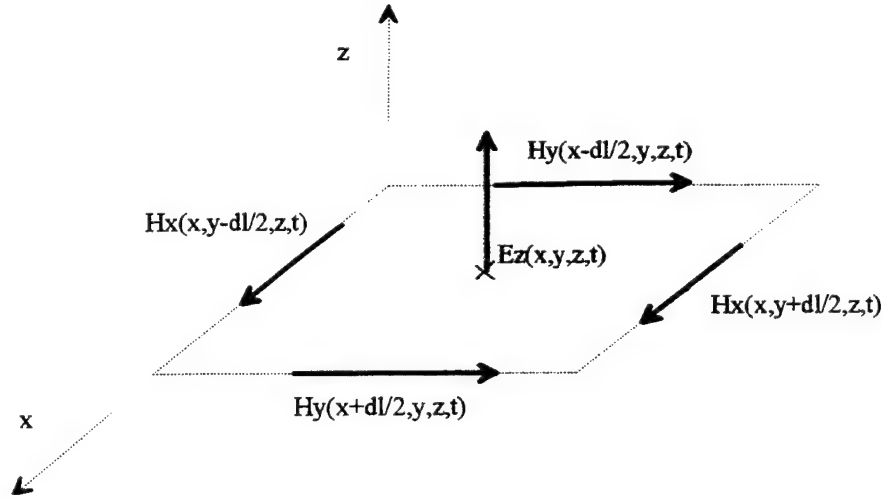


Figure 4.8. A Contour for Updating E_z

Following the same procedure as shown for the $E_x(x,y,z,t)$ update equation, or by a simple cyclic permutation of indices we obtain

$$E_z(x,y,z,t) \approx \frac{1 - \frac{1}{2} \frac{v_0}{v_{grid}} \frac{Z_0 \cdot \Delta l \cdot \sigma_{avgz}(x,y,z)}{\epsilon_{r,avgz}(x,y,z)}}{1 + \frac{1}{2} \frac{v_0}{v_{grid}} \frac{Z_0 \cdot \Delta l \cdot \sigma_{avgz}(x,y,z)}{\epsilon_{r,avgz}(x,y,z)}} E_z(x,y,z,t - \Delta t) + \frac{Z_0 \frac{v_0}{v_{grid}} \frac{1}{\epsilon_{r,avgz}(x,y,z)}}{1 + \frac{1}{2} \frac{v_0}{v_{grid}} \frac{Z_0 \cdot \Delta l \cdot \sigma_{avgz}(x,y,z)}{\epsilon_{r,avgz}(x,y,z)}} \times [H_x(x, y - \frac{\Delta l}{2}, z, t - \frac{\Delta t}{2}) - H_x(x, y + \frac{\Delta l}{2}, z, t - \frac{\Delta t}{2}) + H_y(x + \frac{\Delta l}{2}, y, z, t - \frac{\Delta t}{2}) - H_y(x - \frac{\Delta l}{2}, y, z, t - \frac{\Delta t}{2})] \quad (4.60)$$

The equation simplifies greatly for the case of non-conductive media ($\sigma=0$)

$$E_z(x,y,z,t) \approx E_z(x,y,z,t - \Delta t) + Z_0 \frac{v_0}{v_{grid}} \frac{1}{\epsilon_{r,avgz}(x,y,z)} \times [H_x(x, y - \frac{\Delta l}{2}, z, t - \frac{\Delta t}{2}) - H_x(x, y + \frac{\Delta l}{2}, z, t - \frac{\Delta t}{2}) + H_y(x + \frac{\Delta l}{2}, y, z, t - \frac{\Delta t}{2}) - H_y(x - \frac{\Delta l}{2}, y, z, t - \frac{\Delta t}{2})] \quad (4.61)$$

In the case of free-space ($\epsilon_r=1$), the equation simplifies further

$$E_z(x,y,z,t) \approx E_z(x,y,z,t - \Delta t) + Z_0 \frac{v_0}{v_{grid}} \times [H_x(x, y - \frac{\Delta l}{2}, z, t - \frac{\Delta t}{2}) - H_x(x, y + \frac{\Delta l}{2}, z, t - \frac{\Delta t}{2}) + H_y(x + \frac{\Delta l}{2}, y, z, t - \frac{\Delta t}{2}) - H_y(x - \frac{\Delta l}{2}, y, z, t - \frac{\Delta t}{2})] \quad 4.62$$

B. TRANSPARENT GRID TERMINATION IN 3-D

1. 3-D Grid

The electric and magnetic field update equations have been derived using local coordinate systems, with origins at the centers of the magnetic and electric contours, respectively. These equations now need to be "converted" to a global coordinate system, that is to a 3-D grid of equi-distant sampling points. We assume that our domain is an L by L by L cube discretized using a uniform grid, that is that the discretization step $\Delta l=L/N$

is not changing with position. The electric and magnetic field sampling points (nodes) are "interleaved", that is offset by $\Delta/2$ from each other in x, y, and z-directions. The electric field components are located along the sides of "electric" cells while the magnetic field components are located along the sides of "magnetic" cells.

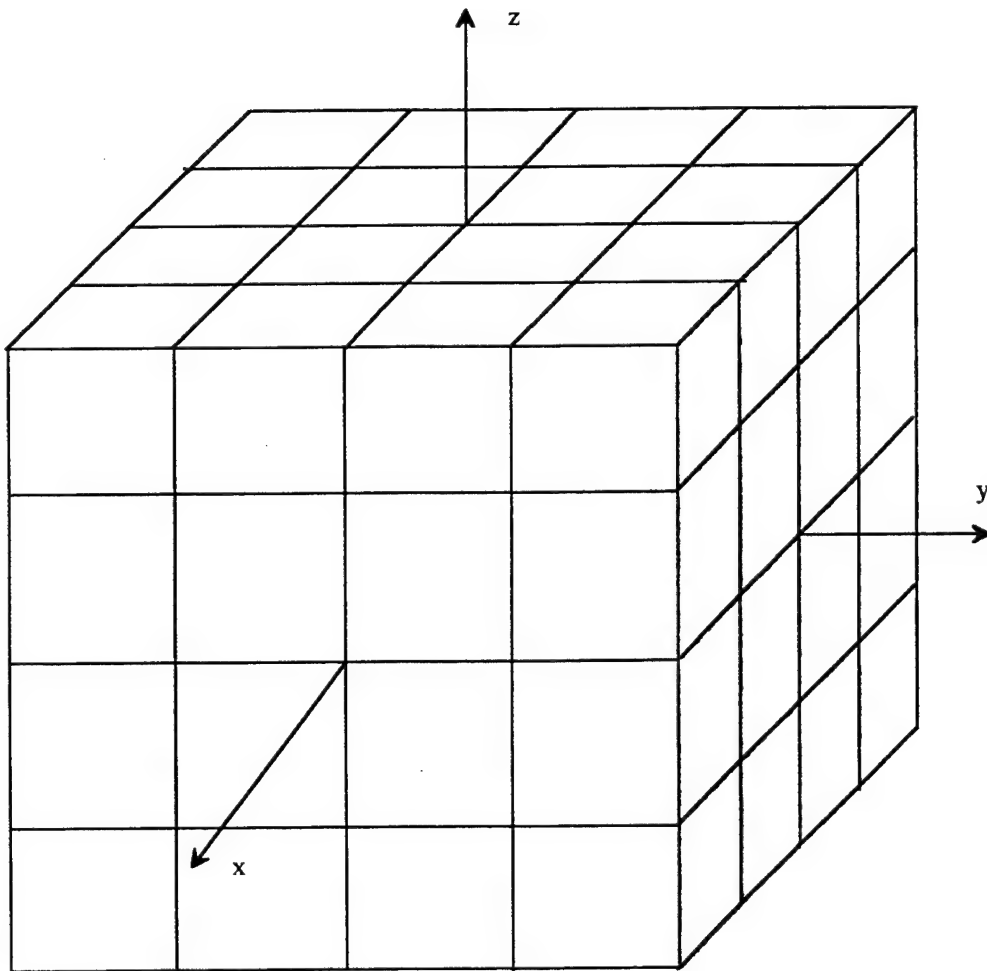


Figure 4.9. 3-D Grid, Electric Cells.

The electric cells are the cells of constant ϵ and σ , while the magnetic cells are the cells of constant μ . The permittivity and conductivity can vary from one electric cell to another in arbitrary manner. The permeability can vary from one magnetic cell to another in an arbitrary manner as well. The electric cells are shifted by $\Delta l/2$ in all three coordinate directions with respect to corresponding magnetic cells. The placement of field components along the cell's sides automatically provides for the continuity of tangential components of electric fields across media interfaces, while the spatial shift of electric vs. magnetic cells provides for electric and magnetic field linkage (coupling). Domain boundaries can coincide with either the faces of electric cells or the faces of magnetic cells, but not both (because of the $\Delta l/2$ spatial shift between the two). Although, in principle, either electric or magnetic cells can be aligned with the grid boundaries, we will select electric cell alignment with the domain boundaries.

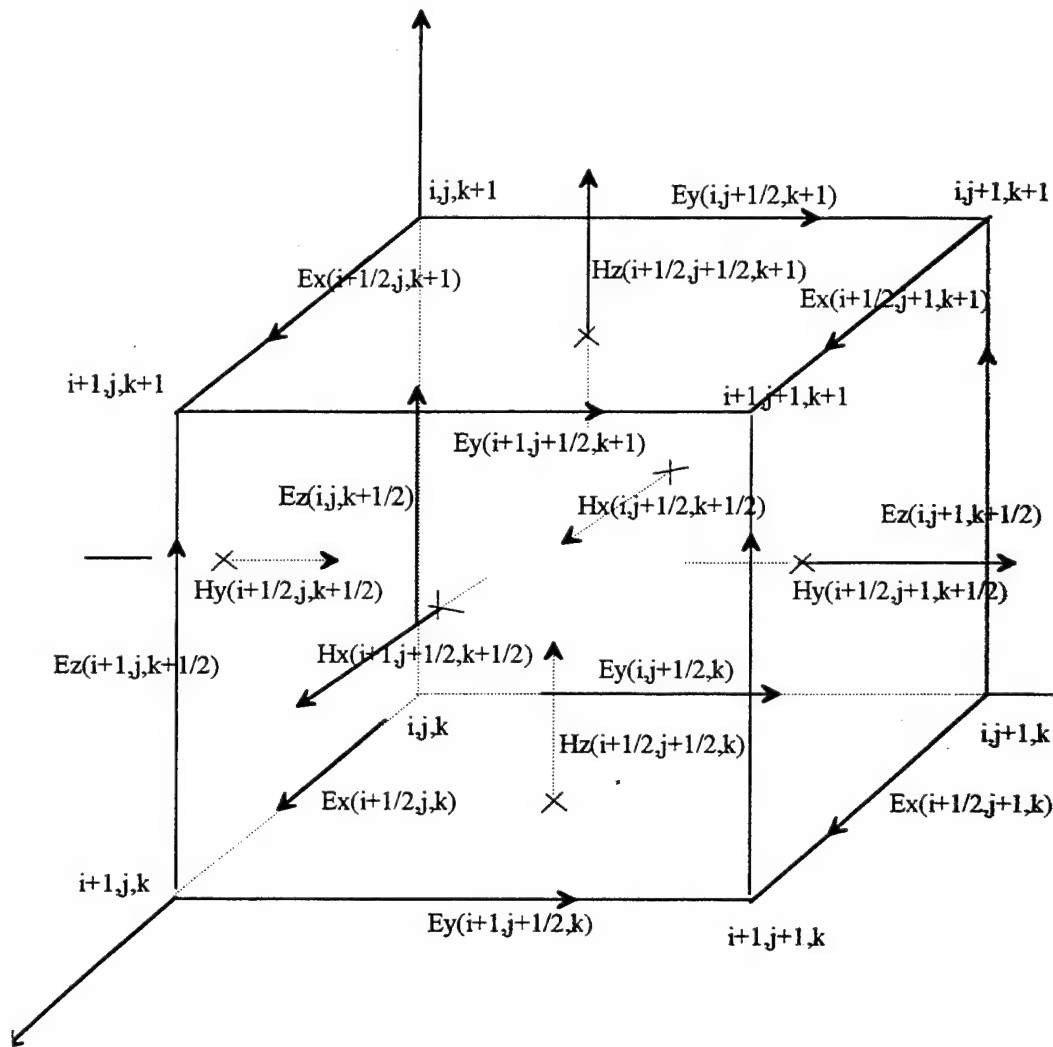


Figure 4.10. Yee Electric Cell and Associated Field Components.

A grid of (N by N by N) electric cells has (N)(N)(N) E_x , E_y , and E_z electric field nodes, (N-1)(N-1)(N-2) H_x , H_y , and H_z magnetic field nodes (Just the opposite would hold for aligning magnetic cells with domain boundaries). 3-D electric and magnetic field "update" equations can now be "converted" to electric and magnetic field grid "update"

equations by replacing the variables x, y, z and t with the grid coordinates of the electric field spatial and temporal sampling points

$$x \rightarrow i\Delta l, i = 0, 1 \dots N \quad y \rightarrow j\Delta l, j = 0, 1 \dots N \quad z \rightarrow k\Delta l, k = 0, 1 \dots N \quad t \rightarrow n\Delta t, n = 0, 1 \dots N_t$$

The notation can be simplified by omitting the common Δl and Δt terms, and using a superscript for the index of the temporal sampling point. The E field grid equations for conductive media are obtained from equations (4.54, 4.57, 4.60)

$$E_x^n(i, j, k) \approx \frac{1 - \frac{1}{2} \frac{\nu_0}{v_{grid}} \frac{Z_0 \cdot \Delta l \cdot \sigma_{avgx}(i, j, k)}{\epsilon_{r, avgx}(i, j, k)}}{1 + \frac{1}{2} \frac{\nu_0}{v_{grid}} \frac{Z_0 \cdot \Delta l \cdot \sigma_{avgx}(i, j, k)}{\epsilon_{r, avgx}(i, j, k)}} E_x^{n-1}(i, j, k) + \frac{Z_0 \frac{\nu_0}{v_{grid}} \frac{1}{\epsilon_{r, avgx}(i, j, k)}}{1 + \frac{1}{2} \frac{\nu_0}{v_{grid}} \frac{Z_0 \cdot \Delta l \cdot \sigma_{avgx}(i, j, k)}{\epsilon_{r, avgx}(x, y, z)}} \times \left[H_y^{n-\frac{1}{2}}(i, j, k - \frac{1}{2}) - H_y^{n-\frac{1}{2}}(i, j, k + \frac{1}{2}) + H_z^{n-\frac{1}{2}}(i, j + \frac{1}{2}, k) - H_z^{n-\frac{1}{2}}(i, j - \frac{1}{2}, k) \right] \quad (4.63)$$

$$E_y^n(i, j, k) \approx \frac{1 - \frac{1}{2} \frac{\nu_0}{v_{grid}} \frac{Z_0 \cdot \Delta l \cdot \sigma_{avgy}(i, j, k)}{\epsilon_{r, avgy}(i, j, k)}}{1 + \frac{1}{2} \frac{\nu_0}{v_{grid}} \frac{Z_0 \cdot \Delta l \cdot \sigma_{avgy}(i, j, k)}{\epsilon_{r, avgy}(i, j, k)}} E_y^{n-1}(i, j, k) + \frac{Z_0 \frac{\nu_0}{v_{grid}} \frac{1}{\epsilon_{r, avgy}(i, j, k)}}{1 + \frac{1}{2} \frac{\nu_0}{v_{grid}} \frac{Z_0 \cdot \Delta l \cdot \sigma_{avgy}(i, j, k)}{\epsilon_{r, avgy}(i, j, k)}} \times \left[H_z^{n-\frac{1}{2}}(i - \frac{1}{2}, j, k) - H_z^{n-\frac{1}{2}}(i + \frac{1}{2}, j, k) + H_x^{n-\frac{1}{2}}(i, j, k + \frac{1}{2}) - H_x^{n-\frac{1}{2}}(i, j, k - \frac{1}{2}) \right] \quad (4.64)$$

$$E_z^n(i,j,k) \approx \frac{1 - \frac{1}{2} \frac{v_0}{v_{grid}} \frac{Z_0 \cdot \Delta l \cdot \sigma_{avgz}(i,j,k)}{\epsilon_{r,avgz}(i,j,k)}}{1 + \frac{1}{2} \frac{v_0}{v_{grid}} \frac{Z_0 \cdot \Delta l \cdot \sigma_{avgz}(i,j,k)}{\epsilon_{r,avgz}(i,j,k)}} E_z^{n-1}(i,j,k) + \frac{Z_0 \frac{v_0}{v_{grid}} \frac{1}{\epsilon_{r,avgz}(i,j,k)}}{1 + \frac{1}{2} \frac{v_0}{v_{grid}} \frac{Z_0 \cdot \Delta l \cdot \sigma_{avgz}(i,j,k)}{\epsilon_{r,avgz}(i,j,k)}} \times \left[H_x^{n-\frac{1}{2}}(i,j-\frac{1}{2},k) - H_x^{n-\frac{1}{2}}(i,j+\frac{1}{2},k) + H_y^{n-\frac{1}{2}}(i+\frac{1}{2},j,k) - H_y^{n-\frac{1}{2}}(i-\frac{1}{2},j,k) \right] \quad (4.65)$$

The equations simplify greatly for the case of non-conductive media ($\sigma=0$)

$$E_x^n(i,j,k) \approx E_x^{n-1}(i,j,k) + Z_0 \frac{v_0}{v_{grid}} \frac{1}{\epsilon_{r,avgx}(i,j,k)} \times \quad (4.66)$$

$$\left[H_y^{n-\frac{1}{2}}(i,j,k-\frac{1}{2}) - H_y^{n-\frac{1}{2}}(i,j,k+\frac{1}{2}) + H_z^{n-\frac{1}{2}}(i,j+\frac{1}{2},k) - H_z^{n-\frac{1}{2}}(i,j-\frac{1}{2},k) \right]$$

$$E_y^n(i,j,k) \approx E_y^{n-1}(i,j,k) + Z_0 \frac{v_0}{v_{grid}} \frac{1}{\epsilon_{r,avgy}(i,j,k)} \times \quad (4.67)$$

$$\left[H_z^{n-\frac{1}{2}}(i-\frac{1}{2},j,k) - H_z^{n-\frac{1}{2}}(i+\frac{1}{2},j,k) + H_x^{n-\frac{1}{2}}(i,j,k+\frac{1}{2}) - H_x^{n-\frac{1}{2}}(i,j,k-\frac{1}{2}) \right]$$

$$E_z^n(i,j,k) \approx E_z^{n-1}(i,j,k) + Z_0 \frac{v_0}{v_{grid}} \frac{1}{\epsilon_{r,avgz}(i,j,k)} \times \quad (4.68)$$

$$\left[H_x^{n-\frac{1}{2}}(i,j-\frac{1}{2},k) - H_x^{n-\frac{1}{2}}(i,j+\frac{1}{2},k) + H_y^{n-\frac{1}{2}}(i+\frac{1}{2},j,k) - H_y^{n-\frac{1}{2}}(i-\frac{1}{2},j,k) \right]$$

In the case of free-space ($\epsilon_r=1$), the equations simplify further

$$E_x^n(i,j,k) \approx E_x^{n-1}(i,j,k) + Z_0 \frac{v_0}{v_{grid}} \times \quad (4.69)$$

$$\left[H_y^{n-\frac{1}{2}}(i,j,k-\frac{1}{2}) - H_y^{n-\frac{1}{2}}(i,j,k+\frac{1}{2}) + H_z^{n-\frac{1}{2}}(i,j+\frac{1}{2},k) - H_z^{n-\frac{1}{2}}(i,j-\frac{1}{2},k) \right]$$

$$E_y^n(i,j,k) \approx E_y^{n-1}(i,j,k) + Z_0 \frac{v_0}{v_{grid}} \times \quad (4.70)$$

$$\left[H_z^{n-\frac{1}{2}}(i-\frac{1}{2},j,k) - H_z^{n-\frac{1}{2}}(i+\frac{1}{2},j,k) + H_x^{n-\frac{1}{2}}(i,j,k+\frac{1}{2}) - H_x^{n-\frac{1}{2}}(i,j,k-\frac{1}{2}) \right]$$

$$E_z^n(i,j,k) \approx E_z^{n-1}(i,j,k) + Z_0 \frac{v_0}{v_{grid}} \times \quad (4.71)$$

$$\left[H_x^{n-\frac{1}{2}}(i,j-\frac{1}{2},k) - H_x^{n-\frac{1}{2}}(i,j+\frac{1}{2},k) + H_y^{n-\frac{1}{2}}(i+\frac{1}{2},j,k) - H_y^{n-\frac{1}{2}}(i-\frac{1}{2},j,k) \right]$$

Similarly, the H-field update grid equations are

$$H_x^n(i,j,k) \approx H_x^{n-1}(i,j,k) - Y_0 \frac{v_0}{v_{grid}} \frac{1}{\mu_{avgx}(i,j,k)} \times \left[E_y^{n-\frac{1}{2}}(i,j,k-\frac{1}{2}) - E_y^{n-\frac{1}{2}}(i,j,k+\frac{1}{2}) + E_z^{n-\frac{1}{2}}(i,j+\frac{1}{2},k) - E_z^{n-\frac{1}{2}}(i,j-\frac{1}{2},k) \right] \quad (4.72)$$

$$H_y^n(i,j,k) \approx H_y^{n-1}(i,j,k) - Y_0 \frac{v_0}{v_{grid}} \frac{1}{\mu_y(i,j,k)} \times \left[E_z^{n-\frac{1}{2}}(i-\frac{1}{2},j,k) - E_z^{n-\frac{1}{2}}(i+\frac{1}{2},j,k) + E_x^{n-\frac{1}{2}}(i,j,k+\frac{1}{2}) - E_x^{n-\frac{1}{2}}(i,j,k-\frac{1}{2}) \right] \quad (4.73)$$

$$H_z^n(i,j,k) \approx H_z^{n-\frac{1}{2}}(i,j,k) - Y_0 \frac{v_0}{v_{grid}} \frac{1}{\mu_{avgz}(i,j,k)} \times \left[E_x^{n-\frac{1}{2}}(i,j-\frac{1}{2},k) - E_x^{n-\frac{1}{2}}(i,j+\frac{1}{2},k) + E_y^{n-\frac{1}{2}}(i+\frac{1}{2},j,k) - E_y^{n-\frac{1}{2}}(i-\frac{1}{2},j,k) \right] \quad (4.74)$$

2. 3-D Grid Termination

The grid equations derived previously are valid for all the nodes *except* for the nodes on the domain boundary. The reason is that the field nodes on the boundary have at most five nearest neighbor nodes while the nodes within the domain boundaries have six nearest-neighbor nodes.

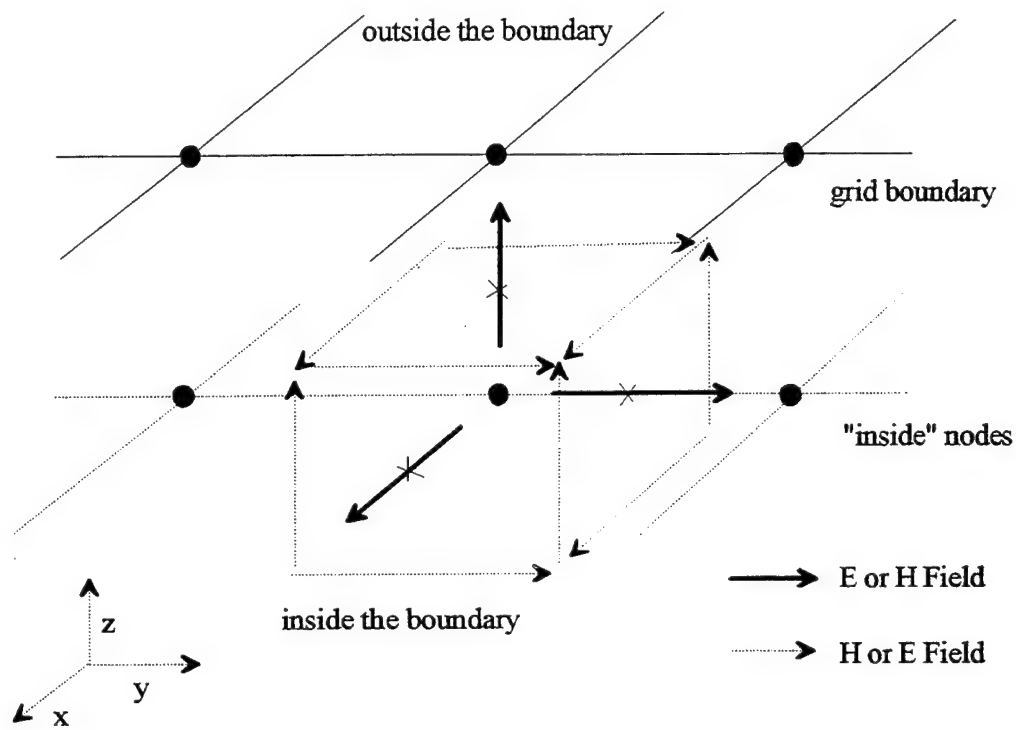


Figure 4.11. Nodes Inside and on a Boundary of a 3-D Grid.

The equations for the field components on the boundary can not be written because the field component on the boundary shown in the figure above can not be updated using the grid equations discussed so far. Extending the ideas of transparent grid termination (TGT) the discrete boundary impulse response (DBIR) applied for 1-D and 2-D problems. Similarly to the 2-D TGT concept, the update equations on the boundary can be devised based upon convolutions of the fields on the just inside boundary and the pre-calculated impulse responses from the just inside boundary to the boundary. The fields on the boundary will be expressed as a superposition of responses, as illustrated in

the figure below for top plane of the boundary. The same applies to other plane of boundary as well.

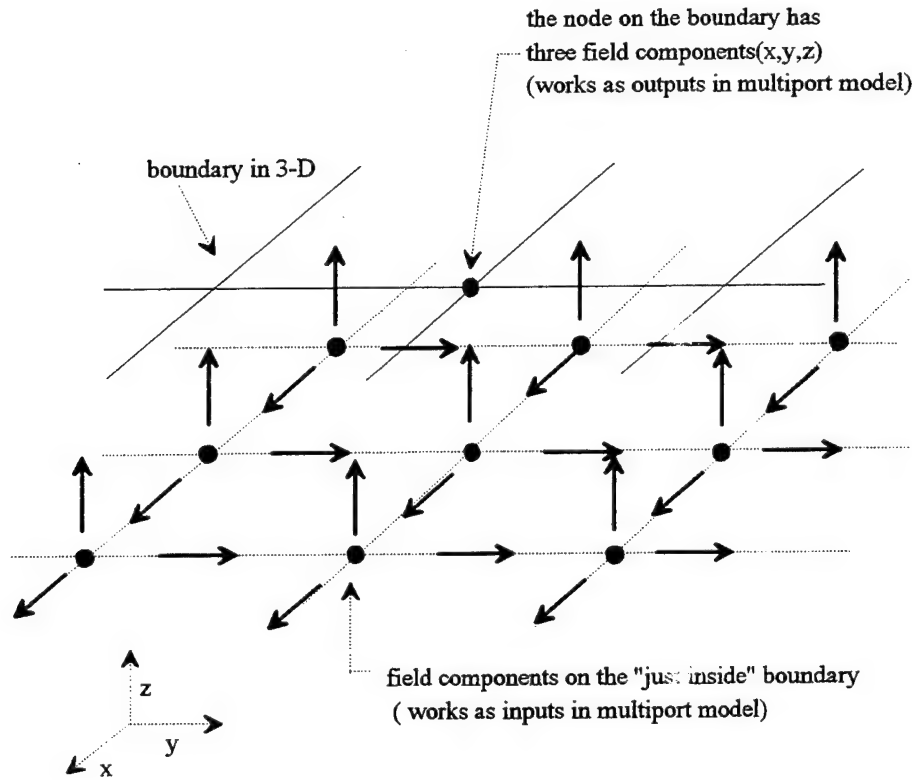


Figure 4.12. Fields on the Boundary as a Superposition of Responses.

The superposition can be also modelled using the concept of a multiport. The nodes on the grid boundary have three field components and those field components can be considered as output ports of a linear multi-port. Assuming that the grid is a cubic with $(N)(N)(N)$ nodes, the total number of output ports will be $3[2(N)(N)+(N-2)4(N-1)]$. The field components on the nodes just inside the grid boundary will be considered as input ports of the linear multiport. There will be a total of $3[2(N-2)(N-2)+(N-4)4(N-3)]$ input

ports. The equivalent multiport model in 2-D TGT can be used in the same manner. The input and output fields can be either electric or magnetic fields. Furthermore, the input and output fields need not be of the same "kind", that is the input fields could be, in principle, E-fields and the output fields could be H-fields, or vice versa. However, we will select the input and output fields to be of the same "kind", that is either all E or all H fields, such that the impulse responses $h_{m,n}(t)$ will be dimensionless. The equations will be derived for E field model, that is with electric fields on the grid boundary. Dual equations for the magnetic fields model can be obtained simply by replacing E's with H's. There are six planes for the cubic grid boundary. However, by splitting the cubic into N pages and making an arrangement for the input and output in the N pages, we can simplify the 3-D TGT model as shown below.

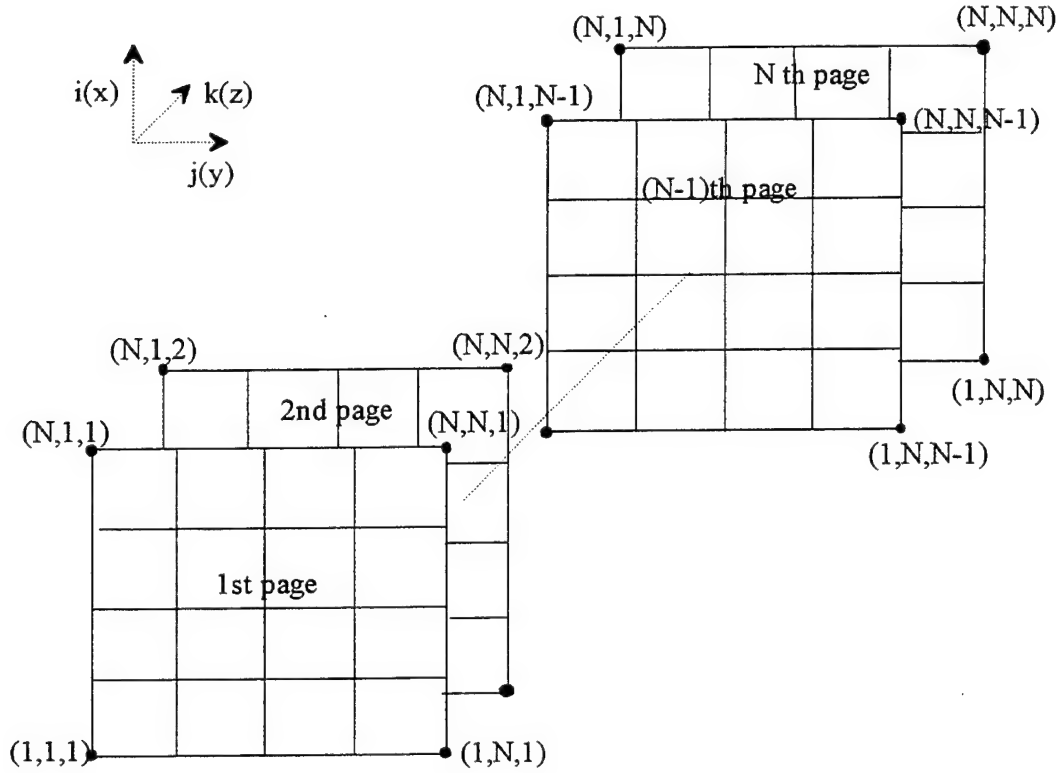


Figure 4.13. Page Arrangement for 3-D Cubic Cell.

The boundary field components for the first page have the electric field $E_x(i,j,1,t)$, $E_y(i,j,1,t)$ and $E_z(i,j,1,t)$. The boundary field components for the second page through $(N-1)$ th page have the electric field components like this. First, for the x components, the 2nd Page has $[E_x(1,j,2,t), E_x(i,N,2,t), E_x(N,j,2,t), E_x(i,1,2,t)]$, nth ($2 < n < N-1$) page has $[E_x(1,j,n,t), E_x(i,N,n,t), E_x(N,j,n,t), E_x(i,1,n,t)]$ and $(N-1)$ th page has $[E_x(1,j,N-1,t), E_x(i,N,N-1,t), E_x(N,j,N-1,t), E_x(i,1,N-1,t)]$. For simplicity, the y,z components have the same global coordinates used in the x components. Finally, the boundary field components on the Nth page have $E_x(i,j,N,t)$, $E_y(i,j,N,t)$ and $E_z(i,j,N,t)$. The limits on the values of i,j,k

on the boundary are 1 and N. Now, the field components on the nodes just inside the boundary exist in the second page through the (N-1)th page. The second page has $E_x(i,j,2,t)$, $E_y(i,j,2,t)$ and $E_z(i,j,2,t)$. For the x components, the third page has $[E_x(2,j,3,t), E_x(i,N-1,3,t), E_x(N-1,j,3,t), E_x(i,2,3,t)]$, mth ($3 < m < N-2$) page has $[E_x(2,j,m,t), E_x(i,N-1,m,t), E_x(N-1,j,m,t), E_x(i,2,m,t)]$. The y,z components have the same global coordinates. Finally, the (N-1)th page has $E_x(i,j,N-1,t)$, $E_y(i,j,N-1,t)$ and $E_z(i,j,N-1,t)$. However, the limits on the values of i,j,k on the nodes just inside the boundary are 2 and N-1. Because the each node on the boundary has three field components, the electric field vectors for the grid on the boundary can be formed as below

$$E_{x_boundary}(t) = [E_{x_1st_page} E_{x_2nd_page} \dots E_{x_(N-1)th_page} E_{x_Nth_page}]^T \quad (4.75)$$

$$E_{y_boundary}(t) = [E_{y_1st_page} E_{y_2nd_page} \dots E_{y_(N-1)th_page} E_{y_Nth_page}]^T \quad (4.76)$$

$$E_{z_boundary}(t) = [E_{z_1st_page} E_{z_2nd_page} \dots E_{z_(N-1)th_page} E_{z_Nth_page}]^T \quad (4.77)$$

where each page field element forms a row vector with the fields at the nodes on the boundary and T indicates transposition (the vector is a column vector, but it has been written as a transpose of a row vector to save space). In an analogous manner an electric field vector can be formed for the nodes just inside the grid boundary

$$E_{x_just_inside}(t) = [E_{x_2nd_page} \dots E_{x_(N-1)th_page}] \quad (4.78)$$

$$E_{y_just_inside}(t) = [E_{y_2nd_page} \dots E_{y_(N-1)th_page}] \quad (4.79)$$

$$E_{z_just_inside}(t) = [E_{z_2nd_page} \dots E_{z_(N-1)th_page}] \quad (4.80)$$

$$E_{just_inside}(t) = [E_{x_just_inside}(t) \ E_{y_just_inside}(t) \ E_{z_just_inside}(t)]^T \quad (4.81)$$

where each page field element forms a row vector with the fields at the nodes just inside the boundary. The electric field on the grid boundary $E_{boundary}(t)$ can be expressed as a

convolution of the electric fields at the layer just inside the grid boundary $E_{just_inside}(t)$ and a *matrix* of impulse responses $H(t)$.

$$E_{x_boundary}(t) = H_x(t) * E_{just_inside}(t) \quad (4.82)$$

$$E_{y_boundary}(t) = H_y(t) * E_{just_inside}(t) \quad (4.83)$$

$$E_{z_boundary}(t) = H_z(t) * E_{just_inside}(t) \quad (4.84)$$

where the $2(N)(N)+(N-2)4(N-1)$ by $3[2(N-2)(N-2)+(N-4)4(N-3)]$ matrix of impulse responses can be written as

$$H_x(t) = \begin{bmatrix} h_{x1,1}(t) & h_{x1,2}(t) & h_{x1,3}(t) & . & . & . & . & h_{x1,M}(t) \\ h_{x2,1}(t) & . & . & . & . & . & . & h_{x2,M}(t) \\ . & . & . & . & . & . & . & . \\ . & . & . & . & . & . & . & . \\ . & . & . & . & . & . & . & . \\ . & . & . & . & . & . & . & . \\ . & . & . & . & . & . & . & . \\ h_{xL,1}(t) & . & . & . & . & . & . & h_{xL,M}(t) \end{bmatrix} \quad (4.85)$$

where $L = 2 \cdot N^2 + (N-2) \cdot 4 \cdot (N-1)$ and $M = 3 \cdot [2 \cdot (N-2)^2 + (N-4) \cdot 4 \cdot (N-3)]$.

$H_y(t)$ and $H_z(t)$ have the same matrix size as $H_x(t)$. The electric field(E_x , E_y , E_z) at a boundary node (identified by a particular value of the index m) can be written as the product of the m -th row of the impulse response matrix $H(t)$ ($H_x(t)$, $H_y(t)$, $H_z(t)$) and the column vector of the electric fields just inside the boundary (identified by index n)

$$E_{x_boundary}(m, t) = \sum_{n=1}^{n=M} h_{x\ m,n}(t) * E_{just_inside}(n, t) = \sum_{n=1}^{n=M} \int_0^t E_{just_inside}(n, \tau) \cdot h_{x\ m,n}(t-\tau) d\tau \quad (4.86)$$

$$E_{y_boundary}(m, t) = \sum_{n=1}^{n=M} h_{y\ m,n}(t) * E_{just_inside}(n, t) = \sum_{n=1}^{n=M} \int_0^t E_{just_inside}(n, \tau) \cdot h_{y\ m,n}(t-\tau) d\tau \quad (4.87)$$

$$E_{z_boundary}(m, t) = \sum_{n=1}^{n=M} h_{z\ m,n}(t) * E_{just_inside}(n, t) = \quad (4.88)$$

$$\sum_{n=1}^{n=M} \int_0^t E_{just_inside}(n, \tau) \cdot h_{z\ m,n}(t - \tau) d\tau$$

The discretized forms of the above equations, involving samples of electric fields at $t=k\Delta t$, are the sums of discrete convolutions. Since a discrete convolution is itself a sum, the result for the boundary nodes will involve double summation.

$$E_{x_boundary}^k(m) = \sum_{n=1}^{n=M} \sum_{p=0}^{p=k} E_{just_inside}^p(n) \cdot h_{x\ m,n}^{k-p} \quad (4.89)$$

$$E_{y_boundary}^k(m) = \sum_{n=1}^{n=M} \sum_{p=0}^{p=k} E_{just_inside}^p(n) \cdot h_{y\ m,n}^{k-p} \quad (4.90)$$

$$E_{z_boundary}^k(m) = \sum_{n=1}^{n=M} \sum_{p=0}^{p=k} E_{just_inside}^p(n) \cdot h_{z\ m,n}^{k-p} \quad (4.91)$$

The convolution equations express the fields at the edges as weighted sums (the weighting coefficients are the values of the discrete boundary impulse responses $h_{m,n}$) of the time histories of the fields "just inside" the grid. In that respect the concept and procedure used in 3-D TGT is the same as those used in 2-D TGT. Also, the impulse responses $h_{m,n}(t)$ converge to zero relatively fast which effectively reduces the number of significant terms in the convolution sums. The convolution sums can thus be truncated such that only a certain number of the most recent values of the electric fields just inside the boundary are needed. The discrete boundary impulse responses $h_{m,n}(k\Delta t)$ need to be determined (and saved) only once, just like in 1-D, 2-D, for a selected grid velocity $v_{grid} = \Delta l / \Delta t$. The impulse responses can be stored in a rectangular matrix form. A particularly suitable matrix form would have $[2(N)(N) + (N-2)4(N-1)]$ rows and $3[2(N-2)(N-2) + (N-4)4(N-3)]N_b$ columns (because the field components at the nodes just inside the boundary consist of E_x, E_y, E_z and the number of each electric field is

$2(N-2)(N-2)+(N-4)4(N-3)]$, where N_h denotes the "truncated" length of the discrete boundary impulse responses. This form is suitable because the boundary electric fields can then be calculated as a product of such a matrix and a column vector constructed of $3[2(N-2)(N-2)+(N-4)4(N-3)]$ subvectors of length N_h . The subvectors represent the N_h most recent values of the electric field at nodes just inside the boundary. The choice of N_h depends on the desired amplitude "resolution". These subvectors are updated at each time step by shifting all of their values down, that is, "further into the past", by one, discarding the last value, and updating the first subvector element with the most recent field value calculated via standard grid update equations. The double summations are thus efficiently executed as matrix-vector multiplications.

In the 3-D TGT, the important thing is how to determine the discretized impulse responses. The discretized impulse responses $h_{x\ m,n}^k$ are determined in a manner analogous to the 1-D, 2-D cases, using the discrete equivalent of the Dirac delta function which we will denote as δ^k . In order to determine the discrete boundary impulse response for a particular input port n , all input ports *except* the n -th input port are set to zero and the Dirac impulse is applied to the n -th input port. Recording all the outputs from $t=0$ to $t=N_h\Delta t$ provides us with $2(N)(N)+(N-2)4(N-1)$ discrete boundary impulses of duration N_h .

$$E_{x_just_inside}^k(n) = \delta^k \quad (4.92)$$

$$E_{x_just_inside}^k(p) = 0 \quad \text{for } p = 1 \dots 2(N-2)^2 + (N-4)4(N-3) \quad \text{and } p \neq n \quad (4.93)$$

$$E_{y_just_inside}^k(p) = 0, E_{z_just_inside}^k(p) = 0 \quad \text{for } p = 1 \dots 2(N-2)^2 + (N-4)4(N-3) \quad (4.94)$$

The $h_{y\ m,n}^k$ and $h_{z\ m,n}^k$ are determined in the same manner as the $h_{x\ m,n}^k$

$$E_{y_just_inside}^k(n) = \delta^k \quad (4.95)$$

$$E_{y_just_inside}^k(p) = 0 \text{ for } p = 1...2(N-2)^2 + (N-4)4(N-3) \text{ and } p \neq n \quad (4.96)$$

$$E_{x_just_inside}^k(p) = 0, E_{z_just_inside}^k(p) = 0 \text{ for } p = 1...2(N-2)^2 + (N-4)4(N-3) \quad (4.97)$$

$$E_{z_just_inside}^k(n) = \delta^k \quad (4.98)$$

$$E_{z_just_inside}^k(p) = 0 \text{ for } p = 1...2(N-2)^2 + (N-4)4(N-3) \text{ and } p \neq n \quad (4.99)$$

$$E_{x_just_inside}^k(p) = 0, E_{y_just_inside}^k(p) = 0 \text{ for } p = 1...2(N-2)^2 + (N-4)4(N-3) \quad (4.100)$$

The each process is repeated $2(N-2)(N-2)+(N-4)4(N-3)$ times and the results for the each case are stored in the $2(N)(N)+(N-2)4(N-1)$ by $3[2(N-2)(N-2)+(N-4)4(N-3)]N_b$ ($[E_x \ E_y \ E_z]$ field vector just inside the boundary) matrix. This matrix is then used to implement the transparent grid termination via the matrix multiplication by the $3[2(N-2)(N-2)+(N-4)4(N-3)]N_b$ column vector of the time-histories of the fields just inside the boundary. Depending on the values of N_b and N , there will be input nodes that are sufficiently far from an output node such that the time it takes for an input impulse to propagate to the output port exceeds N_b . In such a case, the contribution of such an input node to the output node is known to be zero in advance. This may be used to reduce the number of operations in TGT implementation. The process of obtaining the 3-D discrete boundary impulse responses is carried out on a "large" grid whose size should be at least $(N+N_b \text{ by } N+N_b \text{ by } N+N_b)$, or equivalently, the distance from the TGT boundary to the boundary of the "large" grid should be at least $N_b \Delta l/2$. The termination of this "larger" grid (in typical applications $N \gg N_b$ and the "larger" grid would be only incrementally larger) is immaterial, since the reflections off its boundary do not arrive at the output nodes (where they would have corrupted the impulse responses) before the time-stepping has been

terminated. When calculating the discrete boundary impulse responses (DBIR), the nodes interior to the TGT boundary need not be updated since all the nodes on the layer just inside the TGT boundary (the input ports) are zero for $t > 0$ (at $t = 0$ only one node on the layer just inside the TGT boundary has the value of 1). The DBIR calculations thus require updates only for the nodes between the TGT boundary and the large grid boundary which can result in significant computational time savings if $N \gg N_b$. The update equations used for the region between the "inner" (TGT) and the outer boundaries are the free space equations, since this region is assumed to be free space. (The medium between the two boundaries can be any homogenous medium extending to infinity, but the most practical case is the free space.)

C. 3-D TGT RESULTS

The overall procedure for 3-D TGT testing is very similar to that used for 2-D TGT testing. The main difference is in the amount of computer memory needed for 3-D TGT and "infinite" grid implementation. Since 3-D FD-TD calculations require much more computer memory because the number of nodes in 3-D is proportional to N^3 as opposed to N^2 for 2-D (N is the number of cells on each side of the computational domain) this limits the grid size and the duration of impulse responses. We have thus selected a domain with only $N=11$ electric cells on each side (electric cell faces are aligned with the domain boundaries). Note that even such a modest number of cells per each side results in $N^3=1331$ electric cells for the domain volume. Since each cell has three field

components, the total number of electric field components is $3N^3=3993$. The number of magnetic field components is about $3(N-1)^3=3000$. The total number of unknowns is thus about 7000. 3-D TGT is implemented by updating the electric field components on the TGT boundary based on the time histories of electric field components at nodes just inside the TGT boundary. The source is a delta impulse of electric field E field at the center of the grid, with unit-amplitude components E_x , E_y and E_z . The source creates an outgoing spherical wave. If the grid and the TGT were perfect the power within the TGT will be constant until the outgoing wave has reached the nodes in the centers of the six TGT boundary planes (because these nodes are the closest to the source located at the grid center. From then on the power within the TGT should decrease until the outgoing wave has reached the corners of the domain (the nodes furthest away from the source at the domain center). After this time the power within the grid, for a perfect grid and TGT, should be zero. However, since the grid is not perfect, there will be some residual power within the TGT boundary even for an infinite grid. This is the result of the impulse "spreading" as it propagates through the FD-TD grid. Furthermore, the residual power will include the power "reflected" off an imperfect TGT. Again, just like in 2-D, the residual power can be calculated as a function of time for the two cases infinite grid and TGT. The relative difference of the two expressed in dB can be thought of as a measure of performance of the TGT. This quantity can be plotted vs. time (with the time origin defined as the time when the outgoing wave first reaches the TGT) for various impulse response durations. Unfortunately the results for 3-D TGT were not satisfactory. The

TGT tests showed "late-time instability", that is the power within the grid would at first decrease (as it should) but later will start to increase without bounds, which is incorrect. A sample result is shown below (what is the duration of the impulse response for this?)

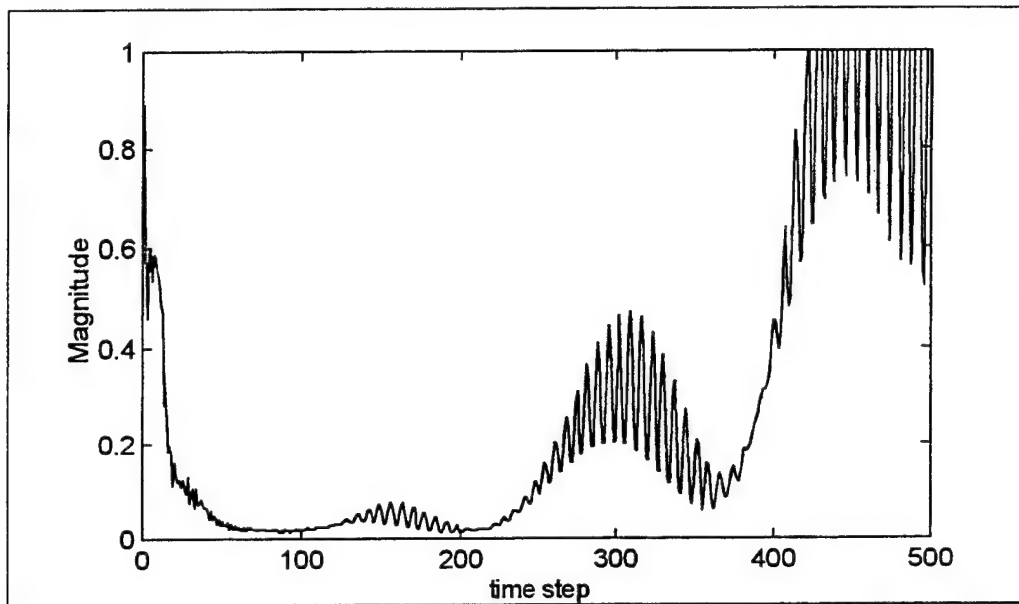


Figure 4.14. Residual Power Within TGT Showing Late-time Instability.

The non-physical oscillatory behaviour of the solution is also evident from the plot of the electric field at a node inside the TGT. The field at first converges to zero as it should, but after about 200 steps it starts to diverge in an oscillatory manner.

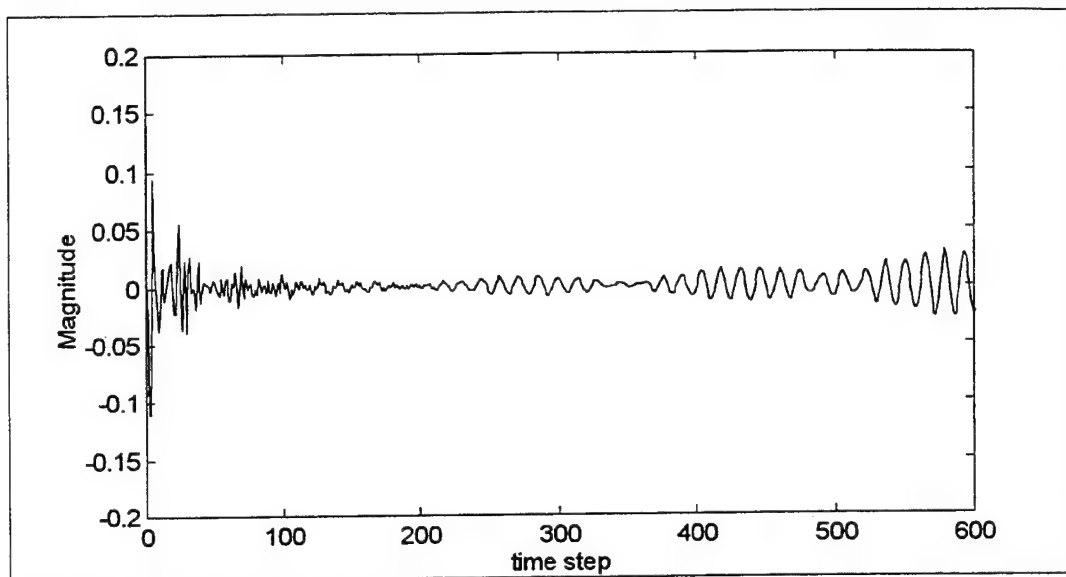


Figure 4.15. Field Strength at a Node observation point within boundary.

For an infinite boundary, the residual power within the TGT boundary decreases to zero as it should. The late-time instability could not be observed because the available PC's did not have enough memory to accomodate the size of the required "infinite" grid.

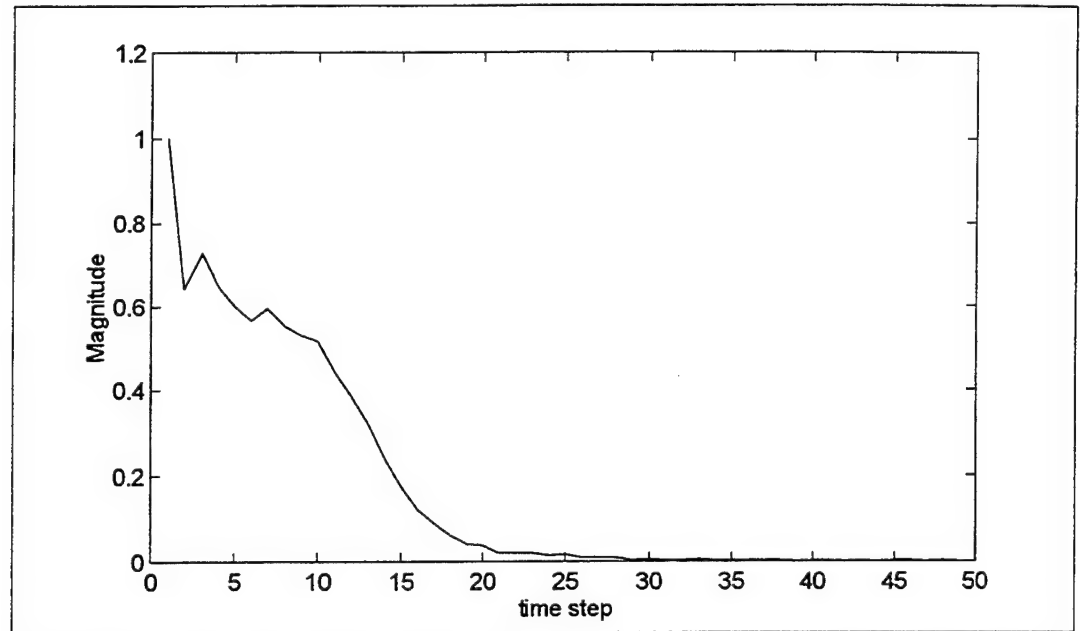


Figure 4.16. Residual Power within TGT for an Infinite Boundary.

V. SUMMARY AND CONCLUSION

A. SUMMARY

In this thesis we have tested the performance of the TGT in 1-D, 2-D and 3-D, based on the residual reflection off the TGT boundary. The power within the TGT boundary was calculated at each time step for an "infinite" grid (that is a grid so large that the reflection off its boundary do not reach the nodes within the TGT boundary before the calculations are completed) and for a much smaller grid with the TGT. For 1-D there were no reflections off the TGT boundary, that is, the outgoing wave was "absorbed" perfectly by the TGT. Note that in 1-D there is no impulse spreading. Therefore, in 1-D, the grid and the TGT can be "perfect". This is not the case in 2-D however. Neither the grid nor the TGT can be perfect, that is there is some pulse spreading and some "reflection" off the TGT. However, the power reflected off the TGT is less than 1% of the residual power due to pulse spreading. Therefore, although the 2-D TGT is not perfect, its performance is excellent since the reflections off the TGT are well below the level of the "distortion" introduced by the grid itself. Furthermore, the power reflected off the TGT boundary depends on the duration of the truncated impulse responses: truncating impulse responses at a later time (increasing the impulse response duration) reduces the reflections off the TGT. Finally, the 3-D TGT implementation was not successful, because of late-time instability problems.

B. CONCLUSIONS AND RECOMMENDATIONS

The results of this study show that TGT concept works for 1-D and 2-D FD-TD electromagnetic field problems. The 3-D TGT implementation was the most difficult, because of the computer memory requirement. Unfortunately, it was not successful due to late-time instabilities. More research is needed to determine and remove the causes of

late-time instabilities in 3-D. A previously completed thesis [Wells] has demonstrated the effectiveness of TGT for 2-D static problems, while this thesis has demonstrated the TGT effectiveness for 2-D time-domain problems. Another possibility for further research is to implement the TGT in the frequency domain, where the time domain convolutions would be replaced by sums of products of complex numbers.

APPENDIX

A. DBIR.M

```

%%%%%%%%%%%%%%%%%%%%%%%%%%%%%%%%%%%%%%%%%%%%%%%%%%%%%%%%%%%%%%%%%%%%%%%%
**** Program : DBIR.M ****
**** This Program Generates TGT Coefficients for 2-D ****
**** TMz fields (Ez, Hx, Hy) ****
**** NOTE: All H-fields have been multiplied by Z0 ! ****
%%%%%%%%%%%%%%%%%%%%%%%%%%%%%%%%%%%%%%%%%%%%%%%%%%%%%%%%%%%%%%%%%%%%%%%%
clear all
clear, flops(0);
tic
    N      = 101;
    Nin    = 21;
    Nout   = Nin + 2;

    h_dur = 40;          % duration of impulse responses
    vr = 1/sqrt(2);       % grid "speed"
    rowsh = 0.5*(N - Nin); % Row "shift" for the "inside" matrix
    colsh = 0.5*(N - Nin); % Column "shift" for the "inside" matrix
    irt   = rowsh + 1;    % Top row for the "inside" matrix
    irb   = irt + Nin - 1; % Bottom row for the "inside" matrix
    icl   = colsh + 1;    % Leftmost column for the "inside" matrix
    icr   = icl + Nin - 1; % Rightmost column for the "inside" matrix
    nodes_out = 4*(Nin+1); % Number of nodes on the boundary
    nodes_in  = 4*(Nin-1); % Number of nodes just inside the boundary

    **** INITIALIZE ARRAYS ****
    Ez = zeros(N,N); Hx = zeros(N-2,N-1); Hy = zeros(N-1,N-2);
    Edbir = zeros(nodes_out,h_dur); Dbir = zeros(nodes_out,nodes_in*h_dur);
    row_pointer = zeros(1,nodes_in); col_pointer = zeros(1,nodes_in);
    col_start = zeros(1,nodes_in); col_stop = zeros(1,nodes_in);

    for m = 1:1:nodes_in          % LOOP OVER INNER GRID NODES
        if (m <= Nin)
            row_pointer(m) = irt; col_pointer(m) = icl + m - 1;          % TOP SIDE
        elseif (m > Nin) & (m <= 2*Nin-1)
            row_pointer(m) = irt + m - Nin; col_pointer(m) = icr;          % RIGHT SIDE
        elseif (m > 2*Nin-1) & (m <= 3*Nin-2)
            row_pointer(m) = irb; col_pointer(m) = icr - (m-(2*Nin-1)); % BOTTOM SIDE
        elseif (m > 3*Nin-2)
            row_pointer(m) = irb - (m-(3*Nin-2)); col_pointer(m) = icl; % LEFT SIDE
        end
        col_start(m) = (m-1)*h_dur+1; col_stop(m) = col_start(m) + h_dur - 1;
    end
    pack

    **** DISCRETE BOUNDARY IMPULSE RESPONSE LOOP ! ****
    ****

    % LOOP OVER INNER GRID NODES as sources
    for m = 1:1:nodes_in
        Ez = zeros(N,N); Hx = zeros(N-2,N-1); Hy = zeros(N-1,N-2);

```



```

Ez(row_pointer(m),col_pointer(m)) = 1;      % Delta pulse excitation along the top
                                             half of the boundary

%%%%%% TIME LOOP %%%%%%
for k = 1:1:h_dur
    Etop = (Ez(irt-1,icl-1:icr+1))';
    Eright = Ez(irt:irb+1,icr+1);
    Ebot = (fliplr(Ez(irb+1,icl-1:icr)))';
    Eleft = flipud(Ez(irt:irb,icl-1));
    Edbir(:,k) = [Etop; Eright; Ebot; Eleft];
    Hx = Hx + vr*( Ez(2:N-1,1:N-1) - Ez(2:N-1,2:N));
    Hy = Hy + vr*(-Ez(1:N-1,2:N-1) + Ez(2:N,2:N-1));

    Ez(2:N-1,2:N-1)=Ez(2:N-1,2:N-1)+vr*(-Hy(1:N-2,:)+Hy(2:N-1,:))
        +Hx(:,1:N-2)-Hx(:,2:N-1));
    Ez(irt:irb,icl:icr) = zeros(Nin,Nin); % Reset Ez inside
end

%%%%%% END OF TIME LOOP %%%%%%
Dbir(:, col_start(m):col_stop(m)) = Edbir;
end
%%%%%% END OF SOURCE LOOP %%%%%%
MFlops = flops/1000000
toc
save dbir_40m Dbir
save par_40m Nin h_dur vr

```

B. TGT_TM.M

```

%%%%%%%%%%%%%%%%%%%%%%%%%%%%%%%%%%%%%%%%%%%%%%%%%%%%%%%%%%%%%%%%%%%%%%%%%%%%%%
%%%%%% Program : TGT_TM.M %%%%%%%%%%
%%%%%%%%%%%%%%%%%%%%%%%%%%%%%%%%%%%%%%%%%%%%%%%%%%%%%%%%%%%%%%%%%%%%%%%%%%%%%%
%%%%%% FD-TD for 2D, TMz fields (Ez, Hx, Hy), cartesian coordinates %%%%%%%%%%
%%%%%%%%%%%%%%%%%%%%%%%%%%%%%%%%%%%%%%%%%%%%%%%%%%%%%%%%%%%%%%%%%%%%%%%%%%%%%%
%%%%%% NOTE: H-fields have been multiplied by Z0 ! %%%%%%%%%%
%%%%%%%%%%%%%%%%%%%%%%%%%%%%%%%%%%%%%%%%%%%%%%%%%%%%%%%%%%%%%%%%%%%%%%%%%%%%%%
%%%%%% Dirichlet b.c. or OPEN boundary simulated via DBIR %%%%%%%%%%
%%%%%%%%%%%%%%%%%%%%%%%%%%%%%%%%%%%%%%%%%%%%%%%%%%%%%%%%%%%%%%%%%%%%%%%%%%%%%%

load dbir_40m
load par_40m

%%%%%% INPUT PARAMETERS %%%%%%

N      = Nin + 2;
nodes_out = 4*(Nin+1);    % Number of nodes on the boundary
nodes_in  = 4*(Nin-1);    % Number of nodes just inside the boundary

% Time Samples
N_samples = 200;

%%%%%% ARRAYS INITIALIZED %%%%%%

Ez = zeros(N); Hx = zeros(N-2,N-1); Hy = zeros(N-1,N-2);
Ebound = zeros(nodes_in*h_dur,1); E_dbir = zeros(nodes_out,1);
time_pointer = zeros(nodes_in,1);

%%%%%% BOUNDARY POINTERS FOR THE TIME HISTORIES OF NODES JUST INSIDE %%%%%%%%%%

for i = 1:nodes_in, time_pointer(i) = (i-1)*h_dur + 1; end

%%%%%%%%%%%%%%%%%%%%%%%%%%%%%%%%%%%%%%%%%%%%%%%%%%%%%%%%%%%%%%%%%%%%%%%%%%%%%%
%%%%%% BOUNDARY POINTERS FOR SPIRAL TO RASTER LABELING CONVERSION %%%%%%%%%%
%%%%%%%%%%%%%%%%%%%%%%%%%%%%%%%%%%%%%%%%%%%%%%%%%%%%%%%%%%%%%%%%%%%%%%%%%%%%%%

```

```

      (can be done only once and stored!!!)

for n = 1:1:nodes_out
    if n <= N
        row_pointer(n) = 1;          col_pointer(n) = n;
    elseif (n > N) & (n <= 2*N-1)
        row_pointer(n) = n - N + 1;  col_pointer(n) = N;
    elseif (n > 2*N-1) & (n <= 3*N-2)
        row_pointer(n) = N;          col_pointer(n) = 3*N - 1 - n;
    elseif (n > 3*N-2)
        row_pointer(n) = 4*N - 2 - n; col_pointer(n) = 1;
    end
end

%%%%%%%%%%%%%%%%%%%%%%%%%%%%%%%%%%%%%%%%%%%%%%%%%%%%%%%%%%%%%%%%%%%%%%%%
%%%%%% START OF TIME-STEPPING LOOP! %%%%%
%%%%%%%%%%%%%%%%%%%%%%%%%%%%%%%%%%%%%%%%%%%%%%%%%%%%%%%%%%%%%%%%%%%%%%%%
    Ez(ceil(N/2),ceil(N/2)) = 1;
    m=0;

for k=1:1:N_samples

    %%%% FIELD UPDATES %%%%

    Hx = Hx + vr*( Ez(2:N-1,1:N-1) - Ez(2:N-1,2:N));
    Hy = Hy + vr*(-Ez(1:N-1,2:N-1) + Ez(2:N,2:N-1));

    Ez(2:N-1,2:N-1) = Ez(2:N-1,2:N-1) +
        vr*(-Hy(1:N-2,:)+Hy(2:N-1,:)+Hx(:,1:N-2)-Hx(:,2:N-1));

    %%%% nodes "just inside", spiral labeling %%%%

    Eupdate = [(Ez(2,2:Nin+1))';Ez(3:Nin+1,Nin+1);(fliplr(Ez(Nin+1,2:Nin)))';
               ;flipud(Ez(3:Nin,2))];

    %%%% FIFO REGISTER-LIKE STORING OF TIME HISTORIES %%%%

    Ebound(2:nodes_in*h_dur) = Ebound(1:nodes_in*h_dur-1);
    Ebound(time_pointer)     = Eupdate;

    %%%% CONVOLUTIONS FOR THE BOUNDARY NODES, MATRIX VERSION %%%%

    E_dbir = Dbir*Ebound

    %%%% CONVERSION FROM SPIRAL BACK TO RASTER LABELING %%%%

    for n = 1:1:nodes_out
        Ez(row_pointer(n),col_pointer(n)) = E_dbir(n);
    end

    Ez(ceil(N/2),ceil(N/2)) = 0;

    %%%% Computation of Residual Power for grid      %%%%
    %%%% since wavefront touching the tgt boundary %%%%

    if (k>=ceil(N/2) & k<=ceil(N/2)+140)

        m=m+1;

```

```
s(m)=0;
for a=1:N
    for b=1:N
        s(m)=s(m)+Ez(a,b)^2;
    end
end

end

end

save s_tgt s
```

LIST OF REFERENCES

1. Yee, K. S., "Numerical Solution of Initial Boundary Value Problems Involving Maxwell's Equations in Isotropic Media," *IEEE Trans. Antennas and Propagation*, vol. 14, 1966, pp. 302-307.
2. Mur, G., "Absorbing Boundary Conditions for the Finite Difference Approximation of the Time Domain Electromagnetic Field Equations," *IEEE Trans. Electromagnetic Compatibility*, vol. 23, 1981, pp. 377-382.
3. Engquist, B., and Majda, A., "Absorbing Boundary Conditions for the Numerical Simulation of Waves," *Mathematics of Computation*, vol. 31, No. 139, July 1977.
4. Lebaric, J.E., Computational Electromagnetics Classnotes at Naval Postgraduate School, 1994.
5. Sadiku, M.N.O., *Numerical Techniques in Electromagnetics*, CRC Press, Boca Raton, FL, 1992.
6. Taflove, A., *Computational Electrodynamics*, Artech House, Norwood, MA, 1995.
7. Kunz, K.S., and Luebbers R.J., *The Finite Difference Time Domain for Electromagnetics*, CRC Press, Boca Raton, FL, 1993.

INITIAL DISTRIBUTION LIST

- | | |
|--|---|
| 1. Defence Technical Information Center
Cameron Station
Alexandria VA 22304-6145 | 2 |
| 2. Library Code 013
Naval Postgraduate school
Monterey Ca 93943-5101 | 2 |
| 3. Chairman Code EW
Electronic Warfare Academic Group
Naval Postgraduate school
Monterey Ca 93943-5126 | 1 |
| 4. Chairman Code EC
Department of Computer and Electrical Engineering
Naval Postgraduate school
Monterey Ca 93943-5121 | 1 |
| 5. Professor J. E. Lebaric, Code EC/Lb
Department of Electrical and Computer Engineering
Naval Postgraduate school
Monterey Ca 93943-5121 | 1 |
| 6. Professor M. A. Morgan, Code EC/Mw
Department of Computer and Electrical Engineering
Naval Postgraduate school
Monterey Ca 93943-5121 | 1 |
| 7. Wang, Kewjin
661-57 Sinlim 13 Dong
Kwanak-Gu, Seoul 151-023
Korea | 2 |